



# LATERALLY LOADED PILE CAP CONNECTIONS

Revised Final Report  
Work Task 4

*by*

Kyle M. Rollins and Tony E. Stenlund

Department of Civil and Environmental Engineering  
Brigham Young University  
368 CB Provo, Utah 84602

*Prepared for*

Utah Dept of Transportation Research Division  
Lead Agency for Pooled-Fund Study  
“Dynamic Passive Pressure on Abutments and Pile Caps”

May 2008



## ABSTRACT

There is presently considerable uncertainty regarding appropriate connection details between driven piles and pile caps. Prior research on the subject suggests that given a proper embedment length, a specialized reinforced connection may not be necessary. Eliminating these costly connection details could save thousands of dollars on both labor and materials. This research study focuses on the importance of the pile-to-cap connection detail with respect to the reinforcement connection and pile embedment length.

Four pile caps were constructed, each with two 40 foot-long steel pipe piles, and were tested with different connection details. Two caps included a reinforced connection detail while the other two relied on their respective embedment lengths. A hydraulic ram was used to apply a cyclic lateral force to each of these pile caps until failure occurred. Load-displacement curves were developed for each pile cap and strain gauge measurements were used to evaluate tension and bending moments in the pile caps. Comparisons are presented regarding the effect of the connection on pile cap response. An analysis has been conducted to best understand possible failure modes; two computer modeling programs were used and their respective results have been presented and compared to the observed readings.

This report provides test data supporting the theory that a proper embedment length acts as an adequate connection in place of a specialized reinforced detail. A pile cap with piles embedded two diameters into the cap performed successfully. In contrast, a cap with piles embedded only one diameter failed after developing a large

crack through the entire cap. For the two pile caps with a reinforcing cage connection; the performance was essentially the same for the piles embedded either six inches (.5 diameter) or twelve inches (one diameter) into the cap. The data produced was found to be very similar to what was estimated by the two programs used for analysis (GROUP 4.0 and LPILE 4.0).

## ACKNOWLEDGMENTS

Funding for this project was provided by Contract No 069148 “Dynamic Passive Pressure of Abutments and Pile Cap” with the Utah Department of Transportation as part of a pooled-fund study supported by Departments of Transportation from California, Oregon, Montana, New York and Utah. Daniel Hsiao served as the project manager for UDOT. This support is gratefully acknowledged. Nevertheless, the opinions, interpretations and recommendations in this report are those of the author and do not necessarily reflect those of the sponsors.

## TABLE OF CONTENTS

<b>1</b>	<b>INTRODUCTION .....</b>	<b>1</b>
1.1	Background.....	1
1.2	Objective and Scope .....	2
<b>2</b>	<b>DESCRIPTION OF PROBLEM.....</b>	<b>3</b>
2.1	Behavior of Laterally Loaded Pile Groups.....	3
2.2	Literature Review .....	4
2.3	H Pile to Pile Cap Connections .....	4
2.4	Pipe Pile to Pile Cap Connections .....	9
2.5	Prestressed Pile to Pile Cap Connections .....	14
2.6	Timber Pile to Pile Cap Connections .....	18
2.7	Related Testing and Analysis Papers .....	19
2.8	Summary of Literature Review .....	23
<b>3</b>	<b>TEST SETUP .....</b>	<b>31</b>
3.1	General Remarks .....	31
3.2	Site Description .....	32
3.3	Pile and Cap Description .....	34
3.4	Instrumentation.....	39
<b>4</b>	<b>ANALYTICAL STUDY.....</b>	<b>54</b>
4.1	Introduction .....	54
4.2	Failure in the Piles.....	55

4.3	Failure in the Cap .....	56
4.4	Failure in the Surrounding Soil .....	58
4.5	Failure in the Connection .....	59
4.6	Rotational Restraint .....	66
4.7	Summary of Predictions .....	67
<b>5</b>	<b>TEST RESULTS.....</b>	<b>68</b>
5.1	General Remarks .....	68
5.2	Pile Cap Test Results.....	69
5.3	Analysis of Longer Piles .....	89
5.4	Comparison of Observed Strain .....	91
5.5	Comparison of Observed Moments.....	97
5.6	Comparison of Test Results.....	101
<b>6</b>	<b>CONCLUSIONS.....</b>	<b>105</b>
6.1	Summary.....	105
6.2	Conclusions .....	106
6.3	Recommendation for Future Research .....	108
6.4	Implementation of Results.....	108
<b>7</b>	<b>REFERENCES .....</b>	<b>110</b>
	<b>Appendix A.....</b>	<b>113</b>

## SYMBOLS AND NOTATION

$a$  = eccentricity of load or distance from last row of trailing piles to point of rotation  
 $A_c$  = cross sectional area of concrete under consideration  
 $A_s$  = area of reinforcement  
 $b$  = width of member  
 $b'$  = pile spacing  
 $b_f$  = flange width of steel pile section  
 $c$  = clear cover of concrete typically 2 to 3 inches  
 $C_m$  = modified characteristic moment parameter  
 $d$  = distance to extreme fiber  
 $D$  = pile diameter  
 $d_b$  = bar diameter  
 $e$  = eccentricity from point of zero moment to the center of the effective embedment  
 $E$  = modulus of elasticity  
 $F$  = the applied force  
 $f'_c$  = compressive strength of concrete (psi)  
 $f_y$  = yield strength of steel  
 $F_y$  = yield strength of steel  
 $h$  = distance between strain gages  
 $I$  = moment of inertia  
 $K_{m\theta}$  = rotational restraint coefficient  
 $K_{\Delta c}$  = axial stiffness at the top of the piles in compression  
 $K_{\Delta t}$  = axial stiffness at the top of the piles in tension  
 $L$  = distance between string potentiometers  
 $L^*$  = distance from lateral loads point of application to the neutral axis of the joint  
 $l_e = L_e = l_e$  embedment length  
 $M$  = observed moment during testing  
 $M'_c$  = modified characteristic moment  
 $M_c$  = original characteristic moment  
 $M_f$  = experimental moment resistance  
 $M_j$  = nominal moment capacity of concrete pile cap  
 $M_p$  = plastic moment  
 $M_r$  = theoretical moment resistance  
 $M_{rc}$  = moment capacity of a concrete filled circular steel pipe  
 $N_u$  = factored axial load normal to cross section  
 $s$  = distance between symmetrically placed  $A_s$  and  $A'_s$   
 $S_u$  = soil undrained shear strength  
 $t$  = thickness of pipe  
 $y$  = distance from the neutral axis to the compression fiber  
 $V_u$  = shear capacity  
 $X_1$  = amount of deflection observed from string potentiometers at location 1  
 $X_2$  = amount of deflection observed from string potentiometers at location 2

$x_i$  = distance from last row of trailing piles to center of pile  
 $z$  = embedment depth of pile top below ground surface  
 $Z$  = plastic modulus of steel section alone  
 $\alpha$  = concrete factor for reinforcement location  
 $\beta$  = concrete factor for coating  
 $\sigma$  = calculated stress  
 $\delta_v$  = vertical translation  
 $\gamma$  = concrete factor for unit weight  
 $\gamma'$  = effective unit weight of soil  
 $\gamma$  = unit weight of soil  
 $\epsilon_c$  = observed strain in compression  
 $\epsilon_t$  = observed strain in tension  
 $\Phi$  = reduction value phi (.75 for shear)  
 $\omega$  = reinforcement index equal to  $A_s/(bl_e)$

# **1 INTRODUCTION**

## **1.1 Background**

Piles are a very common foundation choice for bridges, high-rise buildings and other large structures. These piles must be capable of resisting large lateral forces brought on by earthquakes, wind and wave action. Research has shown that the pile cap connection itself can significantly increase the lateral resistance provided by the foundation against these forces. For example, a pile cap providing a fixed-head boundary will produce a stiffer load-deflection curve than a pile cap which allows rotation. However, relatively little research and testing has been performed to evaluate the effect of the pile to pile cap connection on the degree of fixity and overall response of the pile cap.

This research study has focused on the connection detail between the pile and pile cap and its effect on pile cap stiffness and rotation. In order to analyze a pile head under lateral loading it must be determined whether the connection is in a fixed or pinned condition. From a stiffness standpoint, it is desirable to have a pure fixed head connection yet this is seldom achievable in the field. A design assuming a truly fixed head connection would likely result in underestimated values of deflection, as well as incorrect estimates of the magnitudes and locations of bending moments. On the other

hand a design assuming a pinned connection which fails to resist moments could result in a very costly over design.

Previous research and testing has shown that piles embedded a limited depth into the pile cap will resist only shear and axial loads while piles embedded an adequate depth will resist moments as well and significantly reduce lateral deflections. It has been determined that this boundary condition is a function of the pile-to-cap embedment length with less importance on the connecting steel reinforcement. This report focuses on this connection as a function of reinforced steel and the embedment length. This design must include a connection able to fully develop the piles' capacity while resisting lateral forces and the accompanying moment.

## **1.2 Objective and Scope**

This research has been undertaken to better understand the importance of pile cap connections on lateral pile cap and abutment behavior. The goal in connection design is to provide a connection capable of developing moment capacity equal to the moment demands on the pile while remaining essentially rigid. Ideally, it is desired to eliminate the special reinforcement details and rather provide a proper pile embedment length. This would result in a simpler construction process and lower overall cost. In this study, four pile cap connections involving 12 inch ID pipe piles were tested in the field under full-scale conditions. Connection details included pile embedments of 6 and 12 inches with reinforcing cages extending into the pile cap along with pile embedments of 12 and 24 inches without any reinforcing connection.

## **2 DESCRIPTION OF PROBLEM**

### **2.1 Behavior of Laterally Loaded Pile Groups**

Piles are most often placed in groups with a variety of alignment and spacing arrangements. The piles are then capped with a concrete pile cap which encases the piles. On occasion, individual piles are used, though this is less common in the field. Driven pile foundations typically consist of steel pipes filled with concrete, steel H sections or pre-stressed concrete. Pile groups perform differently than single piles, due to the soil-pile-soil interaction which is a function of pile spacing. The larger the spacing, the less the overlapping of shear zones and the greater the lateral pile resistance.

Typically, the foundation system is designed so that its capacity will exceed that of the column or structural system above ground. This approach ensures that damage will occur above ground where it can more easily be detected and repaired. Therefore, the designer must be certain that the foundation system will develop its full design capacity. For lateral load conditions, the moment capacity of the pile foundation will typically govern the pile section properties. For a fixed-head pile group the maximum negative moment occurs at the base of the pile cap while the maximum positive moment occurs in the pile at a short depth below the base. It is, therefore, desirable to construct a pile cap that will be strong enough so that the pile

can achieve its full moment capacity. In this regard, the connection must be able to resist the large negative moment for the foundation system to be considered efficient. As indicated previously, the moment capacity at the connection depends on both the depth of embedment of the pile and the reinforcement arrangement. This research and testing, which focuses on these issues, is therefore very important to future design and construction of pile systems.

## **2.2 Literature Review**

Due to the extensive use of piles in foundation systems, a number of publications relating to pile cap connections are available in the literature. A literature review was conducted to obtain all available research and/or testing concerning laterally loaded pile caps and their connections. Most of the publications involve laboratory tests on different pile to pile cap connection details; however some of the papers also involve numerical modeling or analytical models based on the test results. The publications reviewed have been divided into five groups: (1) H pile to pile cap connections, (2) Pipe pile to pile cap connections, (3) Pre-stressed pile to pile cap connections, (4) Timber pile to pile cap connections, and (5) Related testing and analysis papers

## **2.3 H Pile to Pile Cap Connections**

Marcakis and Mitchell (1980) developed an analytical model considered to be conservative in determining the capacity of a pile-pile cap connection based on the results of a series of 25 tests involving steel members embedded in reinforced concrete sections. Steel members ranged from welded or embedded H piles, pipe piles filled

with concrete and empty, to standard steel plates. The design method outlined in the 1971 PCI Design Handbook for connections incorporating embedded structural steel was shown to have several inconsistencies. Multiple design charts were then developed with varying material properties, Figure 2-1 shows an example of one of those charts. With most material properties and member dimensions known the designer would choose suitable values of the embedment length ( $L_e$ ), width ( $b$ ), eccentricity ( $e$ ), and be able to enter the appropriate design chart to determine a proper reinforcement connection.

Marcakis and Mitchell (1980) proposed equation 2-1 to compute the ultimate shear force ( $V_u$ ) that can be carried by a pile-pile cap connection. The equation is based on a strut-and-tie approach and uses uniform stress distributions along the embedment zone to determine the required embedment length ( $L_e$ ). The moment capacity of a connection can be determined by multiplying the shear capacity as determined in equation 2-1 by the eccentricity ( $e$ ) from the point of zero moment to the center of the effective embedment (embedment minus cover depth) as shown in Fig. 2-1.

$$V_u = \frac{0.85 f'_c b' (L_e - c)}{1 + \frac{3.6e}{L_e - c}} \quad (2-1)$$

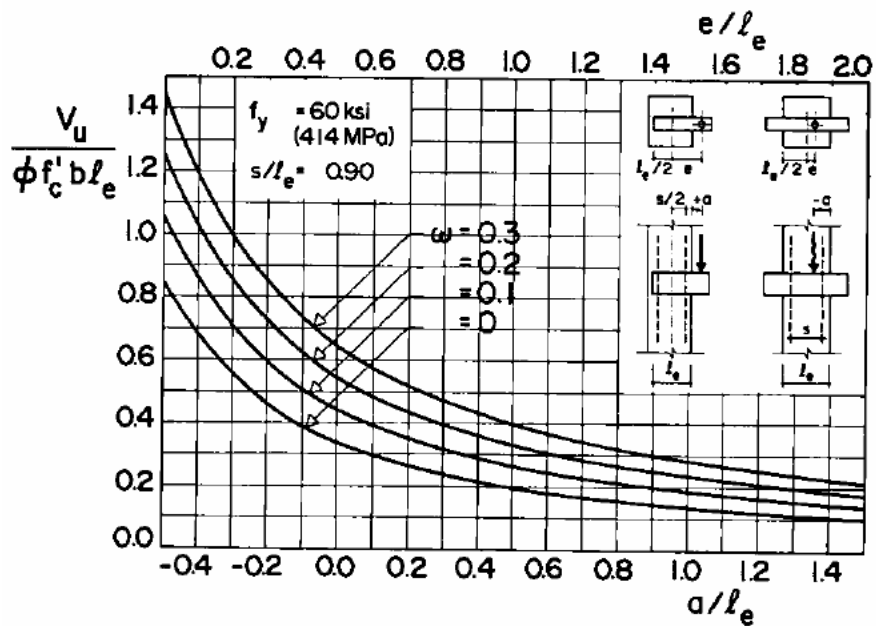
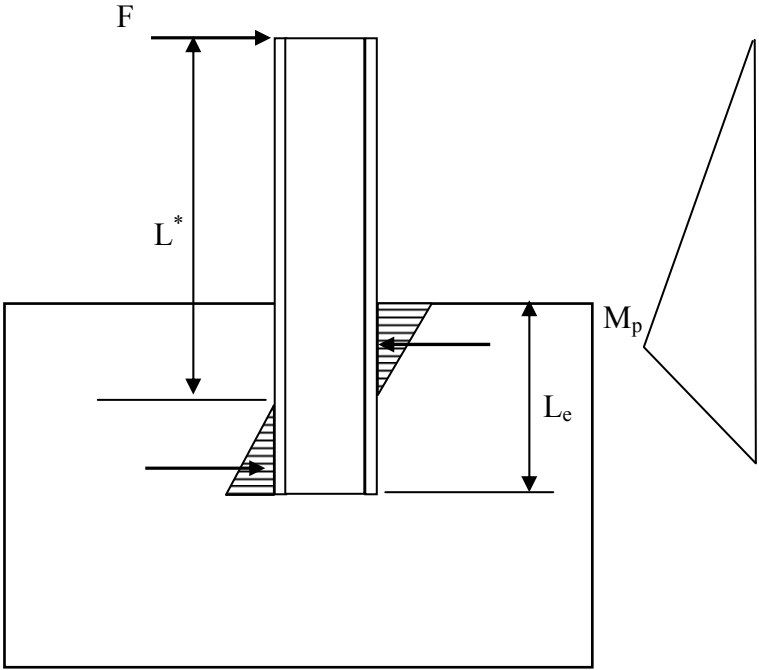


Figure 2-1 Connection design chart by Marcakis and Mitchell.

The effective width ( $b'$ ) is equal to the width of the pile cap or a maximum of 2.5 times the width of the steel section ( $w$ ).

Shama, Ayman, and Mander (2001) used finite element modeling and results from two full scale tests on pile-to-cap connections to develop equations for both new construction and retrofits. Two HP pile-pile cap connections, with deep embedment typical of construction practice in the eastern U.S., were constructed in a laboratory and tested under cyclic axial and lateral loading until failure. A moment capacity equation was developed based on embedment that was proven helpful in predicting connection performance. A pile-to-cap efficiency ratio ( $\rho$ ) was defined which compares the moment capacity of the pile to the moment capacity of the concrete-pile connection.

Figure 2.2 shows the assumed linear stress distribution through the connection zone which is limited to a maximum equal to the compressive strength of the concrete.



**Figure 2-2 Assumed theoretical stress distributions.**

Equation 2-2 was derived to compute the nominal moment capacity of the pile-pile cap connection ( $M_p$ ) based upon the theoretical stress distribution shown in and results from the load tests.

$$M_p = \frac{f'_c b_f L_e^2}{6 + \frac{L_e}{L^*}} \tag{2-2}$$

The moment capacity at the connection is a function of concrete crushing at the pile-pile cap interface, which is related to the concrete compressive strength ( $f'_c$ ), the width

of the H pile ( $b_f$ ), and the length of pile embedment ( $L_e$ ). As the embedment length is increased, the bearing area of concrete increases leading to larger moment capacity.

Shama, Mander and Chen (2002a) investigated the connection capacity of H piles embedded into bent pier caps which are typically located 12 to 15 above the ground surface. Initially, cyclic lateral load tests were performed on five HP 10 x 42 pile sections embedded 1 ft into reinforced concrete pile cap which was 2 ft deep and 2.3 ft wide. Lateral load was applied at 10 ft above the pile cap. The pile caps were reinforced with 4 #9 bars in the top and bottom along with stirrups consisting of #4 bars at 8 inch spacing. Tests were performed about the strong axis on 3 piles and about the weak axis on 2 piles. The 1 ft embedment was sufficient to develop the full moment capacity of the pile in the weak direction, but non-ductile failure eventually occurred for the pile cap for the tests in the strong direction.

Based on the test results, a simplified analytical model was developed to compute moment capacity as a function of embedment depth along with pile and pile cap material properties. These analyses suggested that the embedment depth would need to be increased to a depth between 1.5 and 2 pile widths. Subsequently, another set of lateral cyclic load tests were performed on the same HP sections described previously with embedment of 2 ft into a deeper pile cap. With this embedment depth, the moment capacity of the connection exceeded that of the pile and a ductile failure was observed.

While previous studies involved tests on H piles embedded 1 to 2 ft into the pile cap, engineering practice in the Western US has often designed the pile-pile cap connection to act as a pinned connection. The embedment is only 5 inches deep and

the pile is connected to the pile cap using some type of reinforcing detail. Xiao et al (2006) conducted experimental studies to evaluate the behavior of these shallow embedment connection details. The tests involved cyclic vertical and lateral load tests on five HP 14x89 piles which were embedded 5 inches into the pile cap. Two 2 inch diameter holes were drilled through the web of the H piles and V-shaped reinforcing bars (#8 bars, 2.5 ft long, 60° interior angle) were threaded through the H pile and into the pile cap. The pile cap was 4 ft thick, 4 ft long and 3.5 ft wide and was reinforced top and bottom with a grid of #8 bars at 6 inch spacing in one direction and 7 inches in the other. Vertical stirrups consisting of #5 bars were installed at 12 inch spacing in one direction and 14 inch spacing in the other.

The vertical tests indicated that the V-shaped reinforcing provided only 40 to 70% of the computed ultimate capacity and less than the tensile capacity of the H pile. In addition, the lateral testing showed that the connection did not act as a pinned connection as designed, but sustained a moment ranging from 25 to 66 percent of the ultimate moment capacity of the H pile. To provide any reasonable agreement with the observed moment capacity of the section, consideration had to be given to capacity from both embedment and flexure mechanisms.

#### **2.4 Pipe Pile to Pile Cap Connections**

Steunenberg et al (1998) performed lateral cyclic load tests on a 12 ID steel pipe pile with a 0.5 inch wall thickness which was welded to a 25 x 24 inch x 2 inch thick steel plate. The steel plate was attached to the base of a reinforced concrete pile cap using 30 deformed studs, each 0.59 inches in diameter and 23.6 inches long. The

moment capacity of the connection exceeded that of the pipe pile and the pile failed in a ductile manner.

Silva and Seible (2001) conducted lateral cyclic load tests on two large-scale cast-in-steel-shell (CISS) pile-pile cap connections. The connection details were designed according to Caltrans specifications and built at a 7/12<sup>th</sup> scale. Both piles were composite steel shell piles, the first with an unreinforced concrete core and V-shaped anchor bars and the second with a reinforced concrete core which geometries as shown in Figure 2-3. specifications.

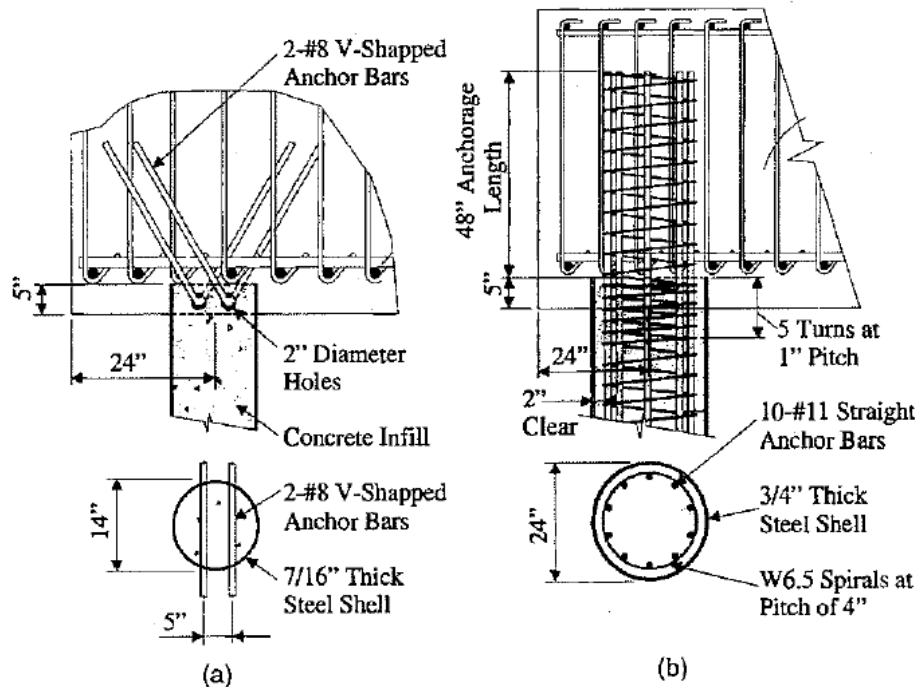


Figure 2-3 Piles and cap configurations.

Test results showed that pile performance due to seismic or any type of lateral force is highly dependent on the embedment length and connection type. Both connection details reached a failure state due to inadequate connections. Another

important observation was that when piles are subjected to combined axial and lateral loads, fracture can occur within the connection reinforcement below the design tension load. Observations from both the tests and analytical data were collected in order to develop limit states and better define and predict damage levels.

The following six limit states were defined by Silva and Seible;

- Pile elastic limit – defined based on a performance level such that any noticeable damage does not require repair. This was the first limit state noticed for both tests and was indicated by the development of thin cracks which emanated at 45 degrees from the pile base to the sides of the cap.
- Pile cap concrete cover spalling – occurs due to rotation and prying and is evidenced by extensive damage to the pile cap concrete cover. Unlike the first test this limit state occurred near failure in test two.
- Pile cap joint region cracking – defined as an onset of joint shear cracking typically occurring simultaneously with the pile elastic limit state and visible in both tests by cracks emanating from the seating region. Also defined when principal stresses in the joint region exceed  $3.5\sqrt{f'_c}$ .
- Pile functional evaluation limit state – moderate damage occurs at this limit state yet the structure does not lose strength and no exposure to reinforcement occurs. Also defined when the anchor bars exceed a strain of 0.0325.
- Pile cap joint shear failure – defined when the principal tensile stresses exceed  $5\sqrt{f'_c}$ , which correspond to poorly reinforced concrete. This was found to occur only in test two.

- Pile safety evaluation limit state – significant damage occurs, requiring repair or replacement of the structure. This was found to be the limit state in test one with the strain in the anchor bars exceeding the maximum allowable of 0.065. Test two failed due to large rotations causing exposure to the pile cap reinforcement along the bottom layer.

A better understanding of the limit states defined above will allow the designer to account for inelastic deformations in the piles, thus reducing the number of piles required and the size of the pile cap. This will also reduce the stiffness in the foundation system thus decreasing the column displacement ductility demand. These significant changes will lead to a more economical foundation design and reduce the damage in the column under a seismic event.

Stephens and McKittrick (2005) performed laboratory tests on five one-half scale steel pipe columns embedded in a concrete pile cap and filled with unreinforced concrete. For each test the pile was embedded 9 inches into the cap with no other reinforcing details provided. A photograph of the test setup is presented in Figure 2-5. With each additional test the amount of steel in the cap, both in the longitudinal and transverse directions, was increased in an effort to evaluate the importance of reinforcing steel in the pile cap to the moment capacity of the pile-pile cap connection. By using one-half scale models there was only 4.5 inches of concrete cover provided around the pile although design guidelines often call for at least one foot of concrete surround each pile.

Tests 1 and 2 had pile cap reinforcing steel ratios in the longitudinal and transverse directions of 0.41 and 0.09%, respectively. With increasing lateral loads

the caps failed through concrete cracking in the cap and it appeared that the reinforcing steel was unable to carry the tension forces. Tests 3 and 3a had increased steel ratios and the same type of failure occurred. Pile Cap 4 had longitudinal and transverse ratios of 2.83 and 0.7% respectively, and this caused a failure in the form of a plastic hinge in the steel pile and only nominal concrete cracking was noticed. With the dramatic increase in steel for Pile Cap 4 as shown in Figure 2-4, constructability concerns developed regarding the amount, size and spacing of the reinforcement.

Hand calculations and Finite Element Modeling were used to analyze each of the four tests. The simple hand calculations proved valuable in predicting the nature of failure though were less accurate in predicting the load at which failure occurred. The finite element analysis did not appear to be capable of modeling accurately the concrete damage under cyclic loads.



**Figure 2-4 Reinforcing cage for pile cap Model 4 Montana State University (Stephens and McKittrick, 2005).**

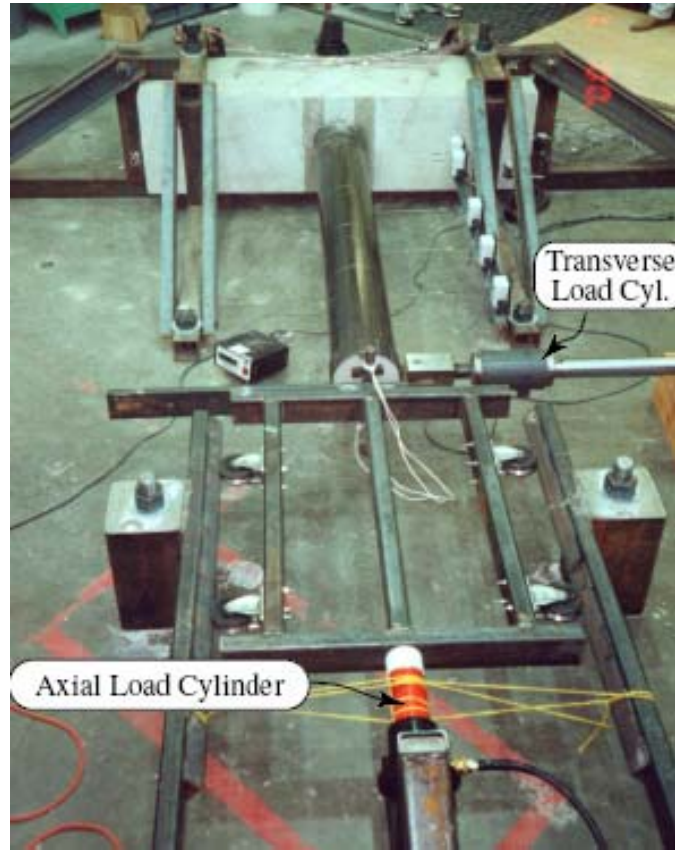


Figure 2-5 Pile and cap setup for testing at Montana State University (Stephens and McKittrick, 2005).

## 2.5 Prestressed Pile to Pile Cap Connections

The Army Corps of Engineers builds many structures such as bridges, locks and buildings that utilize pile foundations. This has been noted as a significant part of the overall cost of construction. To better understand the ability to achieve a fixed head pile-pile cap connection a study was undertaken by Castilla, Martin, and Link (1984). They utilized finite element and finite difference computer modeling programs such as CERL, ANSYS, and COM 622 to better understand the situation.

Although previous Corp design practice assumed that an HP pile embedded one foot into a pile cap would act as a pinned connection, computer analysis in this

study indicated that such a value was unrealistic. According to the analysis, a 1 foot embedment length actually developed between 61 and 83% of the fixed-head moment and therefore could be considered partially fixed. The study concluded that for HP piles the ratio of embedment length to pile width should be greater than two in order to obtain full fixity.

Joen and Pak (1990) investigated a variety of approaches for connecting cast-in-place concrete pile caps to prestressed piles. The piles were 15.7 inch octagonal prestressed concrete piles and the pile cap was 3 feet square in plan. Steel reinforcement ratios in the pile cap were 0.55 and 0.09 percent in the longitudinal and transverse direction, respectively. The connection details included (a) embedding the piles in the cap with an embedment length of 31.5 inch and a spiral encircling the pile along the embedment length, (b) breaking away the concrete on the end of the pile over a 2 ft length and embedding it in the cap to this depth, and (c) simply embedding dowel bars in the pile that extended into the pile cap. During cyclic loading failure occurred by the formation of a plastic hinge in the precast pile at the face of the pile cap and only minor cracking was observed in the pile cap. With the exception of one test, a minimum ductility ratio of eight was observed.

Harries and Petrou (2001) noted the difficulty, time and expense required to provide special connection details for prestressed pile such as those tested by Joen and Park (1990). Their objective was to determine if adequate capacity could be provided by simply embedding the prestressed pile without an special connection detail. The study combined previous test results with results from two new lab tests on full-scale pile-to-pile caps with different connection details to provide evidence that no special

details are necessary if the proper embedment length is provided. The pile-to-cap assembly was tested as a cantilever beam in a horizontal position. Two separate tests were performed using an 18 inch square precast concrete pile embedded 18 inches and 24 inches into a 7 feet x 7 feet x 3 feet pile cap. The precast piles were 18 ft long. Each cap was reinforced with No. 7 longitudinal bars on the top and bottom at 6 inches spacing and No. 3 ties at 6 inches spacing in the transverse direction and through the depth of the pile cap.

Both piles first began to crack at the interface with a moment of 169 ft-kips and yield displacement at the interface was measured to be 1 inch, which occurred at a moment of 246 ft-kips. Harris and Petrou concluded that the embedment lengths were sufficient to develop the moment capacity without a special connection detail. They concluded that an embedment length equal to the pile width would be sufficient to develop the moment capacity of the pile. This condition would provide a “weak pile, strong pile cap” behavior that permits easier inspection and repair in the event of an earthquake.

In contrast to previous tests on prestressed concrete piles where embedment or special connection details were tested, Xiao (2003) conducted large-scale cyclic axial and lateral load tests on prestressed piles with very shallow embedments. The piles represented Caltrans Class 70 full-scale pile. They were 14 inch square and were 67 inches long, with a compressive strength of the concrete was 8.6 ksi. Six 0.5 inch diameter seven wire strands were used for prestressing. The pile segments were confined by ASTM grade A82 w11 wire spirals with a nominal diameter of 9.5 mm spaced at 2 inches. Four #6 bar dowels were cast full-length inside the pile and

extended 34 inches beyond the end of the pile. The end of the pile cap was embedded 3 inches into the pile cap which was 3.16 ft deep x 2.84 ft wide and 5 ft long. The pile cap reinforcement consisted of a top and bottom mat of #8 bars spaced at 5.3 inches in the top and 10.6 inches, respectively.

Despite the shallow embedment, the connection detail was able to resist considerable moment. In order to compute a moment capacity near the measured value, it was necessary to consider moment from bearing on the embedded portion of the pile and moment from flexure at the top of the pile as illustrated in Fig. 2-4. These results are in good agreement with tests on H piles with shallow embedment reported by Xiao et al (2006). Xiao (2003) also found that the moment capacity due to embedment was predicted best by the the PCI Design handbook (PCI, 1999) equation given by

$$V_u = \frac{0.85f'_c b' L_e}{1 + 3.6e / L_e} \quad (2-4)$$

Finally, the dowel connection detail was sufficient to provide the full compressive and tensile capacity of the pile section.

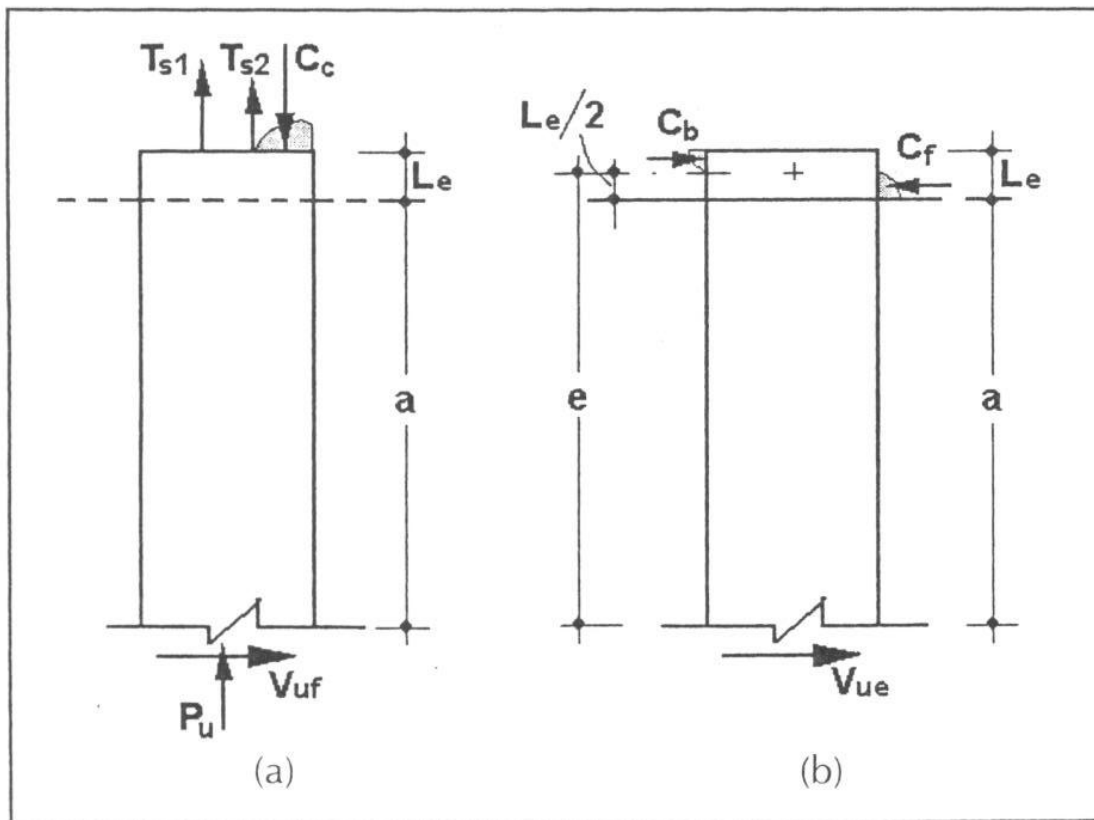


Figure 2-7 Pile end resisting mechanisms (a) flexural resistance and (b) embedment resistance (Xiao, 2003)

## 2.6 Timber Pile to Pile Cap Connections

Shama and Mander (2004) conducted cyclic lateral load tests on two timber piles approximately 9 inches in diameter which were embedded at 1 and 1.5 diameters (9 inches and 14.5 inches) into a pile cap. The pile cap was 3 ft deep, 3 ft wide in the direction of loading, in the direction of loading 3 feet wide and extended 1 foot beyond the edge of the pile on the side. The pile cap was reinforced with a girde of #8 bars at 12 inch spacing in both directions in both the top and bottom of the cap. The testing showed that an embedment of one pile diameter was sufficient to develop the full moment capacity of the pile and provide a ductile response.

## **2.7 Related Testing and Analysis Papers**

In assessing the ultimate moment capacity of a concrete filled pipe, several methods can be employed. Since the goal of the design is for the pile cap connection to exceed the moment capacity of the pile, an accurate assessment of the pile's moment capacity is desired. Bruneau and Marson (2004) conducted full-scale laboratory tests on steel pipe with reinforced concrete infill in an effort to evaluate existing design codes used throughout the world to compute moment capacity. Multiple codes exist throughout the world and each has its own equations and assumptions to determine proper design limits. Unfortunately, the accuracy of the various methods and their relative differences are largely unknown. Four specimens were tested with the load applied laterally at the end of the pipe and the failure occurring at the concrete foundation. Table 1 shows the moment capacity from test data and predictions from five separate codes. It was noted that the AISC LRFD 1994 edition underestimated strength capacities by a significant margin while the Eurocode 4 (1994) proved to be the most accurate.

Equation 2-6 was developed to better calculate the moment capacity of a pipe pile with concrete fill. It was also shown that whether the concrete in the pipe is strengthened with reinforcement or not it still provides confinement and delays local buckling.

**Table 1 Measured to calculated moment capacity ( $M_f/M_r$ ) ratios for specimens tested.**

Code	CFST 64 $P=1000$ kN		CFST 34 $P=1820$ kN		CFST 42 $P=1820$ kN	
	Strength (kN m)	$M_f/M_r$	Strength (kN m)	$M_f/M_r$	Strength (kN m)	$M_f/M_r$
Test data	591		444		928	
AISC LRFD (1994)	362	1.64	234	1.90	681	1.36
CAN/S16.1-M94	314	1.88	255	1.74	608	1.53
Eurocode 4 (1994)	522	1.33	402	1.10	918	1.01
CAN/S16.1-M99 (proposal A)	492	1.20	387	1.15	911	1.02
CAN/S16.1-M99 (proposal B)	519	1.14	380	1.17	897	1.04

$$M_{rc} = (Z - 2th_n^2)F_y + \left[ \frac{2}{5} (.5D - t)^3 - (.5D - t)h_n^2 \right] f_c' \quad (2-6)$$

where

$$h_n = \frac{A_c f_c'}{2Df_c' + 4t(2F_y - f_c')}$$

While piles within pile caps are commonly assumed to be fixed in design, most pile caps exhibit some rotation during lateral loading. Since the pile cap rotation can have a significant effect on the moment which actually develops at the base of the pile cap, an accurate assessment of the rotational stiffness of the pile cap is necessary.

Using data from testing in 1999, Mokwa and Duncan (2003) developed a procedure to estimate the moment restraint which would allow proper estimation of the actual pile head rotational stiffness which would be between the fixed and free conditions. The value of the rotational restraint coefficient,  $K_{m\theta}$  is a function of the amount of movement required to mobilize the tensile and compressive loads in the pile. The amount of rotation is a function of the magnitude of the lateral load and

rotational stiffness  $K_{m\theta}$ . Figure 2-7 shows the free body diagrams used to derive the equation for  $K_{m\theta}$  (equation 2-7).

$$K_{M\theta} = \frac{\Delta M}{\Delta \theta} = \sum_{i=1}^n [K_{\Delta c} (x_i - a)^2] + \sum_{i=1}^n [K_{\Delta t} (x_i - a)^2] \quad (2-7)$$

Figure 2-8 shows one of the load-deflection curves from testing and compares them to the curves predicted using fixed-head and free-head conditions as well as the rotationally restrained stiffness defined using equation 2-7. Clearly the degree of pile head fixity plays a substantial role in the computed load-deflection curves.

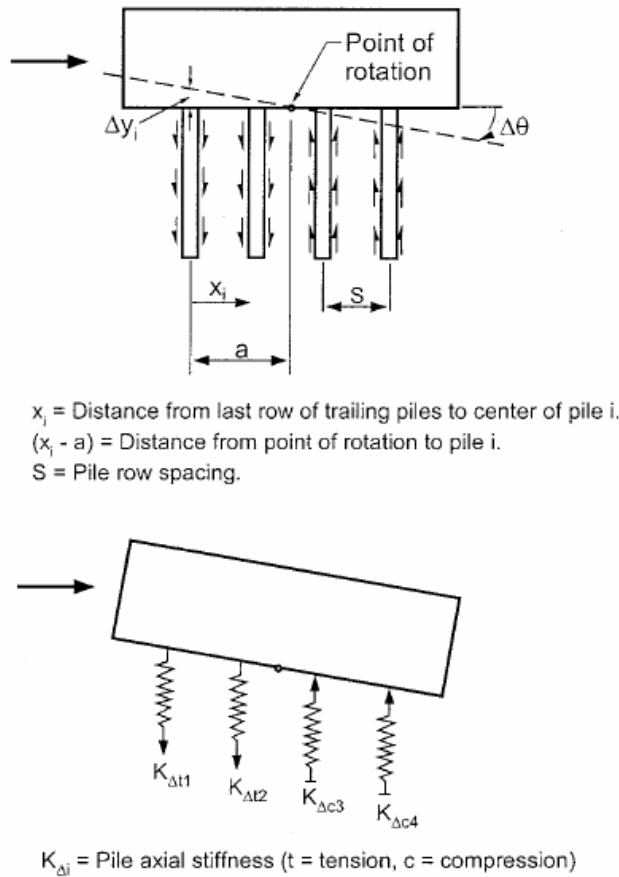
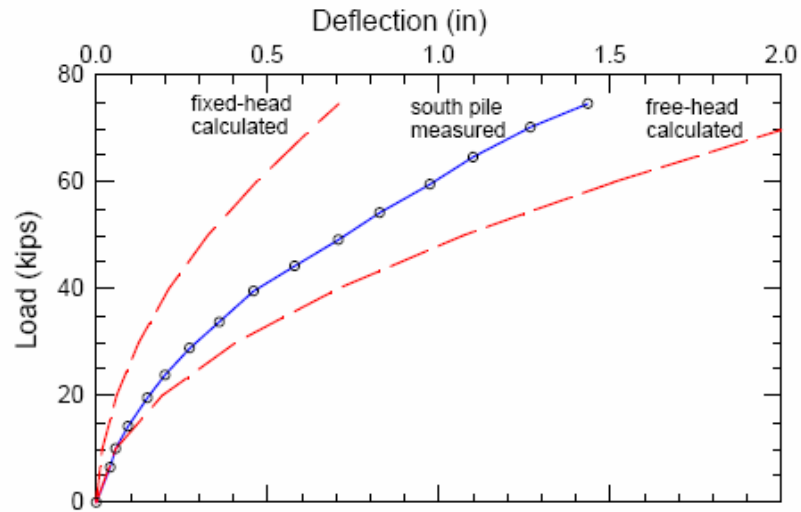
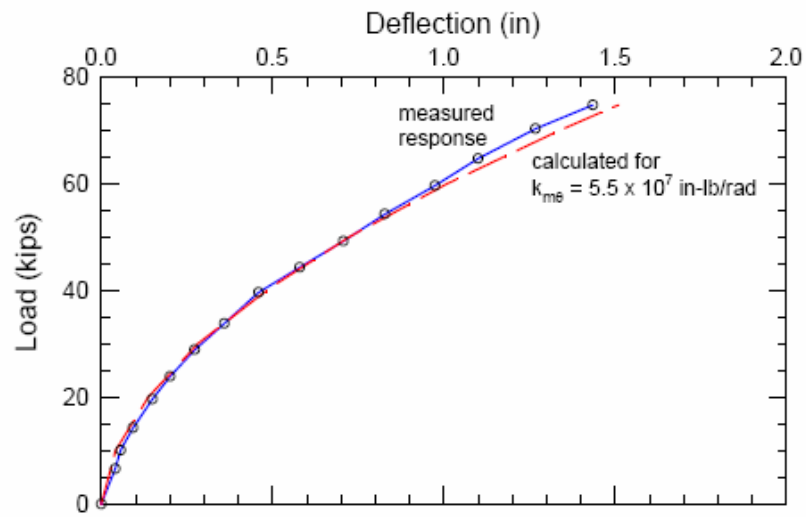


**Figure 2-7 Free body diagrams showing rotational resistance relative to rotation (Mokwa and Dunca, 2003).**



(a) Fixed-head and free-head boundary conditions.



(b) Rotationally restrained pile-head boundary condition, best fit  $k_{m\theta}$  value.

Figure 2-8 Load vs. Deflection curves comparing boundary conditions (Mokwa and Duncan, 2003).

## 2.8 Summary of Literature Review

There has been a significant amount of research conducted pertaining to the lateral resistance of the pile foundation system. There has also been a considerable amount of testing conducted aimed at developing equations to evaluate the moment capacity at the pile to pile cap connection. All of the research and testing reviewed has established the connection detail as a crucial element in developing the piles capacity. Some of the most valuable points are presented here:

1. Rather than relying on rules-of-thumb which specify some minimum embedment length, embedment length and reinforcement details should be designed such that the moment capacity of the connection exceeds that of the pile. As a result, embedment requirements will increase with pile size and pile moment capacity. (e.g. the embedment length of a steel pipe pile would be greater than for a timber pile)
2. Marcakis and Mitchell (1980) produced multiple design charts based on testing which enable the designer to determine proper embedment for steel piles. An example of these charts is presented in Figure 2-1. Equation 2-1 was developed incorporating the importance of the embedment length by calculating the stresses at the connection face.
3. Shama et al (2001) derived Equation 2-2 to predict required embedment lengths based upon the theoretical stress distributions shown in and results from load tests. They found that moment capacity at the connection is a function of the concrete crushing strength at the pile-pile cap interface.

4. Although tests conducted by Joen and Park (1990) highlight the successful performance of precast prestressed piles with special connection details, Harries and Petrou (2001) contend that an adequate connection can be provided more economically by simply increasing the embedment length. Parametric studies with prestressed piles suggest that the embedment length should be taken as the larger of the pile diameter or 12 inches.
5. A number of studies (Joen and Park 1990, Shama et al 2002a, Xiao 2003, Xiao et al 2006) have found that piles with shallow embedment do not normally act as “pinned” connections, but provide considerable moment capacity. Accurate assessment of moment capacity requires consideration of shear and moment capacity from embedment and flexure mechanism. These findings also suggest that an economical connection detail could be achieved with shallow reinforcement and some type of reinforcement cage
6. Two testing programs found that standard connection details used by Caltrans involving shallow pile embedment and V-bar anchors, did not provide adequate tensile or compression capacity (Silva and Seible 2001, Xiao et al 2006). These details were also insufficient to develop full moment capacity. .
7. One-half scale single piles were tested at Montana State University (Stephens and McKittrick 2005) with various amounts of steel in the cap which showed that the moment capacity of the pile system is also a

function of reinforcement ratio in the pile cap. Premature failure of the cap can prevent development of the moment capacity of the pile.

8. A number of design equations have been proposed to estimate the moment capacity of a pile-pile cap connection; however, the available inventory of test data is insufficient to validate the equations for anything but a very limited set of connections. As a result, recommendations on required embedment length vary widely.

Table 2 summarizes the publications reviewed that directly pertain to a pile caps connection under lateral loads. While much research and testing has been conducted on pile groups, only a few are related to the connection between the pile and pile cap; those that have been reviewed are summarized in this table. By preparing this table it is noted that only a few tests have been performed all of which have been conducted in a laboratory with a similar test setup.

### **2.8.1 Limitations of Current Understanding**

Because relatively few tests have been performed on pile to pile cap connections, significant uncertainty exists regarding appropriate embedment lengths to achieve a given moment capacity. This is particularly true when flexure at the top of the pile cap do to dowels or other reinforcements may provide some increase in moment capacity. Although several equations have been developed, the existing data set is insufficient to validate these equations generally. Furthermore, the connection type for which the least testing has been performed is the concrete filled pipe pile.

**Table 2 Summary of reviewed pile cap tests.**

<b>Investigator</b>	<b>Test</b>	<b>Pile characteristics</b>	<b>Cap Characteristics</b>	<b>Connection</b>	<b>Objective</b>
Shama et al (2000)	Test 1 and 2 Full Scale Laboratory	HP10X42	7' x 9' x 3' CIP	12" embedment	Define criterion for pile system retrofits
Shama et al (2002a)	Tests 1-5 Full-scale Laboratory	HP10x42	3' x 14' x 2' CIP	12" embedment	Evaluate adequacy of embedment for moment capacity
Shama et al (2002b)	Tests 1-3 Full-scale Laboratory	HP10x42	3' x 10' x 3.5'	24" embedment	Evaluate adequacy of retrofit and design equations
Xiao et al (2006)	Tests 1-5 Full-scale Laboratory	HP14x89	4' x 3.5' x 4'	5" embedment with V bars	Evaluate shallow embedment
Steunenberg et al (1998)	Test 1 Full-scale Laboratory	Hollow 12' pipe pile with 0.5" wall	2.4' x 5.6' x 2.6'	Plate with 30 studs	Evaluate plate/cap interaction
Silva and Seible (2001)	Test 1 Full Scale Laboratory	24" Steel Pipe with unreinforced concrete fill	24' x 24' x 5' CIP	5" embedment with 2 #8 V-shaped bars 30" long	Evaluate tensile capacity, moment capacity and limit states
	Test 2 7/12 <sup>th</sup> Scale Laboratory	14" Steel Pipe with reinforced concrete fill	24' x 24' x 5' CIP	5" embedment with 10 #11 bars 53" into cap	Evaluate tensile capacity, moment capacity and limit states

Stephens and McKittrick (2005)	Tests 1-5 ½ scale Laboratory models	8" Steel Pipe with unreinforced concrete fill	69"x 18"x 18" CIP	9" embedment	Test system capacity with various steel reinforcement ratios in the pile cap
Joen and Park (1990)	Tests 1-2	16" octagonal prestressed piles	3' x 6.5' x 3' CIP	2' embedment and external reinforcing cage	Compare various connection details
	Tests 3-4	16" octagonal prestressed piles	3' x 6.5' x 3' CIP	2' of concrete removed from cage	
	Tests 5-6	16" octagonal prestressed piles	3' x 6.5' x 3' CIP	2" embedment and dowels extending into cap	
Harries and Petrou (2001)	Tests 1 & 2 Full Scale Laboratory	16" octagonal prestressed piles	7' x 7' x 3' CIP	18" and 24" embedment	Show that no special connection detail is required
Xiao (2003)	Tests 1-3 Full-Scale Laboratory	14" square prestressed piles	2.8' x 5' x 3.2' CIP	3" embedment 4 #6 dowels	Evaluate effect of shallow embedment
Shama and Mander (2004)	Tests 1-2 Full-scale Laboratory	9" diameter timber piles	3' x 10' x 3'	9" and 13.5" embedment	Evaluate embedment effect of moment capacity

Previous research has been conducted exclusively under lab conditions with the load applied at some distance from the base of the pile cap. Under field conditions the load is not all applied at one location but is distributed along the length of the pile due to soil-pile interaction. This factor, which may effect connection capacity, has not been investigated (Xiao et al, 2003, Xiao 2006). In addition, the pile caps in the laboratory testing have been completely fixed against rotation, while under field conditions, the cap may rotate to some degree decreasing the moments which develop. These limitations indicate the need to better understand how a pile group will react under field conditions. This study addresses these limitations by applying the force on the pile cap while the pile remains in the ground.

Some laboratory tests highlight the potential for eliminating special reinforcing details and developing moment capacity in the connection exclusively with embedment. Eliminating special reinforced connections has not yet been accepted in design. In fact much of the current pile group design includes not only a special reinforced connection detail but also a significant embedment length. Alternatively, recent laboratory test suggest that successful performance can potentially be achieved with minimal embedment and an appropriate reinforcing segment.

The current research involves full scale field tests which will consider soil-pile interaction effects and allow the cap to move and rotate as it might in an actual seismic event. The research will involve pile-pile cap connections with varying embedment depths and reinforcement details which can be compared for cost and effectiveness. This research is designed to contribute to a better understanding of how pile groups act

under large lateral forces where shear, bending and axial forces are all acting on the connection.



## **3 TEST SETUP**

### **3.1 General Remarks**

A total of four pile caps were tested each supported by two piles driven to a depth of 40 feet. These four pile caps were laterally loaded independent of each other using a hydraulic ram. As indicated in the literature review, the majority of tests involving pile caps have been performed on either scale models or on laboratory specimens. These tests are significant in that they consider the complete pile/pile cap/soil system under in-situ conditions rather than a laboratory setting. Also, prior testing has fixed the pile cap and applied the lateral force to the tip of the piles without soil involved. However, under in-service load conditions, the pile cap would not be fully fixed. This test setup also takes into account the pile group interaction effects while the prior testing typically included only single piles.

The purpose of this study is to compare the performance of four connection details between the piles and the pile cap. There are two basic details involved with the connection between the pile and the pile-cap. The first detail involves the length to which the pile is embedded into the pile cap and the second is the reinforcement connection extending from the pile cap a proper development length into the pile. Therefore, each of the four pile caps were configured with the same geometry with the exception of the connection.

Prior research has shown that a proper embedment length alone can be sufficient to develop the moment capacity of the pile and it may suffice to ignore any type of reinforcement connection which can be very costly to both fabricate and construct in the field. Another type of practice, although less common, involves leaving the piles hollow. The lack of concrete makes a reinforced connection more difficult to fabricate and analyze. As shown in the literature review section, a length equal to at least one pile diameter should be embedded into the pile cap to fully develop the moment capacity of the pile. To evaluate this finding under field conditions, it was decided to test a pile cap with piles embedded one pile diameter and compare its performance with pile caps that have shorter as well as longer embedment lengths.

### **3.2 Site Description**

The site used for the construction and testing of all four pile caps was located at 700 West and South Temple in Salt Lake City Utah. This is a Utah Department of Transportation (UDOT) test site where other pile testing had been performed previously. The soil profile at the test site can be seen in Figure 3-1 along with all the soil properties developed from previous field testing (Rollins et al, 2003). The soil profile generally consists of stiff clay with two thin sand layers to a depth of 4.09 m which is the depth range which has the greatest effect on the lateral pile response. The water table was located at a depth of approximately 1.07 m during the time of the testing. The piles extended through an underlying soft clay layer and into a stiffer

clay layer below. A picture of the site prior to construction of the pile caps is provided in Figure 3-2.

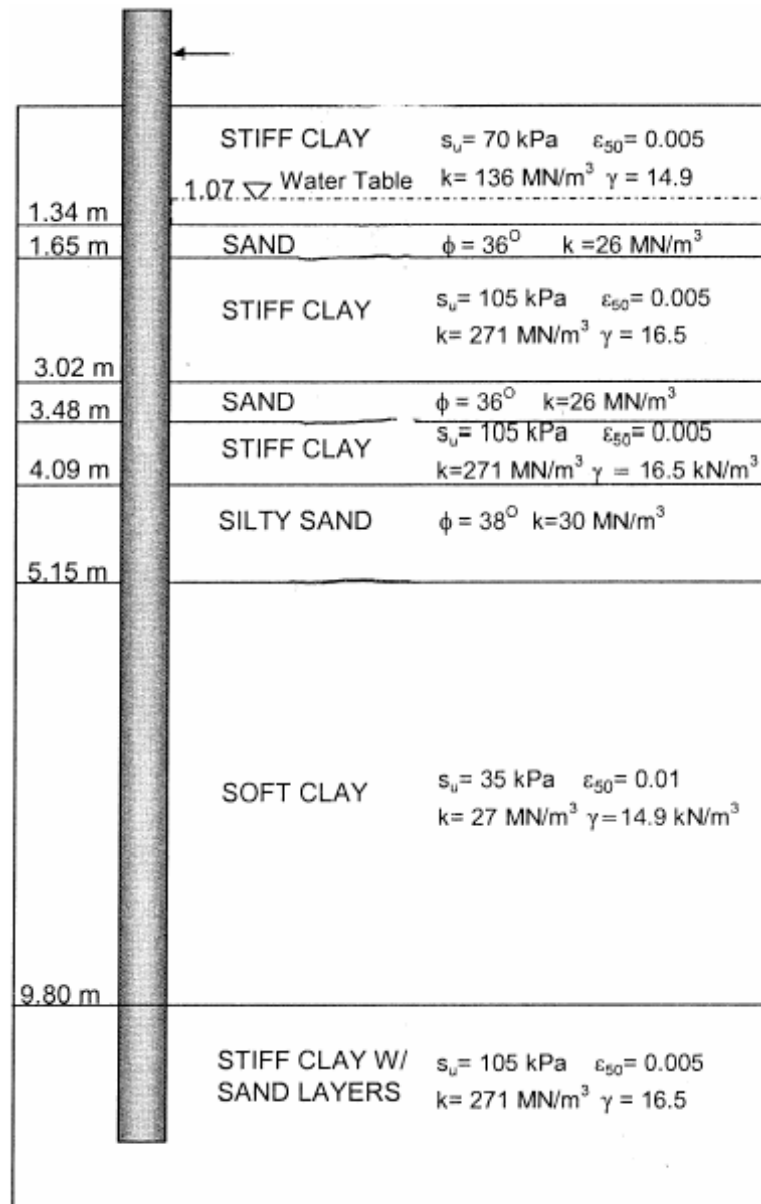


Figure 3-1 Soil Profile for the South Temple, Salt Lake City Test Site.



**Figure 3-2 Photograph of the South Temple, Salt Lake City Test Site.**

### **3.3 Pile and Cap Description**

The pile caps for all of the tests consisted of a 6 ½ foot long x 3 ft high x 3 ft wide concrete block. Each pile cap was connected to two circular steel pipe piles which had been driven to a depth of 40 feet and were spaced at 3 ½ feet on centers. Each pile had an inside diameter of 12 inches with a 3/8 inch wall thickness. All pile caps were reinforcing with grids of #7 bars spaced at 6 inches on centers in the longitudinal and transverse directions both top and bottom with a minimum 3 inches of clear cover on the top and 3 inches on the bottom. The materials used in the construction of all four pile caps were consistent with what is typically used in the field, that is: concrete with a 4,000 psi compressive strength and rebar with a yield

strength of 60,000 psi. The steel pipe piles had a modulus of elasticity of 29,000 ksi and a yield stress of 57,000 psi.

Figure 3-4 through Figure 3-8 show the piles and caps for each test and Table 3 summarizes the connection details for each cap. Small holes were cut in the piles so that the longitudinal bars from the bottom reinforcement grid could extend through the piles; however, the transverse bars were cut off to prevent an excessive amount of holes in the piles. Figure 3-3 is an isometric view of the piles and cap. This drawing shows an embedment length of 12 inches which varies with each test.

**Table 3 Summary of connection details for each pile cap test.**

<b>Pile Cap</b>	<b>Pile Embedment</b>	<b>Connection Steel</b>	<b>Cap Steel</b>
1	6 inches	4-#6 bars, 6.25 ft long, #4 Spiral @ 6" pitch	#8 @ 6" grids top and bottom
2	12 inches	4-#6 bars, 6.25 ft long, #4 Spiral @ 6" pitch	"
3	12 inches	None and no concrete in pile	"
4	24 inches	None, but concrete fill in pile	"

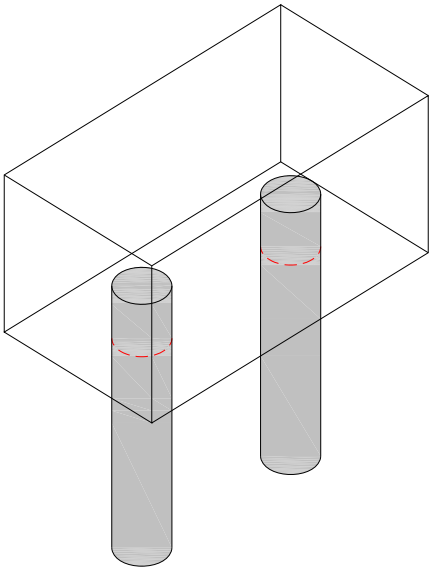


**Figure 3-3 Isometric view of typical pile cap configuration.**



**Figure 3-4 Photograph of the pile cap reinforcing and forms prior to concrete placement at the South Temple, Salt Lake City Test Site.**

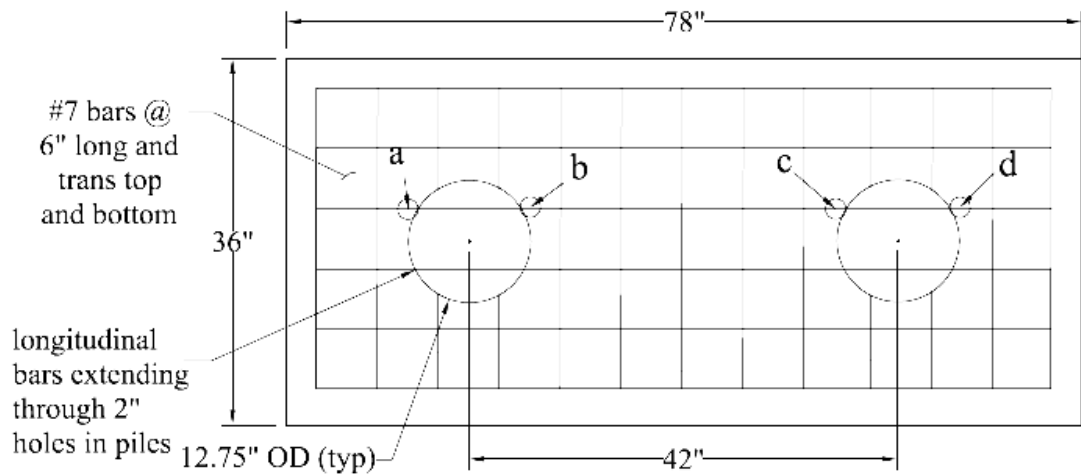


**Figure 3-5 Pile Cap plan view dimensions (typical all caps).**

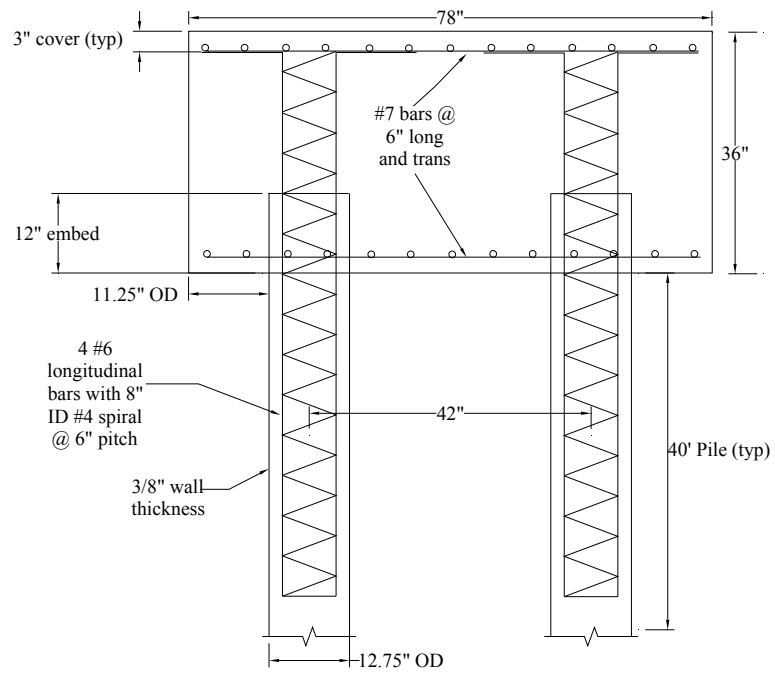
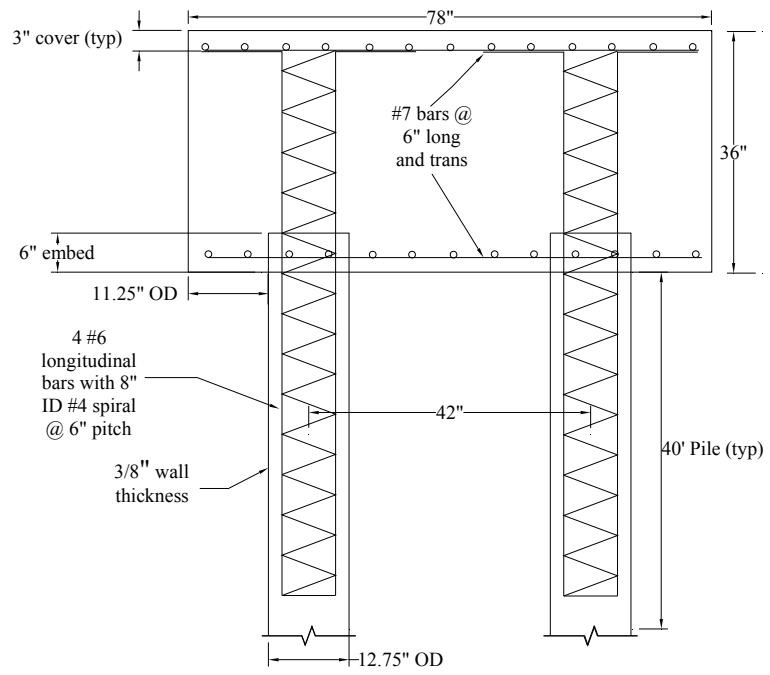


**Figure 3-6 Dimensions for Pile Cap 1 (above) and Pile Cap 2 (below).**

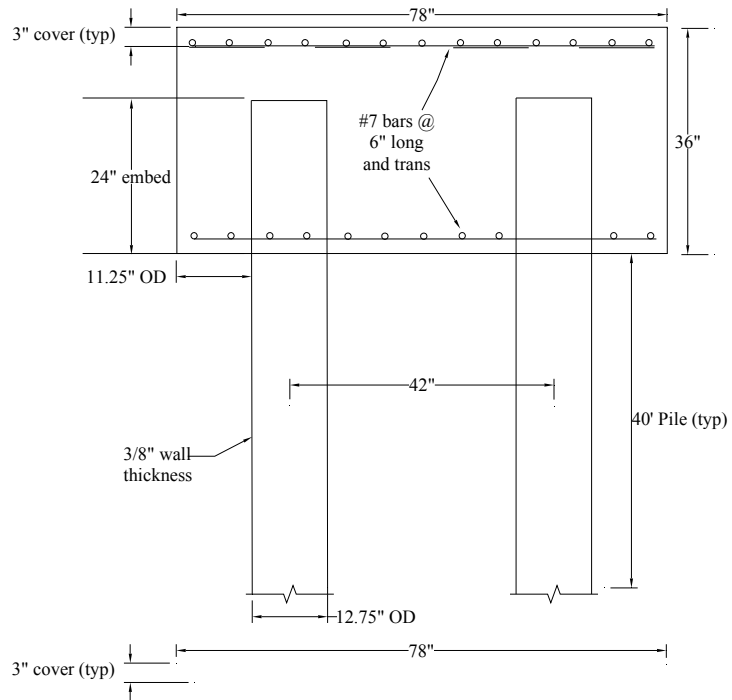
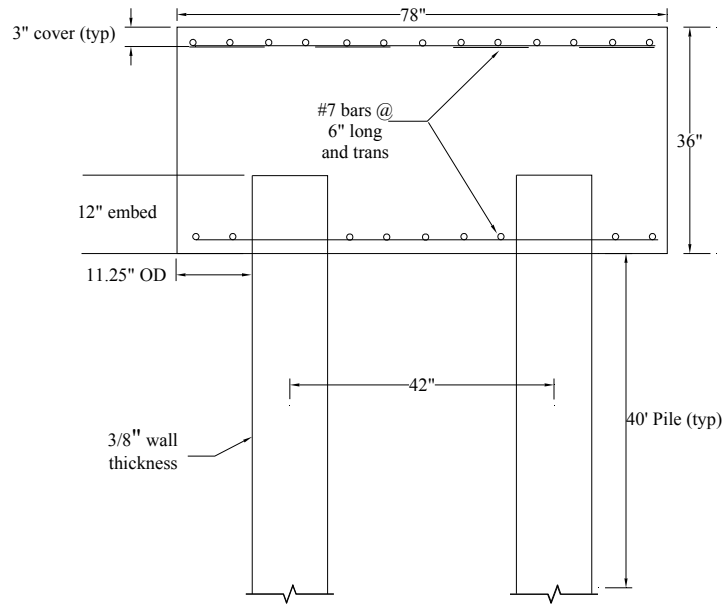


**Figure 3-7 Dimensions for Pile Cap 3 (above) and Pile Cap 4 (below).**

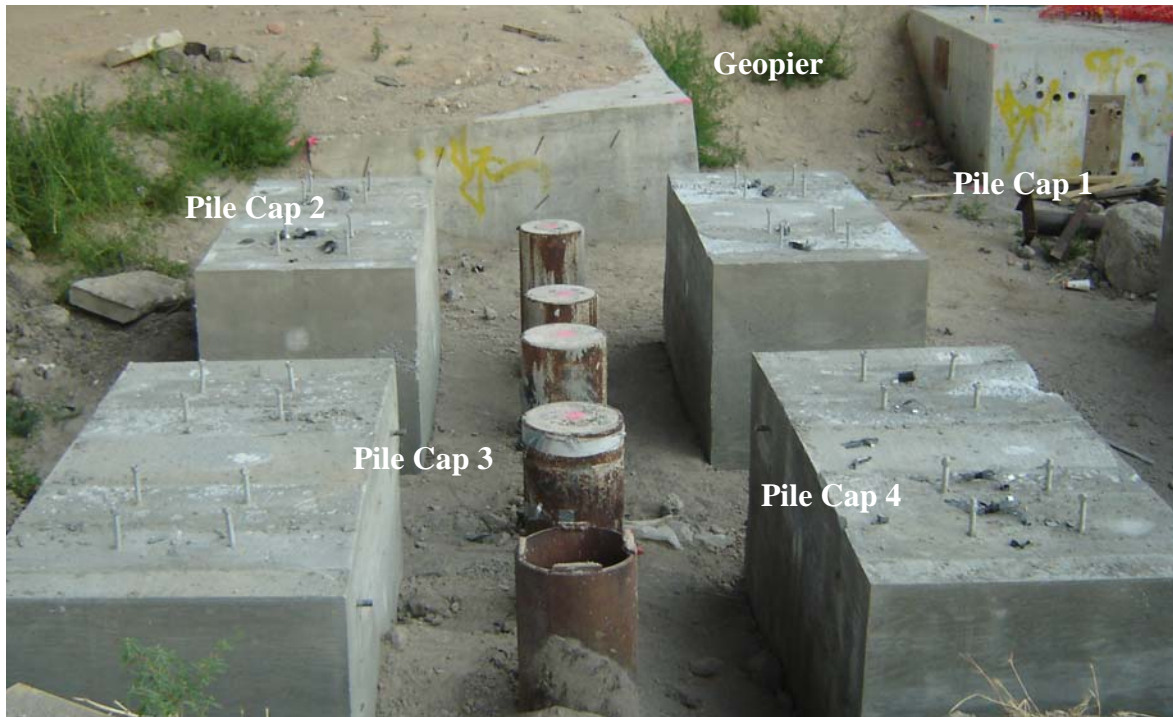


**Figure 3-8 Photograph pile caps after concrete placement but prior to testing at the South Temple, Salt Lake City Test Site.**

### **3.4 Instrumentation**

Electrical resistance type strain gauges (Texas Measurements Group type FLA-6-11) were installed on the reinforcing bars as well as on the piles. In order to properly install these strain gauges, each gauge location was thoroughly prepared by grinding, sanding, and cleaning a flat, smooth area on either the pile surface or reinforcing steel bars. Figure 3-5 shows the reinforcing grid in the longitudinal and transverse directions in a plan view. This is typical of all caps; also shown is the location of the strain gauges (a, b, c, and d) installed on the bottom grid which is also typical of all four caps. Strain gauges are represented as circles on the drawings and labeled with a letter corresponding to its respective location; this is consistent throughout this report.

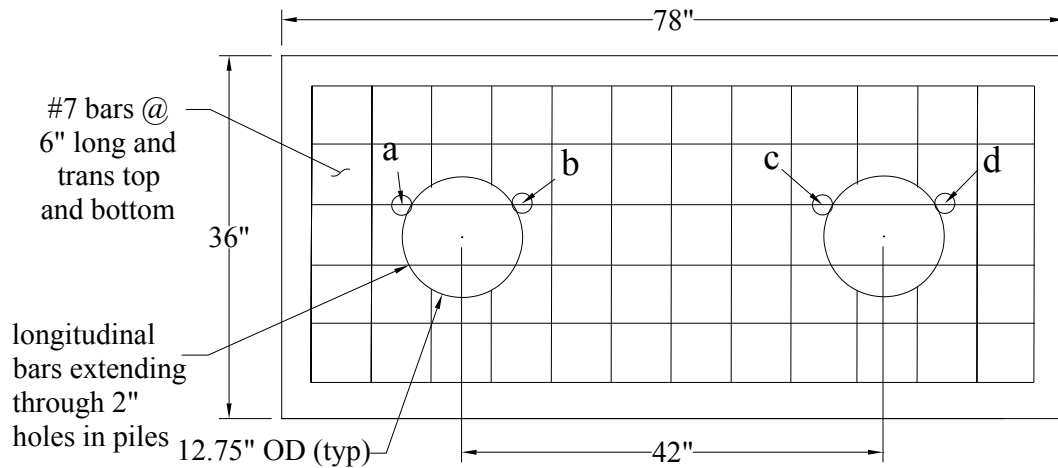
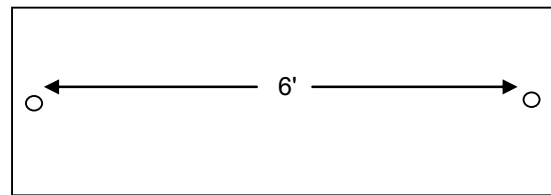


**Figure 3-9 Pile-Cap and instrumentation plan view typical all caps.**

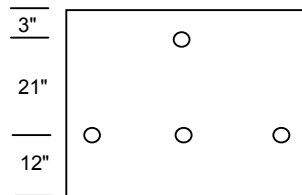
To determine the displacement and rotation of each cap as a function of the applied force, six string potentiometers (string pots) were installed on the exterior of each cap to be tested. Two were placed on the top of the cap at a center location and spaced six feet apart so that they were approximately 3 inches from the front and back edges of the cap as shown in Figure 3-10. These two string potentiometers measuring displacements made it possible to calculate the pile cap rotation.

Along the front of the cap four additional string potentiometers were installed as shown in Figure 3-10. Three were placed at the elevation of the loading point, one foot above grade with one potentiometer at the center of the cap and two spaced at a distance of 3 inches from the edge of the cap on either side. The last string pot was located 21 inches directly above the center string potentiometer which placed it about 3 inches below the top of the cap. The displacement readings of three lower string potentiometers yielded an average displacement value and provided an indication of

rotation of the cap about the vertical axis, while the difference between upper and lower displacements was used to calculate a rotation value about a horizontal axis and confirm the rotation obtained by the two string potentiometers that were placed on the top of the cap. Figure 3-11 shows a photograph of the setup of the string potentiometers. It is important to notice in the photograph that each string pot was connected to an independent reference frame that was not in contact with the pile cap, but was supported at a minimum distance of 10 to 15 feet from the test cap. This setup was the key to obtaining undisturbed displacement and rotation values.



Plan



Elevation

**Figure 3-10 String potentiometer locations (typical all caps).**



**Figure 3-11 Photograph of string potentiometers setup (typical all caps).**

#### **3.4.1 Test Layout for Pile Cap 1**

In the first of pile cap 1, an embedment length of 6 inches was provided along with a reinforcing bar connection detail consisting on 4 #6 longitudinal bars embedded 48 inches down into each pile and extending 33 inches above grade surrounded by an 8 inch diameter #4 spiral at a 6 inch pitch. Each vertical bar included a one foot section after a 90° bend which was tied to the top reinforcement grid. Both piles were filled with concrete. This is a standard UDOT connection detail and a cross section can be seen in Figure 3-12, with Figure 3-13 showing a cross section of the front elevation. A photograph of the connection provided for Pile Cap 1 is also presented in Figure 3-14. Twenty quarter bridge, resistance type strain gauges (Texas Measurements Group type FLA-6-11) were installed on Pile Cap 1: four along the bottom reinforcing grid, six on each of the vertical connecting bars, and two on each

of the piles at grade, their locations are shown in Figure 3-12. Despite preparations for protecting the gauges prior to pouring the concrete, some of the gauges malfunctioned and did not provide useable data.

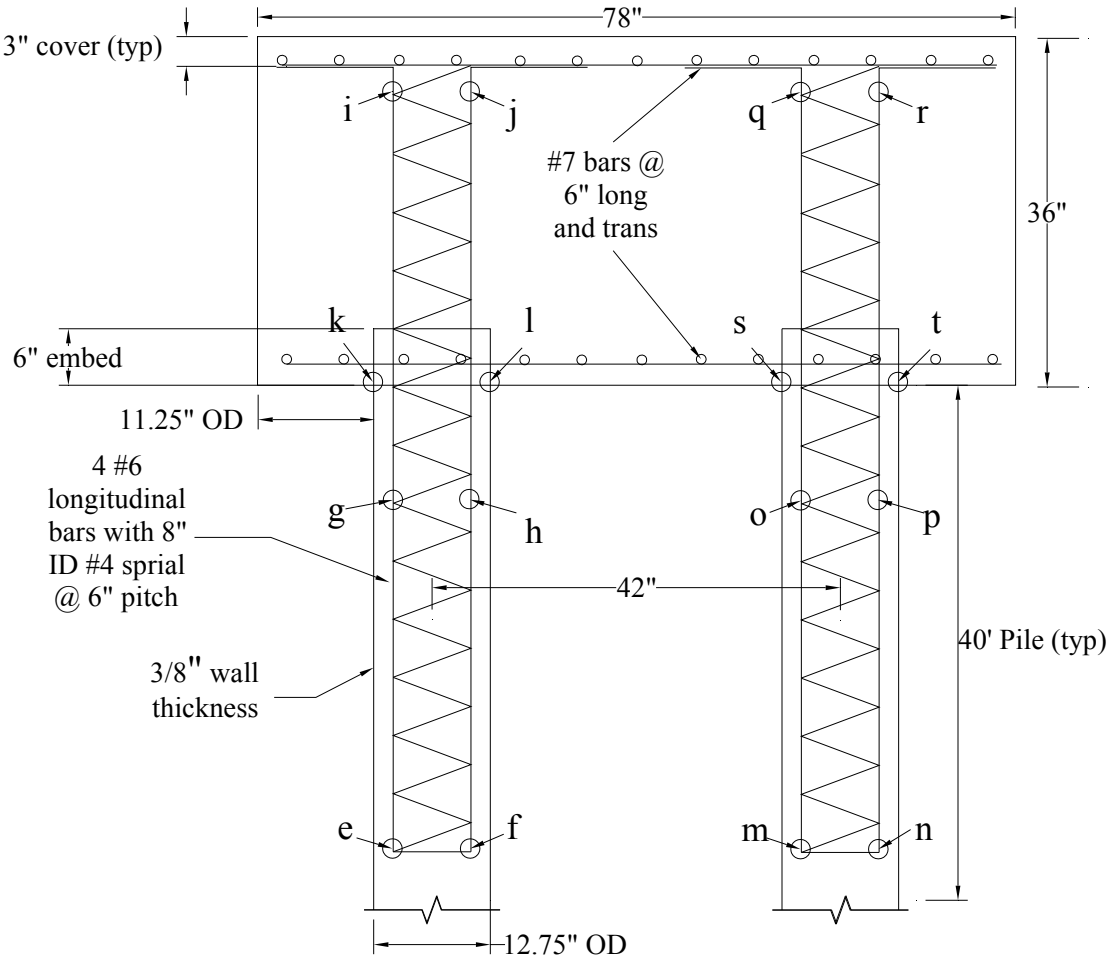
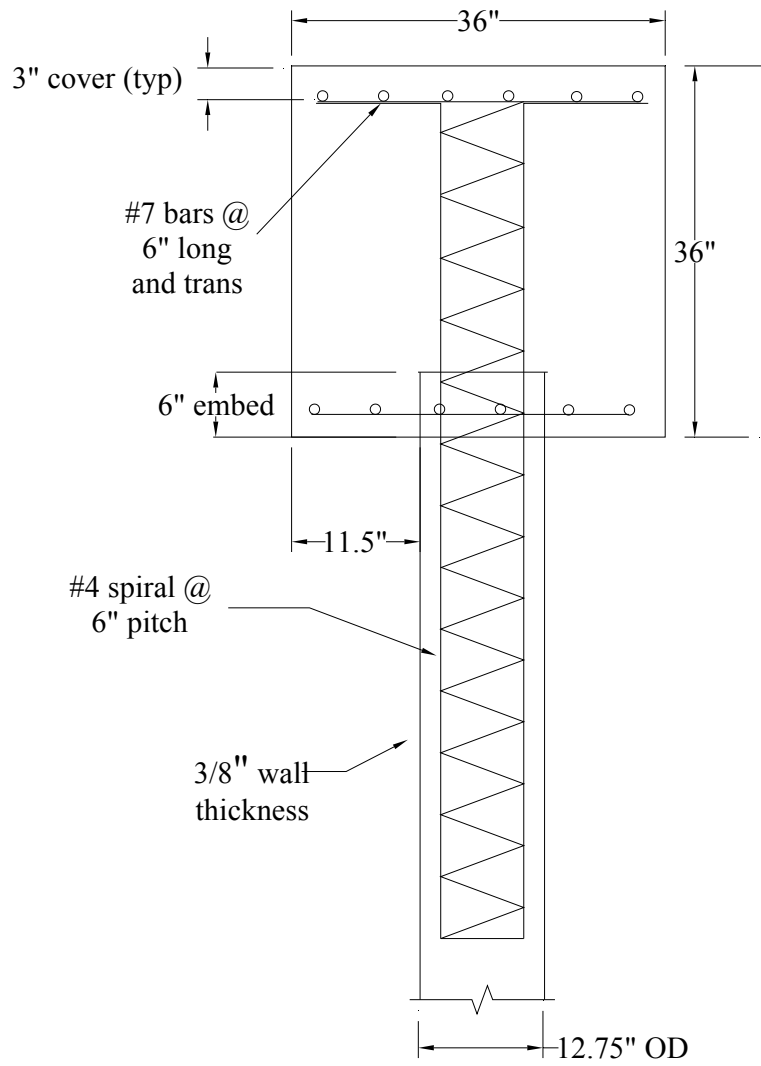


Figure 3-12 Pile Cap 1 with construction details and instrumentation layout.



**Figure 3-13 Front elevation view of Pile Cap 1.**



**Figure 3-14 Photograph of Pile Cap 1 reinforcing.**

Pile Cap 1 was approximately 8 feet from a large Geopier cap and it was therefore convenient to use the Geopier cap as a reaction for applying the load. As shown in the photo in Figure 3-15 a swivel head was attached to the back face of the pile cap with four 1 inch diameter cast-in-place all thread bolts embedded 5 inches into the cap and tied to two vertically placed rebar that were tied to the bottom and top reinforcing grids. The swivel head was then bolted to a 300 kip load cell which was in turn bolted to the hydraulic ram. The hydraulic ram was bolted to a circular steel spacer that was then bolted to the Geopier cap. Since the center of the pile cap was slightly off the edge of the Geopier cap, two angle pieces had to be attached to the Geopier cap to completely support the hydraulic ram as it connected to the cap. All of

these connections were designed so that a load of 150 kips could be applied without causing distress to any of the elements.

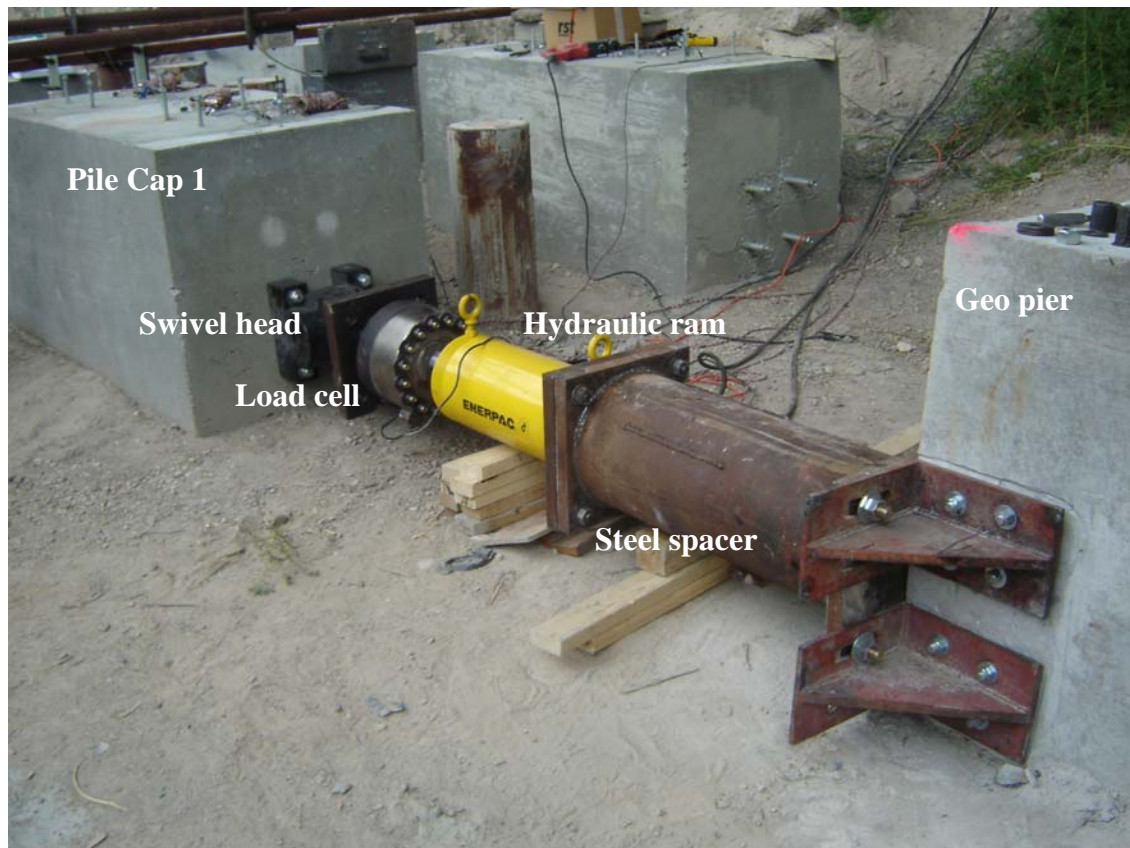


**Figure 3-15 Photograph of test set-up for Pile Cap 1.**

### **3.4.2 Test Layout for Pile Cap 2**

As shown in Figure 3-16, the connection detail for pile cap 2 was essentially the same as that for pile cap 1, except that the embedment length of the steel pipe pile was increased from 6 inches to 12 inches. Also shown in Figure 3-16 is the location of strain gauges which are identical to those for Pile Cap 1. Both piles were also filled with concrete.

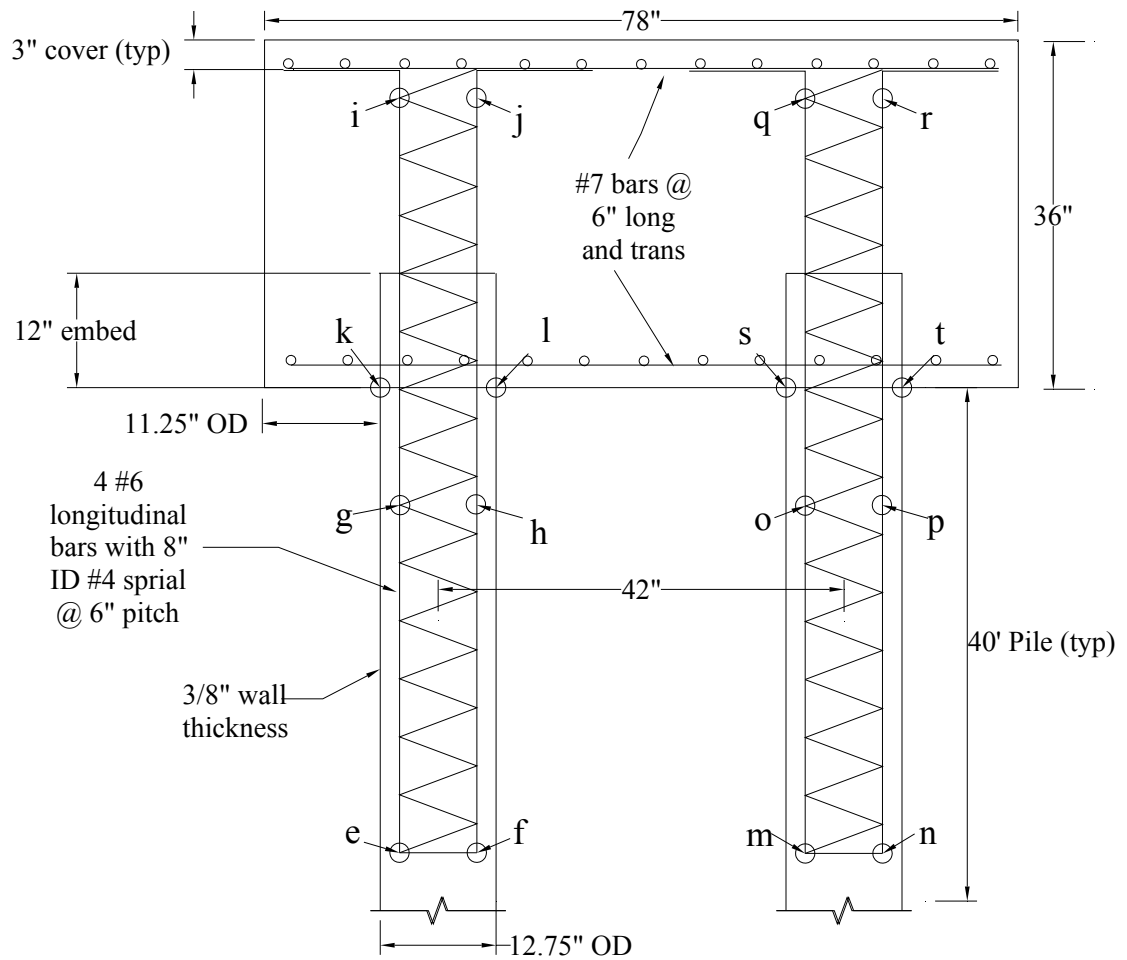


**Figure 3-16 Pile Cap 2 with construction details and instrumentation layout.**

Figure 3-17 shows a photograph of the test setup for Pile Cap 2, the same connections were utilized and the Geopier (not pictured) was used again as a reaction to counter the applied force.



**Figure 3-17 Photograph of test set-up for Pile Cap 2.**

### **3.4.3 Test Layout for Pile Cap 3**

The third pile cap also provided a 12 inch embedment length; however no reinforcing cage connection detail was provided as shown in Figure 3-18. The piles were capped off with a metal plate and remained hollow as requested by the Oregon Department of Transportation. This simulates the typical pile embedment detail used in Oregon; however, Oregon also provides additional vertical and transverse steel reinforcement to the pile cap itself which was not included in this study. This was done so that effects of pile embedment only could be isolated. Due to a lack of reinforcing detail the location of strain gauges was limited and only eight were used: four along the bottom reinforcing grid as with all the caps and four on the piles as shown in Figure 3-18.

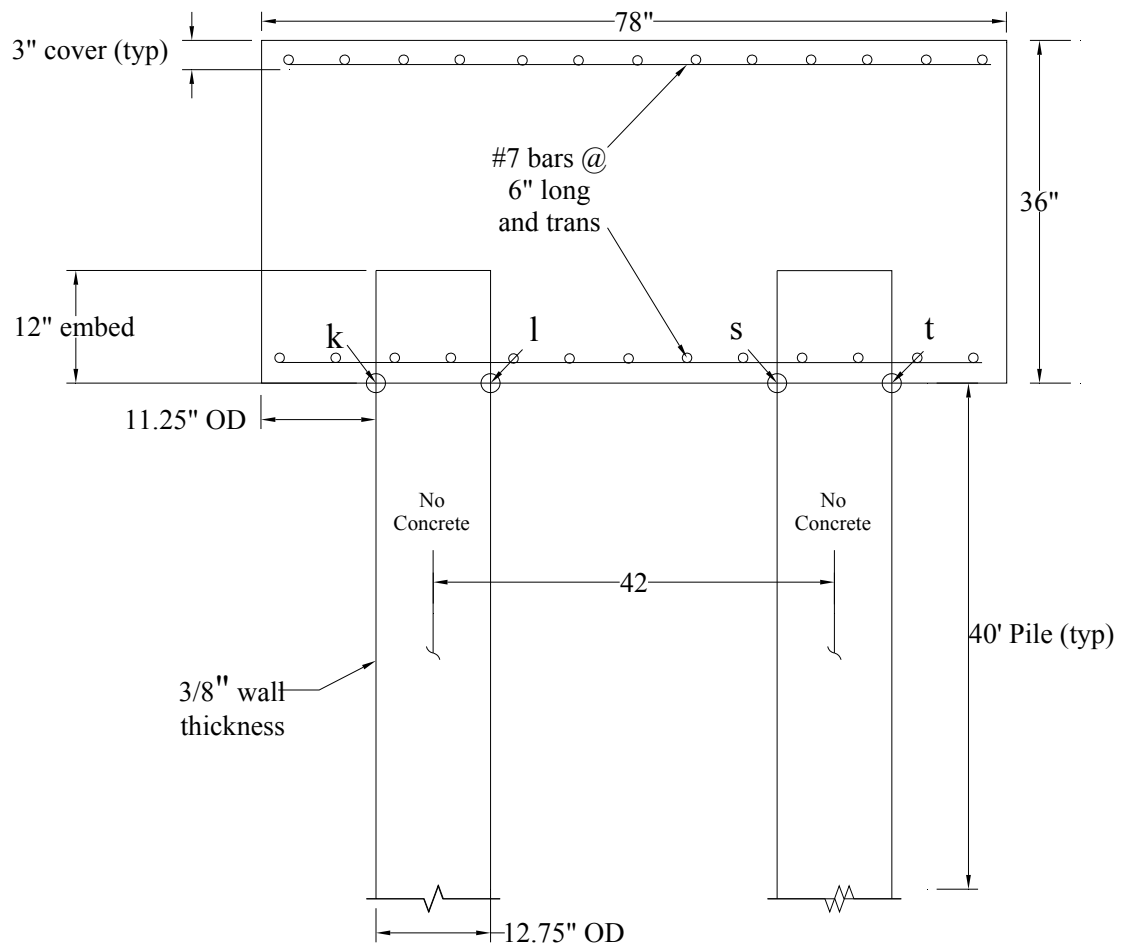


**Figure 3-18 Pile Cap 3 with construction details and instrumentation layout.**

Figure 3-19 provides a photograph of the pile cap, hydraulic ram set-up and reference frame during the test on Pile Cap 3. The Geopier cap was again used to provide the reaction for the load test by placing a steel strut between Pile Cap 2 and the Geopier Cap. Figure 3-20 shows a closer view of the test setup for Pile Cap 3

including the positions and anchoring used for the string potentiometers. A more compact swivel head was used due to the space constraints between the pile caps.

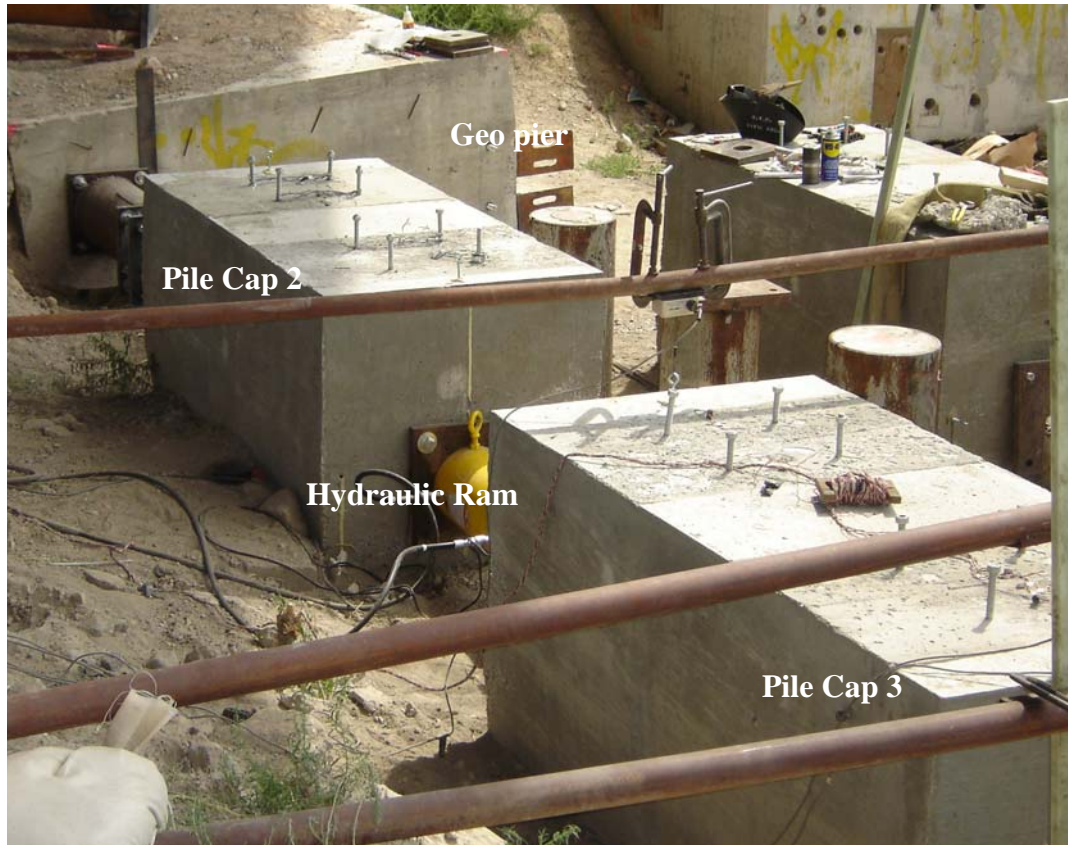


**Figure 3-19 Photograph of equipment arrangement for test on Pile Cap 3.**



**Figure 3-20 Side view of test setup prior to loading Pile Cap 3.**

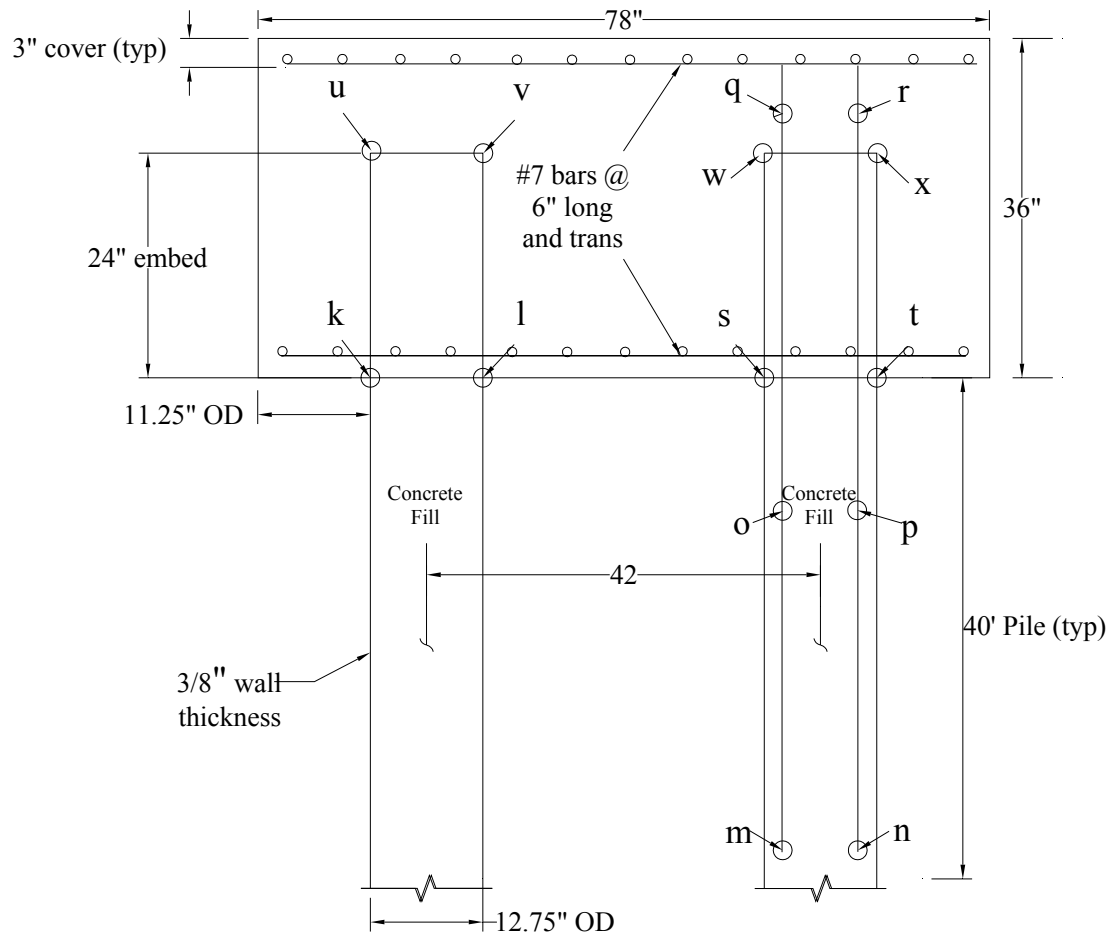
#### **3.4.4 Test Layout for Pile Cap 4**

Figure 3-21 shows the loading arrangement for the test of Pile Cap 4. A different hydraulic jack was used, and a strut was placed between Pile Cap 1 and the Geopier cap to provide the reaction for the test.

The geometry of Pile Cap 4 is shown in Figure 3-22. A 24 inch pile embedment length was provided but no reinforcing cage connection detail was included. However, both piles were filled with concrete in contrast to Pile Cap 3 where the piles were left hollow. Since the rear pile had been previously filled with concrete, strain gauges were not able to be installed.



**Figure 3-21** Photograph of test layout for test on Pile Cap 4.



**Figure 3-22 Pile Cap 4 with construction details and instrumentation layout.**

Two #6 rebar were placed in the front pile with six strain gauges attached as shown in Figure 3-22. With the increase in embedment length an additional 4 strain gauges were installed on the tops of the piles as shown in Figure 3-22.

## **4 ANALYTICAL STUDY**

### **4.1 Introduction**

Hand calculations and computer modeling were used to better understand how the pile caps would perform under lateral loads. Hand calculations were used to evaluate the potential for failure of individual elements and the computer models were used to explain the configuration as a system. Multiple failure scenarios were developed and their respective capacities determined by either hand calculations or computer modeling. In some cases, results were available from both methods and could be compared. There were two computer modeling programs available for calculations; LPILE 4.0, and GROUP 4.0. LPILE analyzes a single pile with user-defined soil and pile parameters. GROUP analyzes a group of piles with their respective soil and pile properties. Both programs account for group interaction effects as well as the pile head boundary conditions. Neither program considers the size, placement, or strength characteristics of the cap or the embedment length of the pile.

There were four major areas of concern: failure in the pile, failure in the cap, failure in the surrounding soil, and failure in the connection between the cap and pile. It was intended that failure would occur in the connection; therefore the pile and cap details were designed to both fit the criteria specified by the Utah and Oregon

Departments of Transportation as well as allow the failure modes to occur in the connection. It was predicted that even though the pile caps were to be laterally loaded that there would also be large tensile and compression forces acting on the piles and cap as well as large moments. It was therefore necessary to estimate multiple failure scenarios which will be discussed in this chapter.

#### **4.2 Failure in the Piles**

Generally, all the piles had the same material properties and geometries. The only variance was test piles for Pile Cap 3 that remained hollow while the test piles for the other pile caps were filled with concrete. Areas of concern regarding failure in the piles alone were that of excessive moments; this being the most common type of failure from testing conducted at Montana State University. The shear strength of a hollow pile was estimated to be approximately 484 kips therefore shear strength calculations with concrete and/or rebar were not necessary.

According to analyses using LPILE, the hollow pile would have a 3,100 kip-in moment capacity while the concrete filled pile would have over a 3,500 kip-in moment capacity.. Moment capacities obtained from equation 2-3 (Bruneau and Marson 2004) showed little variation from these values. Although filling the piles with concrete only increased its moment capacity by 13% it is still recommended that piles be filled with concrete to delay local buckling GROUP estimated that the largest moment would occur at grade on the front pile, and would not exceed 2,000 kip-in for a lateral load of 130 kips. GROUP accounts for rotation effects due to the pile geometry and loading. LPILE, on the other hand, estimated that with a lateral load of

130 kips the moment would exceed 3,500 kip-in assuming that the pile was in a fixed-head condition.

### 4.3 Failure in the Cap

The caps themselves are also subject to moments as well as tension, compression and shear forces. Calculations using equation 4-1 estimated the cap moment capacity to be approximately 6,000 in-kips which greatly exceeded the moment to be applied. The one way shear strength of Pile Caps 1, 2, and 4 were also predicted to exceed the stresses applied during loading and to not be a concern, the one way shear strength equation is presented in equation 4-2.

$$M_u = .9A_s f_y \left( d - \frac{A_s f_y}{1.7 f_c' b} \right) \quad (4-1)$$

$$V_n = 2\phi \sqrt{f_c'} A_c \quad (4-2)$$

However, questions remained as to how Pile Cap 3 would respond with the applied force acting in a direct line with the connection and with no vertical reinforcement to hold the cap to the pile. GROUP estimated that tensile forces within the cap would reach 80 kips. The tensile capacity of the pile cap was estimated to be 192 psi by equation 4-3. In this equation the moment (M) was taken as 280 ft-kips, I as 22.8 ft<sup>4</sup> and y as 2.25 feet. The moment was determined conservatively by multiplying 80 kips by the pile spacing of 3.5 feet, the moment of inertia (I) was determined by considering the concrete that was in direct assistance to resist the

tensile forces (3 feet wide and 4.5 feet long), and  $y$  was half of the 4.5 foot long section. Figure 4-1 is a diagram showing the forces and assumptions made in these calculations. These values should produce a conservative estimate for the tensile stress. Since this stress is considerably lower than the 400 psi tensile strength of the concrete it is expected that the cap will not fail in direct tension.

A more likely scenario would be a combination of both shear and tension. For members under combined axial and shear force loading, ACI Code modifies the ultimate shear force equation 4-2 as shown in equation 4-4. With  $N_u$  equal to a negative 80 kips and  $A_c$  equal to  $13.5 \text{ ft}^2$ , equation 4-4 yields a shear strength of 169 kips; which is also below the force to be applied.

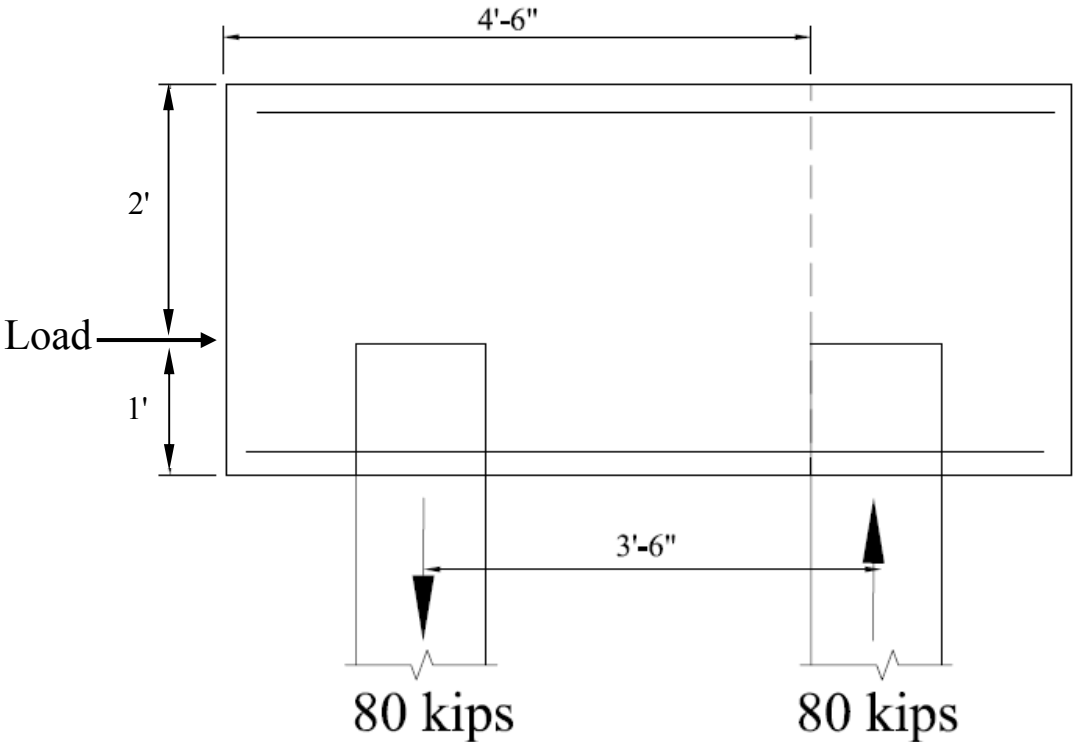


**Figure 4-1 Tensile failure analysis diagram.**

$$\sigma = \frac{My}{I} \quad (4-3)$$

$$V_n = 2\phi\left(1 + \frac{N_u}{500A_c}\right)\sqrt{f_c'}A_c \quad (4-4)$$

Although not supported on the opposite face as load is applied, the pile cap most closely resembles a deep beam. If modeled as a deep beam there is inadequate reinforcement to resist the large tensile and shear forces that may develop and a one-way shear failure is possible. There is a large amount of steel located within the cap, yet this steel including the piles are not in locations to provide direct assistance to resist a one-way shear failure.

Cracks in deep beams have been observed to occur at stresses somewhere between one-third to one-half of the ultimate strength (MacGregor and Wight 2005). To fit the criteria of a deep beam it can be assumed that the front pile is the location of the support and therefore the area of concern is only 4.5 feet long and 3 feet wide which yields a one-way shear capacity of 184 kips; one-third to one-half of this value is less than the load to be applied, and one way shear is of concern.

#### **4.4 Failure in the Surrounding Soil**

The computer modeling program GROUP proved invaluable in analyzing each test. By inputting the soil profile and each layer's respective thickness and strength properties an estimation of the soil reaction vs. length along the piles was obtained. The soil profile and properties used in analyses are presented in Figure 3-1. When

piles are driven at relatively close spacing the shear zones for adjacent piles overlap reducing the lateral resistance. Such group interaction effects are often accounted for using  $p$ -multipliers to reduce the soil resistance of  $p$  value. Using relationships developed by Rollins et al (2006)  $p$ -multipliers were estimated to be 0.82 and 0.61 for the front and trailing row piles, respectively. The unit side resistance along the length of the pile was estimated based on the undrained shear strength in the clay or the penetration resistance in the sand. Group analyses indicated that the trailing row pile would begin to pull-out of the ground when the lateral force reached about 80 kips. At a load of about 130 kips the pile cap would deflect significantly and the pile cap would have essentially failed at that point. Once a pile has displaced vertically more than 0.1 to 0.2 inch the majority of side friction is mobilized and additional loading would cause a magnification of both deflection and rotation. This appears to be an important failure mode for pile caps 1, 2, and 4.

#### **4.5 Failure in the Connection**

It was desired that failure in the connection would occur prior to any other type of failure such that a comparison between all four of the tested connections would be possible. There were also multiple types of possible failures within the connections to be considered.

##### **4.5.1 Tensile Failure of the Reinforcement**

The tensile capacity,  $T$ , of the reinforcement is given by the equation,

$$T = A_s f_y \quad (4-5)$$

where  $A_s$  is the cross sectional area of the reinforcement and  $f_y$  is the yield strength.

The connection design, consisting of 4 #6 bars with a yield strength of 60 ksi would be able to resist over 106 kips of tensile force. As shown previously, the pile would pull out of the ground at an axial load of 80 to 90 kips and therefore the reinforcement design was considered adequate.

#### 4.5.2 Reinforcement Pull-Out Failure in Pile

To develop the full tensile capacity of the reinforcing steel, the embedment length must be sufficient so that the bond strength between the concrete and the reinforcement is not exceeded. The required embedment length is known as the development length. Pile Caps 1 and 2 were considered within this scope and Pile Cap 3 and 4 while having no reinforcement connection were clearly not considered. According to ACI code provisions, the development length,  $l_d$ , is given by the equation

$$l_d = \frac{f_y d_b \alpha \beta \lambda}{25 \sqrt{f'_c}} \quad (4-6)$$

with variables as defined at the beginning of the report. UDOT has specified a development length of 4 feet for #6 bars in their connection detail; however, calculations using the ACI equation indicate that only 29 inches of embedment are required. Therefore, the 4 foot embedment depth specified by UDOT was used and considered more than sufficient.

### 4.5.3 Reinforcement Pull-Out of Cap

After determining that the reinforcement embedment into the pile exceeded the required development length it was then necessary to check the development length into the pile cap to ensure that this connection would also be adequate. Pile Caps 1 and 2 had both reinforced connections and a hook in the rebar as shown in the profile drawings. Using equation 4-7 with a #6 bar and 4000 psi concrete, the development length provided by the hook,  $l_{dh}$ , was 14 inches which is based on a bend of at least 12 bar diameters, therefore only 15 inches of additional development length is required. In order to fully develop the reinforcement the bars must extend from the piles into the pile cap 15 inches and then hook at a 90 degree angle a distance of 12 bar diameters. The design specifications that Utah DOT provides for embedment into the cap is 27 inches from the top of the pile which excludes any type of hook, therefore once again the provided details are more than adequate.

$$l_{dh} = \frac{1200d_b}{\sqrt{f'_c}} \quad (4-7)$$

### 4.5.4 Concrete Pull-Out of the Pile

Another potential failure mechanism to be considered for Pile Caps 1 and 2 is if the tensile forces within the pile exceed the bond strength between the steel pipe and the concrete infill so that the reinforced concrete section pulls out of the pile. Using a bond strength of 45 psi between a steel pipe pile and concrete infill, this failure type was predicted not to be a concern provided a monolithic pour of a minimum of 4.5

feet. The worst case to consider would be Pile Cap 1 with only 6 inches embedment which still provides 6 inches on the exterior of the pile and 54 inches on the interior extending to the tip of the reinforcing bars. This analysis indicates that before the concrete can be pulled out of the pile the reinforcing steel will yield.

#### **4.5.5 Bond Strength between Exterior of Pile and Concrete**

Pile Caps 3 and 4 did not have a reinforced connection detail and with such high axial loads to be considered it was necessary to calculate a possible slipping to occur between the exterior of the pile and the surrounding concrete. Pile Cap 4 had two differences compared to Pile Cap 3. First, the concrete in the pile and cap were poured monolithically providing added strength and second the embedment length was 24 inches which was twice as long as for Pile Cap 3. Using the same conservative value of 45 psi for the steel to concrete bond strength, the capacity of the interface for Pile Cap 4 was found to be 90 kips; this includes the bond strength around the perimeter of the pile. This load is close to the ultimate side friction capacity of the pile although with the very low bond strength value of 45 psi used in the calculation, this failure mode is not considered to be of high concern. These same calculations suggest that the interface capacity for Pile Cap 3 would be only be 50 kips. Therefore, failure at this interface could occur before the pile pulls out of the ground. However, these calculations did not account for the influence from the bottom reinforcing grid which includes the pile cap longitudinal bars extending into the piles through 2 inch holes; this is expected to provide additional pull-out resistance.

#### 4.5.6 Bearing at Connection Interface

The calculations influenced by the embedment length were that of excessive bearing at the embedment interface. As shown in the literature review, several of pile cap tests showed extensive failure in this region. The photograph in Figure 4-2 is presented to show how many of the tests previously conducted have failed in the connection area due to concrete crushing and/or bearing failure (Stephens and McKittrick, 2005). Tests conducted in this study are different in that the pile cap was not completely fixed against rotation as was the case with the laboratory tests, such as those conducted by Montana State University. Other steel to concrete connection tests, such as those performed by Marcakis and Mitchell (1980) and Mattock and Gaafar (1982), also fixed the embedment region while applying the force at some distance away from the connection such that a large moment could be developed at the interface. Based on tests of brackets, Mattock and Gaafar (1982) developed the equation below to predict the ultimate shear force that could be applied for an embedment depth,  $L_e$ .

$$V_u = 54\sqrt{f'_c}\left(\frac{b'}{b}\right)^{.66} \beta_1 b L_e \left[ \frac{.58 - .22\beta_1}{.88 + \frac{a}{L_e - c}} \right] \quad (4-8)$$

Using equations 2-1, 2-2, and 4-8 the required embedment lengths as a function of applied load have been computed and the results are presented in Figure 4-3. As noted previously, the equations used to develop Figure 4-3 were developed through a series of tests in which the embedded steel received the force while the

concrete in which the steel was embedded remained fixed. However, in the field tests the load on the pile is actually distributed over a length rather than being applied at a single point as in the lab testing. To provide an equivalent moment arm, the computer program GROUP was used to compute the maximum moment and shear force at the base of the pile cap and the maximum moment was divided by the shear force to determine the point of action for the force. An alternative approach would be to use the computer program to find the distance to the point of zero shear force in the pile. As it turns out, both approaches yield a reasonably similar results.

As shown in Figure 4-3, all the equations show inadequate embedment for Pile Cap 1, which only a 6 inch embedment length, when lateral load exceed 20 to 40 kips. Therefore, a bearing failure in the pile cap would be expected. In addition, for applied loads greater than about 80 kips the equations predict that Pile Caps 2 and 3, both with 12 inches of embedment length, would also be close to failure.

It should, however, be noted that these equations do not account for the additional moment capacity which could be provided by a flexural mechanism as was observed in several of the laboratory tests involving piles with shallow embedment (Xiao 2003 and Xiao et al 2006).



Figure 4-2 Failure of pile caps tested at Montana State University.

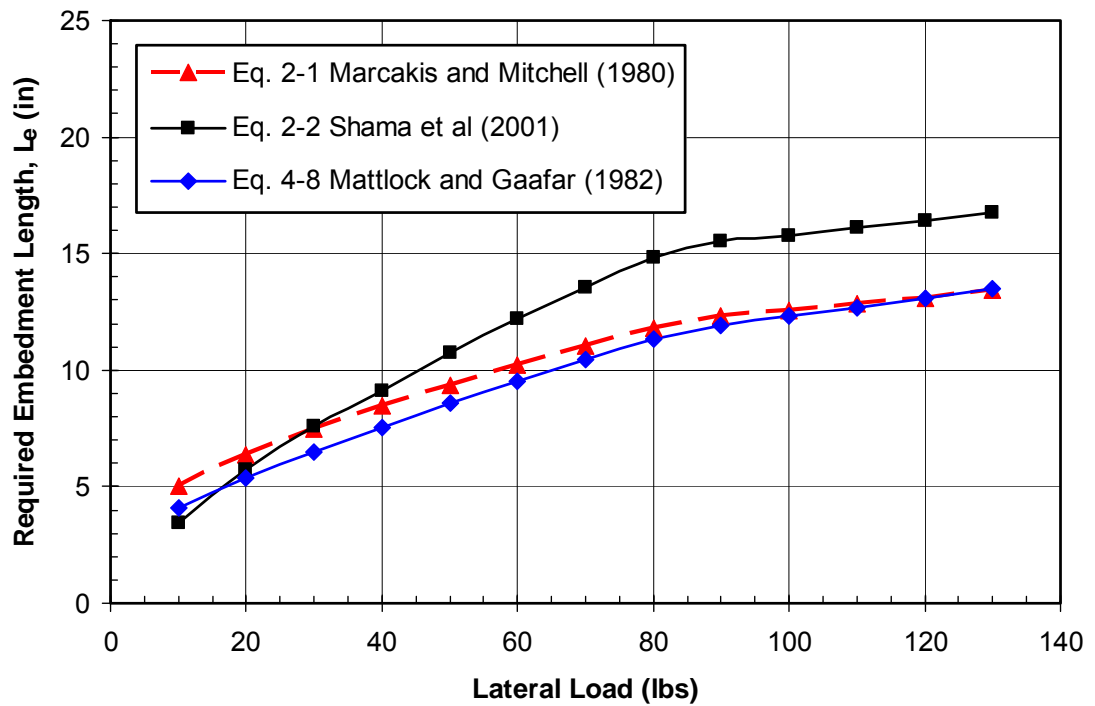


Figure 4-3 Required embedment using moment and load from GROUP.

#### **4.6 Rotational Restraint**

In general, it is desirable to determine accurately the boundary conditions of the connection in order to properly design and/or analyze the connection between the pile and the cap. In terms of stiffness, it is desirable to achieve a fixed head condition such that zero pile head rotation occurs, yet this is seldom achievable in practical cases. In contrast, a free-head or pinned connection which allows full pile head rotation is seldom seen in practice and assuming this boundary condition could result in a very costly over design. On the other hand, assuming a completely fixed condition when it is really not the case, could have the opposite effect which would lead to under design and hence an increased potential for failure. As indicated in the literature review, Mokwa and Duncan (2003) developed a method to calculate the rotational spring stiffness of a pile head for pile caps which are intermediate between fixed-head and free-head boundary conditions. Using Mokwa and Duncan's method, a value  $K_{M\theta}$  of 90,859 kip-ft was determined and was used as an input in the computer modeling program GROUP. This value, as will be seen further on in this paper, was found to produce results which were very similar to a fixed head condition and also very accurate regarding deflection and rotation compared to the data observed during testing.

#### **4.7 Summary of Predictions**

After conducting this analytical review, predictions can be made regarding each pile cap test. A failure would be expected in the connection for Pile Cap 1 at a relatively small lateral load ranging from 20 to 40 kips, assuming that the concrete cover spalls off. Connection failures would also be expected in Pile Caps 2 and 3 at higher lateral loads just about the time that the rear piles start pulling upward. Although flexural capacity might help increase the moment capacity of Pile Caps 1 and 2, there is no reinforcement to increase moment capacity in Pile Cap 3. In addition, if Pile Cap 3 acts as a deep beam, shear failure could occur at the elevation of the tops of the pile. The pile embedment of 24 inches for Pile Cap 4 should be sufficient to prevent failure in the pile cap; however, the back pile would be expected to pull out of the ground at higher load levels.

## **5 TEST RESULTS**

### **5.1 General Remarks**

All of the full-scale pile to pile cap tests conducted previously have been laboratory tests where most problems can be observed and corrected relatively easily. Field testing is more challenging, yet can potentially produce more valuable data because the test conditions are closer to actual conditions. Each lateral load test utilized a hydraulic ram to produce the lateral force which pushed the pile cap at a predetermined location one foot above grade. Five load cycles were applied at each deflection increment with slight variances that are noted. Three types of instrumentation were used for gathering data: string potentiometers to measure the amount of displacement, strain gauges to measure the amount of strain, and a load cell to determine the applied force. Each test lasted an average of 90 minutes due to the loading sequence as well as inspections of equipment and the pile cap.

The behavior of each pile group was predicted using the computer programs LPILE and GROUP. The soil input parameters used in the analyses were summarized in Section 3.1 and the pile material properties were defined in Sections 3.2. Analyses were performed using free-head, fixed-head and elastically restrained pile head boundary conditions. Because GROUP does not account for connection stiffness, the computed pile group response was the same for all four pile caps.

## **5.2 Pile Cap Test Results**

Contrary to expectations, the pile to pile cap connection details for Pile Caps 1 and 2 performed very well. No cracking or other distress was observed in these pile caps during testing. At higher load levels the rear piles began to pull out and lateral pile cap deformations became excessive. In contrast, Pile Cap 3 experienced connection failure which led to cracking throughout the length of the cap while both piles remained in the ground with no noticeable movement. Pile Cap 4 performed as expected with no distress to the pile to pile cap connection. A detailed summary of the results from each of the four tests is provided in the subsequent sections of this report. In addition, the measured results are compared with predicted behavior using GROUP and other analyses.

### **5.2.1 Pile Cap 1**

As indicated previously, the connection detail for Pile Cap 1 consisted of a pile embedded 6 inches into the cap along with a reinforcing cage which extended to the top of the cap. Full details and specs for pile cap 1 are provided in Chapter 3. As shown in the load versus time plot presented in Figure 5-1, the load test was performed using nine load increments. The initial applied load was selected to obtain deflection increments of about 0.25 inch for deflections less than 1 inch and at deflection increments at 0.5 inch at higher deflection levels. At each increment, four additional cycles of load were applied using a “load controlled” approach where cycles were applied to a specified load as shown in Figure 5-1 after which the load was decreased to zero. Prior to loading to the next desired increment, the pile cap was

pulled back, as close as possible, to its initial position. This general cyclic loading procedure was continued on all four tests.

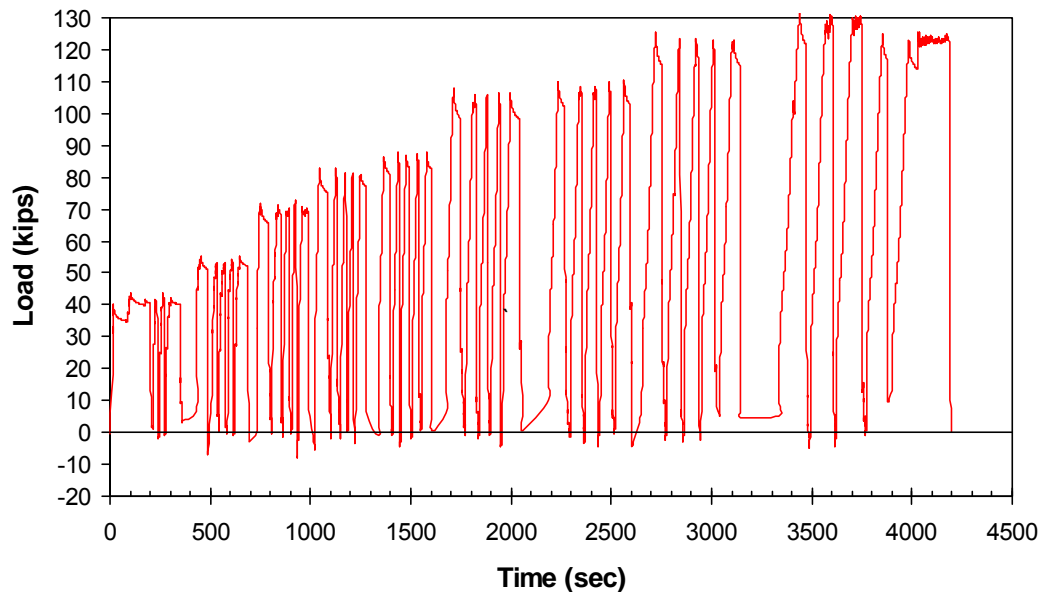


**Figure 5-1 Pile Cap 1 load vs time plot showing loading sequence.**

Figure 5-2 shows a plot of the complete load-deflection curve during the load testing. In the test on Pile Cap 1, the pile cap was repeatedly loaded to a specified load with each cycle at a given increment. Unfortunately, progressively higher deflections were achieved with each load cycle and eventually the load would produce a deflection which exceeded the subsequent target deflection level for the next increment. The progressively increasing deflection at a given load is evident in Figure 5-2 particularly at higher levels. To prevent this from occurring in future tests, a deflection control approach was adopted for subsequent tests in which cycles were applied to a given deflection rather than a given load.

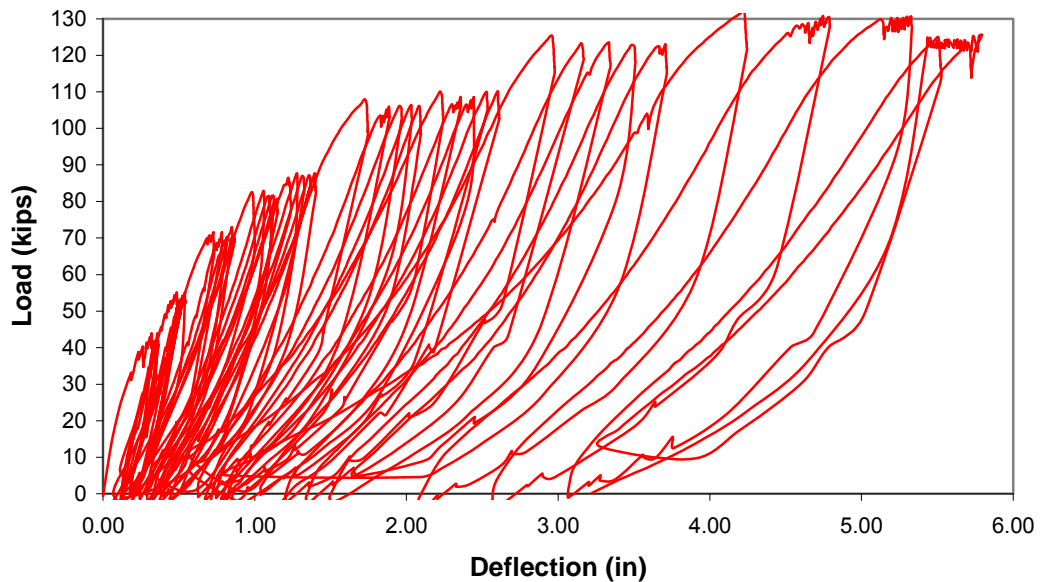


**Figure 5-2 Complete cyclic load vs. deflection curves for Pile Cap 1.**

The peak load versus deflection curves for the first and fifth cycle of loading are presented in Figure 5-3. Typically the decrease in load for a given deflection level was between 5 to 15%. Figure 5-3 also provides load vs. deflection curves computed using GROUP with three pile head boundary conditions, namely; fixed head, elastically restrained, and pinned. The value for the rotational stiffness in the elastically restrained case was calculated using equations developed from Mowka, and Duncan (2003) and was considered to be the most accurate for analysis. Nevertheless, the two curves for the fixed-head and elastically restrained pile head condition are relatively similar in this case. The percent error between the measured and computed load was typically less than 5 to 10% for a given deflection for Pile Cap 1. The

discrepancy between the measured and computed load-deflection curves appears to increase somewhat at the higher load levels (>100 kips).

The computed load vs. deflection curve for the free-head boundary condition is much flatter than the measured curve and highlights the error which could occur if the improper boundary condition were used in design.

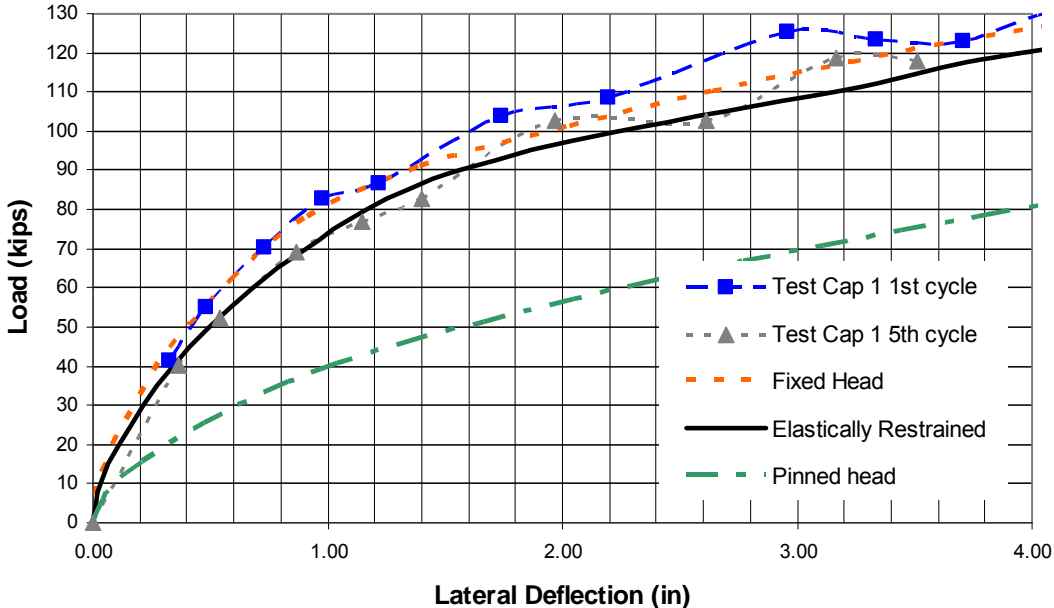


Figure 5-3 Comparison of measured and computed load vs. deflection curves for Pile Cap 1

The measured rotation versus load curve for the first cycle of loading is plotted in Figure 5-4. The rotation was calculated using the deflection measured by the string potentiometers located strategically on both the top face and front face of the cap. Unfortunately, string potentiometer 11 malfunctioned, which was not noticed until all four tests were completed. Therefore, wherever string potentiometer 11 was installed, the corresponding data had to be discarded. During testing of Pile Cap 1 this string

potentiometer was positioned on the top face of the cap. Therefore, rotation ( $\Theta$ ) was computed using the deflection data on the front face of the cap using the equation

$$\theta = \arctan\left(\frac{X_1 - X_2}{L - \delta_v}\right) \quad (5-1)$$

where  $X_1$  and  $X_2$  are the deflections on two adjacent string potentiometers,  $L$  is the distance between the two string potentiometers, and  $\delta_v$  is the vertical translation of the string potentiometers. In equation 5.1,  $L - \delta_v$  is used rather than  $L$  to correct for string pot displacements caused by vertical translation as illustrated in the drawing in Figure 5-5.

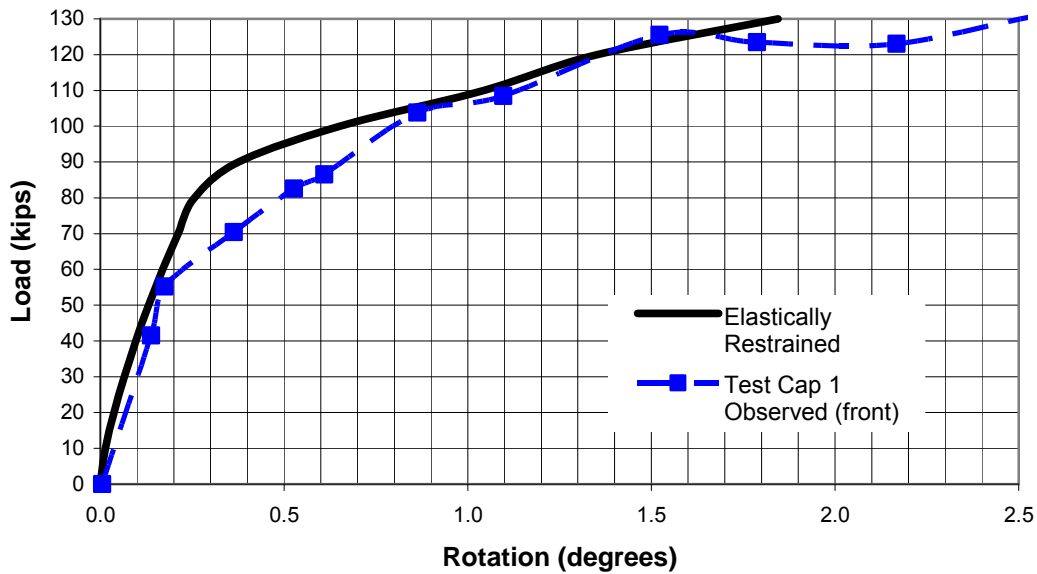
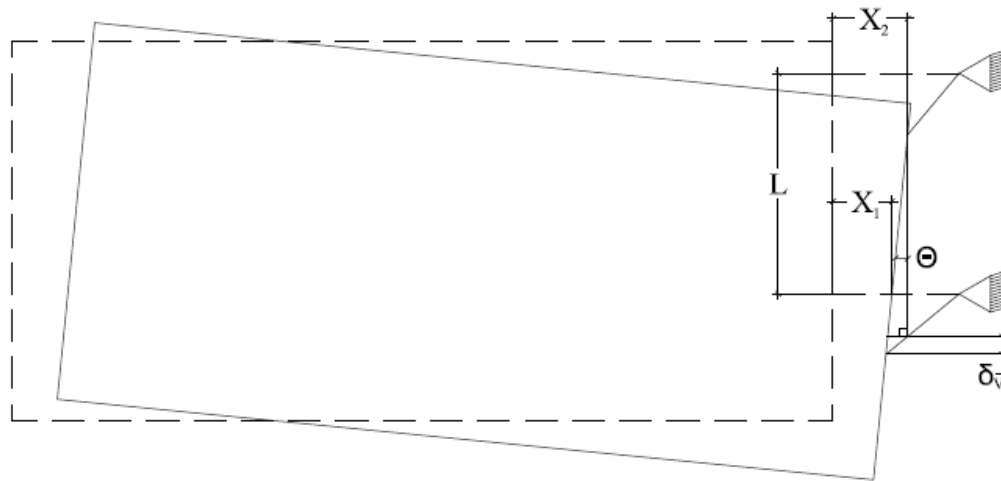


Figure 5-4 Comparison of measured and computed load vs. rotation curves for Pile Cap 1.

The measured load vs. rotation curve is also compared with the curve calculated using GROUP in Figure 5-4. Generally, the agreement is very good. As GROUP predicted, pile cap rotation increased significantly at a lateral load of 80 kips as was observed in the experimental data.



**Figure 5-5 Drawing showing arrangement of string potentiometers used for pile cap rotation.**

Both the load versus deflection and the load versus rotation curves remained approximately linear until a load of about 80 kips was reached. At this point, a shear crack was observed radiating outward at about a 45 degree angle from the back pile. At this point the uplift force on the back piles apparently began to exceed the side resistance between the pile and the soil. Soon after this, increased rotation and deflection were observed as shown in Figures 5-3 and 5-4.

The strain gauge readings on a reinforcing bar on the back pile are plotted in Figure 5-6. The tensile strain in the back pile also increased significantly as the lateral load increased to 100 kips. This behavior is consistent with an increase in axial pile force which led to pile pullout. Although the strain level is far below the tensile

capacity of the bars, Figure 5-6 confirms the need for some type of connection between the pile and cap. It explains that as the load is transferred, the reinforcing bars pull the pile out of the ground. As will be shown later in this report, if a proper connection is not provided, the pile cap rotates while the pile remains in the ground with little or no disturbance to the piles. No evidence of cracking or distress was observed in the pile cap connection and the pile did not appear to pull out of the cap despite predictions from equations 2-1, 2-2 and 4-8 as discussed previously. It was thus concluded that the connection detail was adequate for the shear and moment levels reached during this test. While the pile cap and connection remained essentially elastic throughout the loading sequence, the pile cap failure was considered to fall under the category of excessive deflection under load. This was due to the piles pulling out of the ground as shown in the photograph in Figure 5-7.

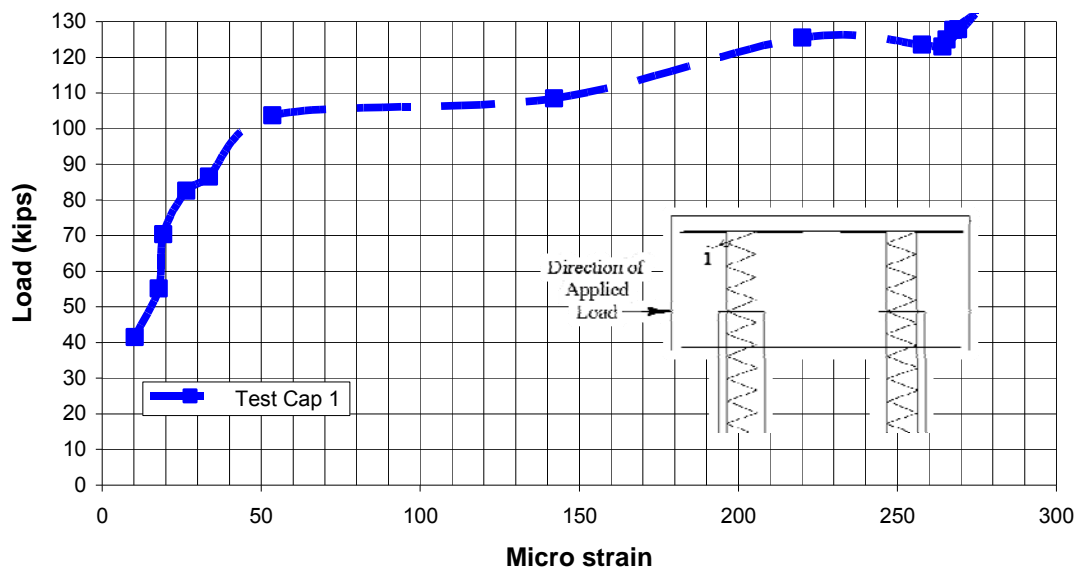


Figure 5-6 Observed micro strain at location i on vertical reinforcement.



**Figure 5-7 Photograph of Pile Cap 1 at failure showing uplift of the back pile.**

### **5.2.2 Pile Cap 2**

The pile to pile cap connection for Pile Cap 2 varied from Pile Cap 1 only in the embedment length of the piles. In Pile Cap 2 the piles were embedded 12 inches into the cap rather than 6 inches as in Pile Cap 1 (refer to chapter 3 for Pile Cap 2 details and specs.) The measured load-deflection curve from the test on Pile Cap 2 is shown in Figure 5-8. It was expected that Pile Cap 2 might experience smaller deflections and rotations due to the increased embedment, however this was not the case. For a given load, slightly larger deflections were observed for Pile Cap 2 relative to Pile Cap 1. Nevertheless, the two load versus deflection curves were still

within about 5% of each other. Therefore, the differences could have been a combination of other scenarios ranging from imperfections in construction, slightly different soil parameters or the different loading scenario. The decrease in peak lateral resistance from the first to the fifth cycle

Also shown in Figure 5-8 is the predicted load-deflection computed by GROUP. The same general trends are observed as with Pile Cap 1. Initially, the response is relatively stiff and linear and the deflections are small. However, at a load of about 80 kips there is a significant change in slope as the back pile begins to pull out of the ground at which point the lateral deflections increased. The load-deflection curve observed during the test on Pile Cap 1 was slightly higher than predicted by GROUP while the curve for the test on Pile Cap 2 was slightly lower. However, the percent difference in load predicted by GROUP for a given deflection for Pile Cap 2 was typically less than about 5% as was the case for Pile Cap 1.

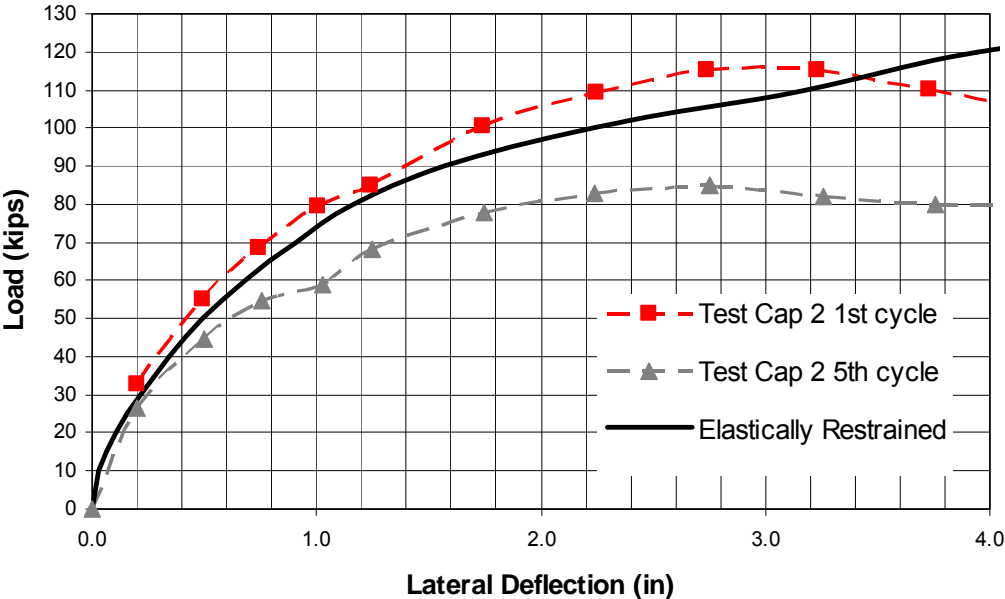


Figure 5-8 Comparison of measured and computed load vs. deflection curves for Pile Cap 2.

Figure 5-9 shows the observed rotation of Pile Cap 2 as a function of load. Rotation was computed using two string pots on the top face and two string pots along the front face and the agreement between the two measurements is consistent and reasonably good. Figure 5-9 shows plots of load versus rotation from both sets of string pots. Small rotations were again observed until 80 kips at which point the piles began to lose side friction and the amount of rotation was magnified. The measured load versus rotation curves again compare favorably with the curve predicted by GROUP. It is important to note how similar all three of these curves are to each other and that they are slightly lower than what was observed with Pile Cap 1.

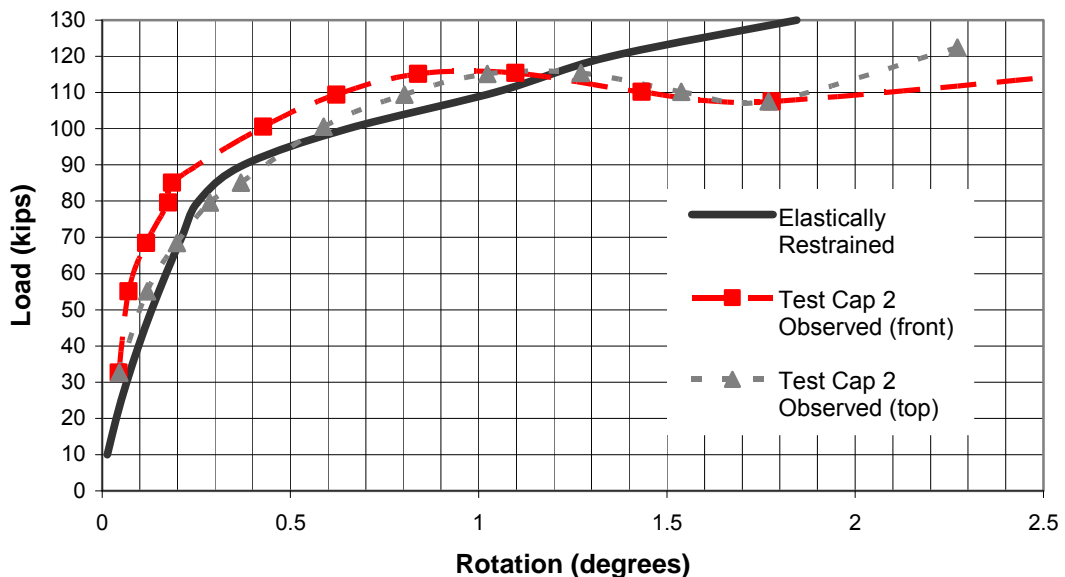
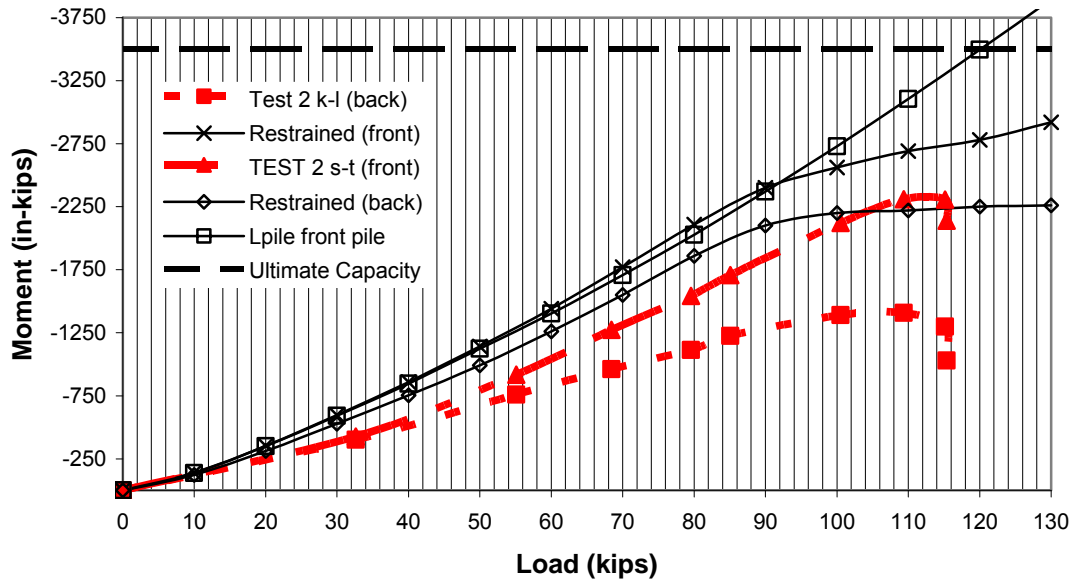


Figure 5-9 Pile Cap 2 observed vs. estimated rotation.

Plots of maximum negative moment versus load at the base of Pile Cap 2 are presented in Figure 5-10 based on strain gauge measurements. Figure 5-10 shows five

different curves and one horizontal line that represents the ultimate capacity of the pile. The two solid curves represent the maximum negative moment predicted by GROUP for the front and back row piles, the two dashed lines represent the observed moments from Pile Cap 2 derived from the strain gauges, and the black dashed line represents what was predicted by LPILE. It should be noted that the front pile was both predicted and observed to develop a larger moment for a given load. The agreement between measured and predicted moment is reasonably good until the load reaches about 80 to 90 kips. This is the load at which GROUP predicted uplift to begin to cause failure. LPILE on the other hand does not predict failure even when the moment capacity is exceeded by the applied moment; it continues to predict an approximate linear curve. It is noted that LPILE only analyzes a single pile and does not account for axial uplift. In addition, to determine the moments shown in Figure 5-10 for a group of two piles, equivalent lateral forces were determined from GROUP and these respective forces applied to a single pile model in the LPILE program.

Both the computed and measured moments are still less than the ultimate moment capacity for the pile. Therefore, the connection capacity was not fully developed. Nevertheless, the connection performed better than would have been expected based on Eqs. 2-1, 2-2, and 4-8.



**Figure 5-10 Computed and measured maximum negative moment vs load at grade.**

As shown in Figure 5-10 the observed moments varied quite significantly from the prediction by GROUP once the back pile began to lift up and cause the cap to rotate. As shown, LPILE does not predict this sort of failure since it only analyzes a single pile and does not account for uplift. Therefore, the moment versus load curve is a relatively linear curve as shown in Figure 5-10. GROUP does predict this rotation and failure scenario and as shown predicts that once the piles began to uplift and rotate significantly that the moments only gradually increase rather than continue this linear relationship as was observed.



**Figure 5-11 Pile Cap 2 failure in pullout.**

There was some question on the mode of failure. While it was considered that the piles pulled out of the ground, another possibility was that the piles remained in the ground and the concrete lost its friction with the pile and slipped. Figure 5-11 shows a close up of the back pile for Pile Cap 2. It is seen here that a cavity was formed around the pile and that it did indeed pull out of the ground. There is no evidence of slippage between the pile and the cap. It was observed during both the loading and unloading parts of each cycle that the pile and cap remained completely connected with one another.

### **5.2.3 Pile Cap 3**

As explained in Chapter 3; Pile Cap 3 and Pile Cap 4 did not have a reinforcing bar connection detail; rather, their connection capacities were dependent upon their respective pile embedment lengths. For Pile Cap 3 the pile was embedded

one foot into the cap while for Pile Cap 4 the pile was embedded 2 feet. From a construction and economics standpoint, it would be desirable if these two connection details could provide the same or similar capacities to that measured for the connection details involving reinforcing cages. In the field, construction is much simpler and less expensive if the reinforcing cage connection is left out and only a minimum embedment length is provided.

Another important fact to reiterate is that Pile Cap 3 not only lacked the reinforced connection detail but also the piles remained hollow (refer to Chapter 3 for Pile Cap 3 specs). Although filling the pile with concrete would improve its moment capacity, the pile was left hollow to simulate typical practice by the Oregon DOT which does not fill the piles with concrete.

The same basic loading sequence used for the tests on Cap 1 and Cap 2 was followed for Pile Cap 3 with one exception. As cracking developed at the elevation at which the force was applied, a significant amount of concern arose. It was feared that the connection of the loading equipment to the pile cap would fail if the pile cap were pulled back to its initial position prior to loading to the next deflection target. Therefore, after a zero load was registered, the applied load was increased to the next target deflection.

As indicated previously, less data was collected from this test than for the other caps because without a reinforcement detail only a few strain gauges were able to be installed and half of them failed either during construction or during loading. Nevertheless, sufficient basic information was obtained to help understand the behavior of the test cap.

During the first push of the 5<sup>th</sup> load increment corresponding to 1.25 inches deflection and 80 kips of lateral force, a loud popping sound was heard. Observations indicated that a crack had developed along the front of the pile cap and approximately one foot above grade as shown in Figure 5-12. The combined shear and tensile forces apparently developed within the cap and exceeded the concrete capacity in the absence of vertical reinforcing steel. Without this vertical steel, the stresses resulted in a shear crack due to a block failure.

During the next load increment, at approximately 90 kips, another popping sound was heard and additional cracks were noticed. These cracks began near the top of the back pile and propagated across the cap at the same elevation as the top of the embedded piles. The crack then joined the previous crack near the front of the pile cap. The new crack on the back and side of the cap can be seen in Figure 5-13. Again it appears that the applied force exerted by the hydraulic ram was not transferred to the pile as it was during the other tests due to the lack of vertical reinforcement with the center section of the pile cap. The cracks shown in Figure 5-13 continued to propagate until failure occurred as shown in Figure 5-14.

The load versus deflection curve observed during testing of Pile Cap 3 is shown in Figure 5-15. Despite the cracking and shear failure exhibited in this test, the load-deflection curve is surprisingly similar to that for the other tests. With the excessive amount of cracking it appeared that the back pile did little in resisting deflection, yet either the front pile compensated or the remaining concrete was sufficient to transfer load between the two piles. The cracking occurred at the location



**Figure 5-12 Initial cracking on the front face and side of Pile Cap 3.**



**Figure 5-13 Cracking at a 90 kip load on the back and side of Pile Cap 3.**



Figure 5-14 Shear crack in Pile Cap 3 at failure.

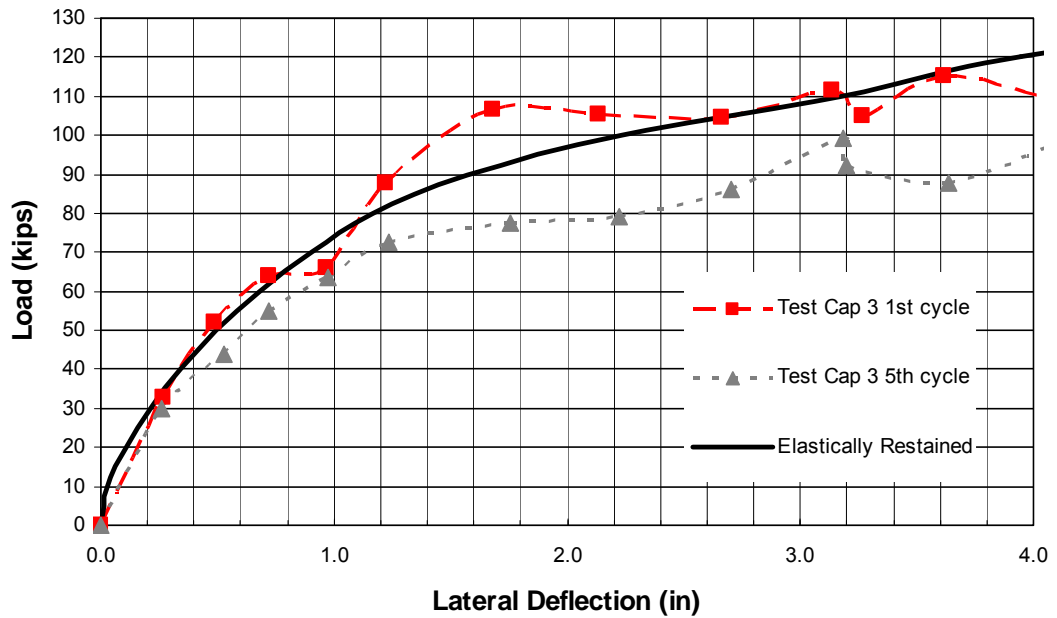


Figure 5-15 Comparison of computed and measured load vs. deflection curves for Pile Cap 3.

where the front face string pots were located, therefore, their respective data may not be entirely accurate. The load-deflection curves for the 1<sup>st</sup> and 5<sup>th</sup> cycles of loading are relatively close together until the load level at which cracking developed in the pile cap. However, after cracking the drop in lateral force from the 1<sup>st</sup> to the 5<sup>th</sup> cycle became more pronounced.

#### **5.2.4 Pile Cap 4**

As explained in Chapter 3 of this report, Pile Cap 4 included a pile embedment length of 24 inches which is twice as long as the embedment for the prior two tests. However, Pile Cap 4 did not include a reinforcing steel connection detail. The test was conducted to determine if the embedment length would be long enough to act as a reinforced connection such that the full capacity of the piles could be developed. Because the first two tests both had adequate connections and the back piles pulled out of the ground, it was concluded that if the connection were adequate, Pile Cap 4 would also fail by having the back pile pull out of the ground.

The loading sequence followed the same pattern as was followed in the prior two tests. The measured load versus deflection and load versus rotation curves are presented in Figure 5-16 and Figure 5-17, respectively. Once again the measured curves are compared with the curves predicted by GROUP. In general, the measured load versus deflection curve is 5 to 10% higher than the curve predicted by GROUP. However, the measured curve is still very similar to that obtained for Pile Caps 1 and 2 where vertical reinforcing steel was used in the connection detail.

Similar to Pile Cap 2 two rotation values were computed using two string pots on the top face of the cap and two string pots of the front face. The top face values are thought to be more accurate because they span a distance of 6 feet which is much greater than the front face string pots which span roughly 1.83 feet. The greater span should lead to a lower chance of error in the rotation computation; however, as the pile caps rotate and translate simultaneously it becomes difficult to estimate the actual rotation from the top string pots. The rotation computed from the front face string pots is consistently higher than that computed from the top face string pots for a given load. The percent difference between the two rotations becomes smaller at higher load levels, but a significant error is apparent at lower load levels. The computed load versus rotation curve is in good agreement with the measured curve, based on the top face string pots at loads less than about 90 kips, but then overestimates the measured rotation at higher loads.

Based on the test results, the 2 foot pile embedment length used in Pile Cap 4 was sufficient to provide tensile capacity such that the piles and cap remained in complete connection and the back pile eventually pulled out of the ground. As in previous cases, pile pullout resulted in a significant increase in deflection and rotation as shown in Figure 5-16 and Figure 5-17, respectively. Figure 5-18 provides a photograph showing how the back pile lifted up and out of the ground causing the deflection and rotation.

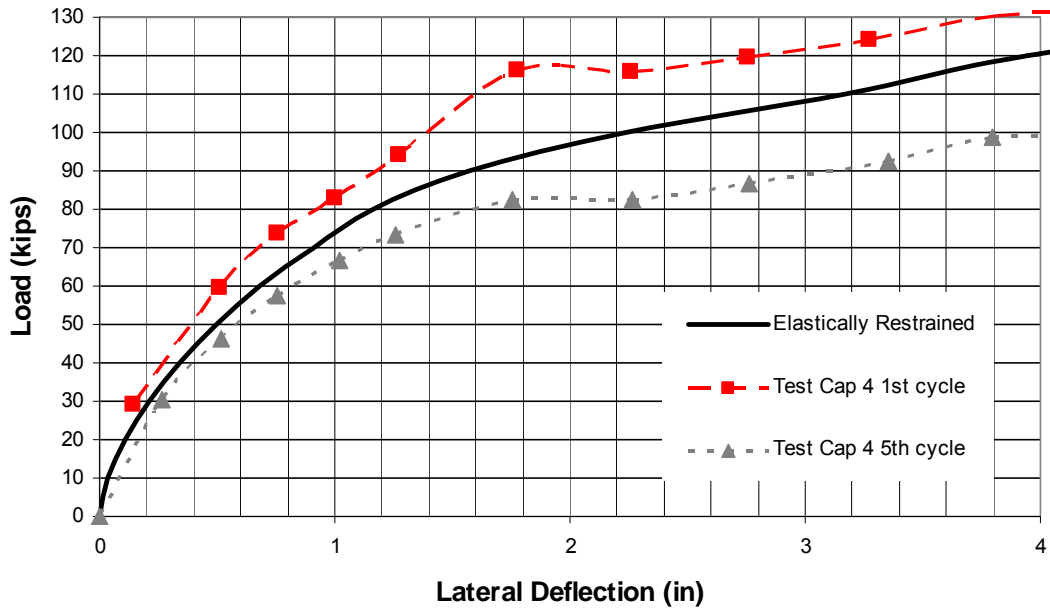


Figure 5-16 Comparison of computed and measured load vs. deflection curves for Pile Cap 4.

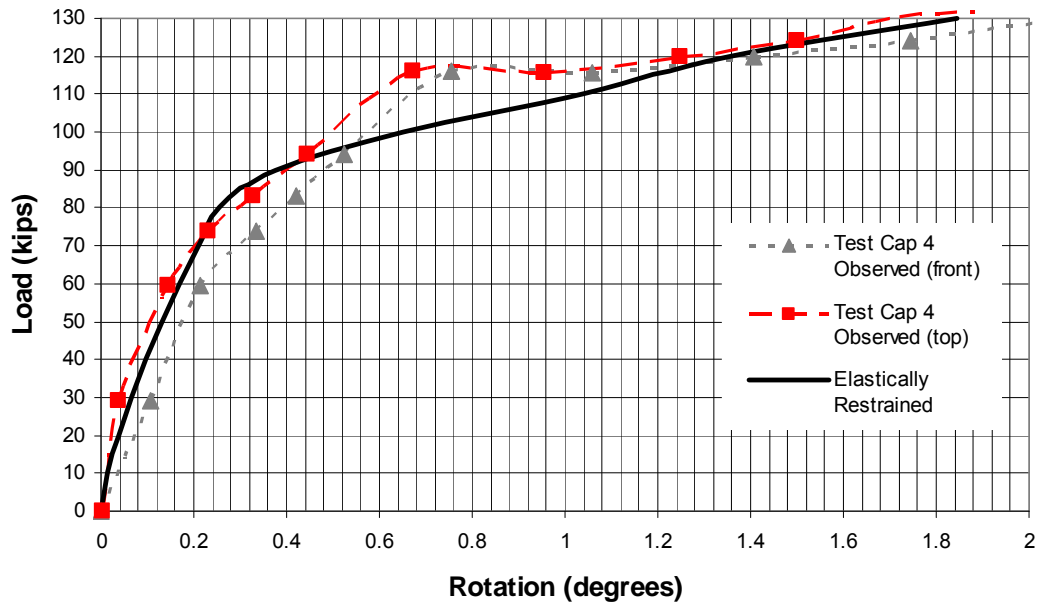


Figure 5-17 Comparison of computed and measured load vs. rotation curves for Pile Cap 4.



**Figure 5-18 Photograph of Pile Cap 4 after pullout failure.**

### **5.3 Analysis of Longer Piles**

Because the available piles were only 40 ft long, the piles pulled out prior to developing moment equal to the moment capacity of the pile. Therefore, it was desirable to determine what effect longer piles might have played on the load vs. deflection, load vs. rotation, and load vs. moment curves for the pile cap. Figures 5-19 through 5-21 below show three configurations that were analyzed in GROUP. The 40 foot pile is the same as was tested while the 60 foot and 80 foot piles were analyzed assuming that the additional lengths consisted of the same soil as was present in the last layer of the soil profile.

As shown in Figure 5-21 a 60 foot pile would have been ideal for this testing. The longer pile would have had more resistance against pull out and allowed the

capacity of the connection to be fully utilized. It also would have allowed more load to be applied to the cap with lower amounts of rotation and deflection.

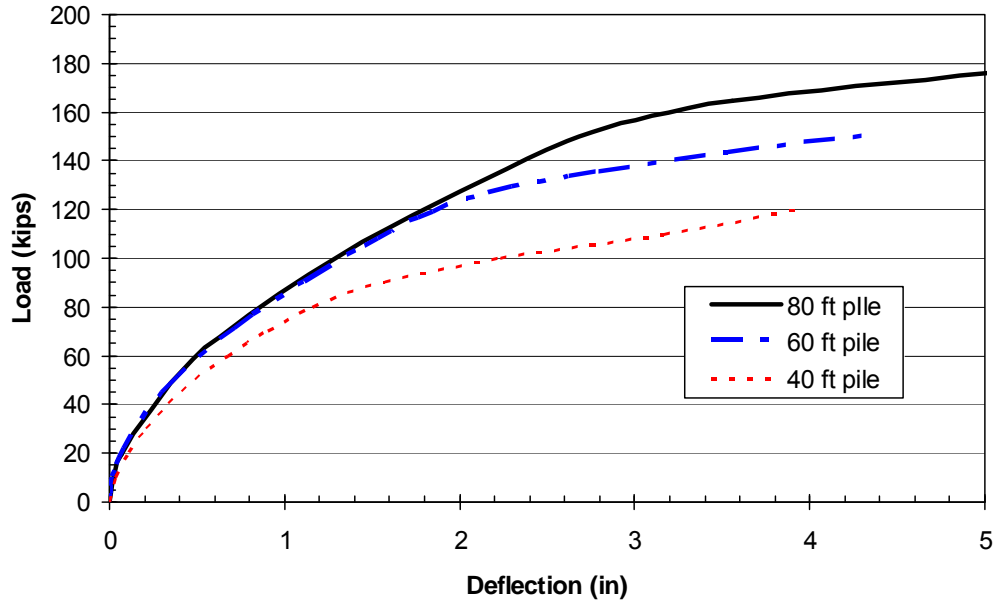


Figure 5-19 GROUP predicted load versus deflection curves for piles of variable length.

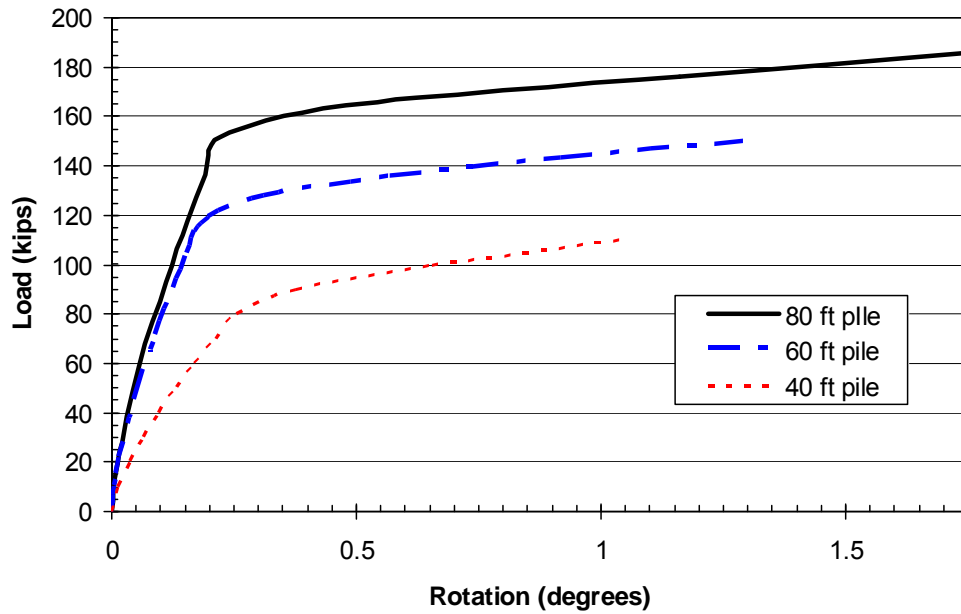


Figure 5-20 GROUP predicted load versus rotation curves for piles of variable length.

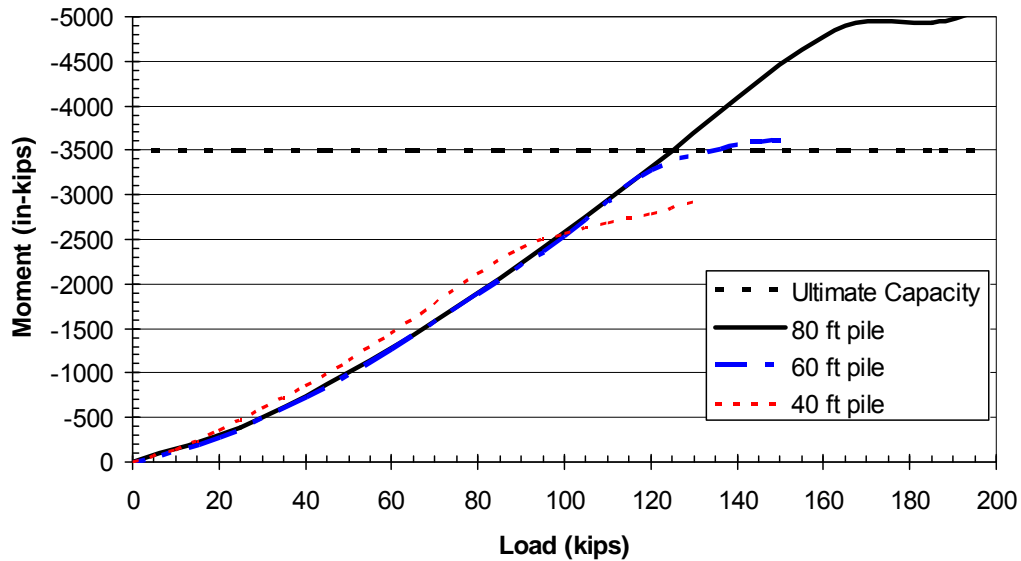


Figure 5-21 GROUP predicted moment versus load curves for piles of variable length.

#### 5.4 Comparison of Observed Strain

A portion of the strain gauges produced either insignificant data or failed during loading; nevertheless, a proper comparison of those that functioned was conducted to better understand the nature of force transfer within the pile and pile cap. Shown in Figure 5-22 through Figure 5-28 are strain gauge values in microstrain as a function of applied load. The location of each of these gauges is given in the figure caption and located on the pile at grade. In addition, a drawing of the location of the strain gauge on the pile cap is inserted in each figure. Please refer to section 3.4 for the exact locations of these gauges. The charts in figures below show the similarities within the tests and provide a good understanding of the forces within the pile cap system. As expected, the strain gauges located on the side closest to the force were in compression while the gauges on the opposite side of the pile were in tension. If the piles were in

pure bending, the tensile and compressive strains would be equal but be opposite in sign. In cases such as this, where both axial forces and bending moments are present, the strain values will be different. In this case, the axial force is proportional to the average strain, whereas the bending moment is proportional to the difference in strain.

The strain readings allowed a moment to be computed and these moments are presented subsequently in this report when relevant. As the strain versus load curves generally show, the strain on each pile face increased until the back piles began pulling out and the pile cap started rotating and deflecting a large amount. At this point, the strain gauges reached a maximum and then began to decrease towards zero. The strains on opposite faces of the back pile are much higher in tension than in compression suggest that there is significant moment plus a tensile force at the pile cap-ground interface. However, the difference in strain on the front and back faces of the front pile is relatively small, while the average strain level is lower than on the back pile. These observations suggest that the bending moment is higher on the front pile but that the axial force is smaller than on the back pile.

Strain gauges located along the reinforcement 4 feet below grade (locations e, f, m, and n) yielded very small strains which were similar to what was estimated by GROUP and LPILE; therefore their respective strain charts are not presented. The strain gauges at locations g, h, o, and p, which were approximately one foot below grade, measured the largest strains of the strain gauges located on the reinforcement; yet lower than those gauges located on the piles themselves at the base of the pile cap. Figure 5-26 and Figure 5-27 show the strain readings near the middle of the vertical reinforcing bars approximately one foot below grade and on both sides of the front

pile. Similar to strain gauges on the front piles at grade, the gauges on opposite sides of the pile develop close to equal and opposite suggesting the pile is dominated by bending stresses.

The gauges located at the top of the reinforcement at locations i, j, q, and r yielded very similar results with respect to each other. Each showed a small amount of strain until the lateral load increased enough that the cap began to rotate and then the strain increased dramatically. This is shown in Figure 5-28, and the other strain gauges at these locations measured very similar strain levels. This observation suggests that tension is developing in the piles after the cap begins to rotate. This tension is developed as the reinforcing steel acts to hold the pile and the pile cap together.

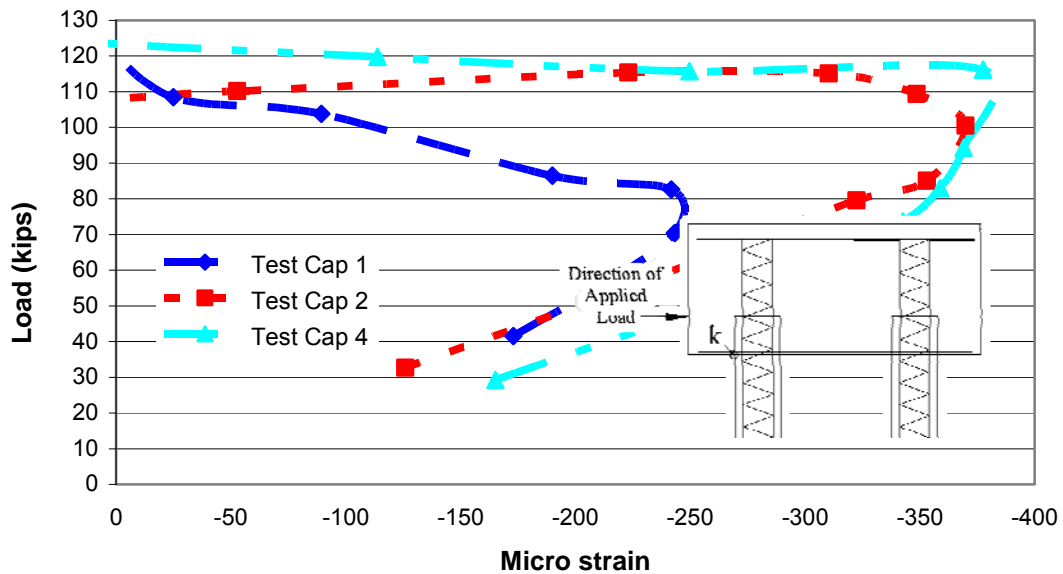


Figure 5-22 Strain gauge readings at location k.

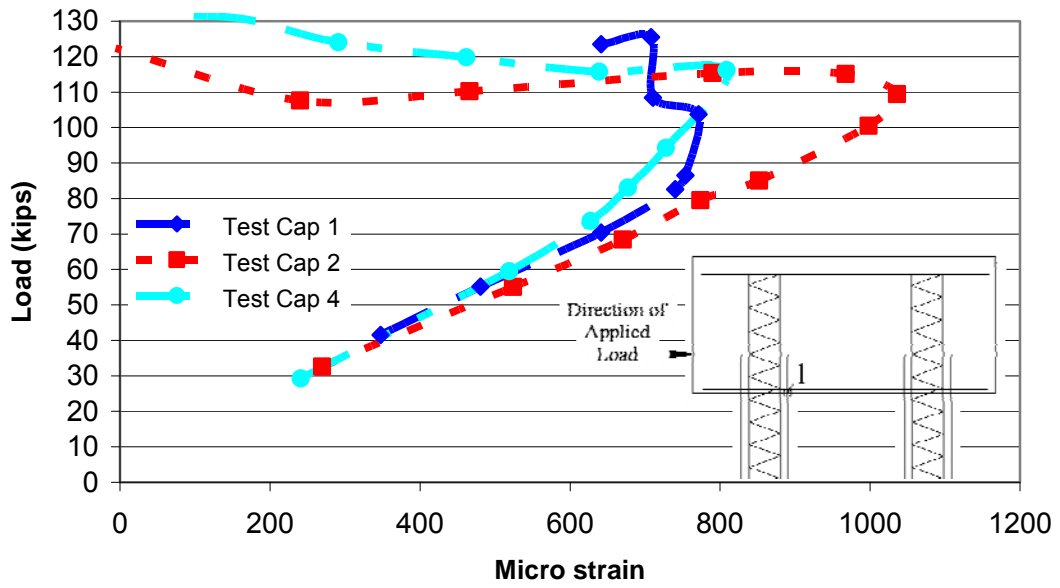


Figure 5-23 Strain gauge readings at location 1.

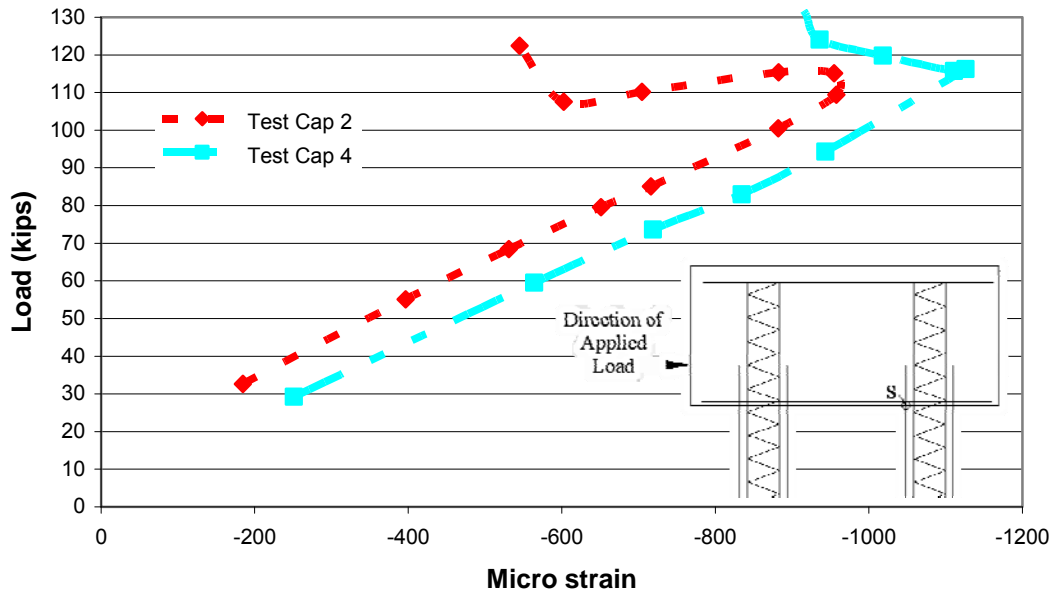


Figure 5-24 Strain gauge readings at location s.

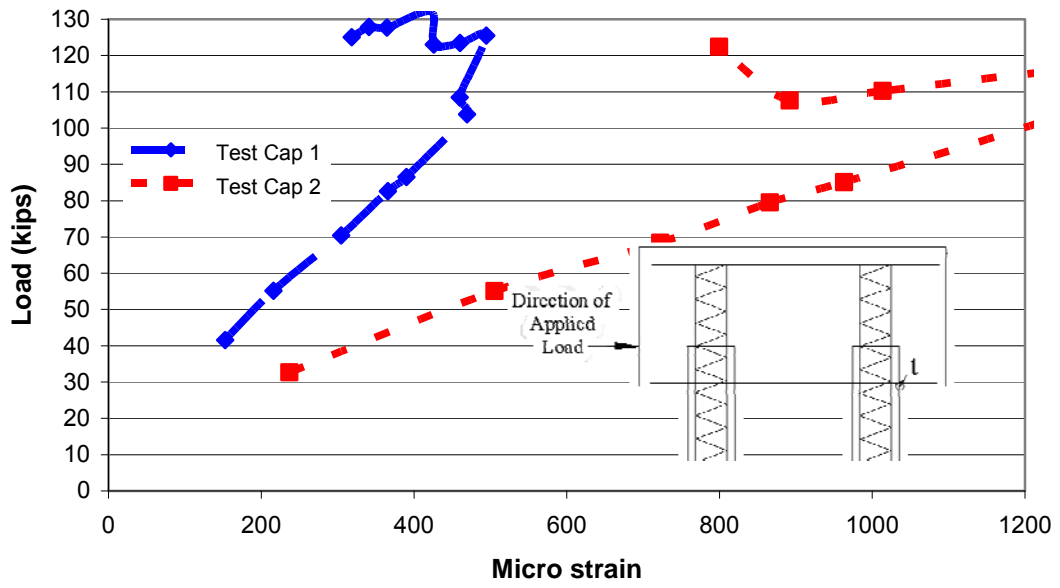


Figure 5-25 Strain gauge readings at location t.

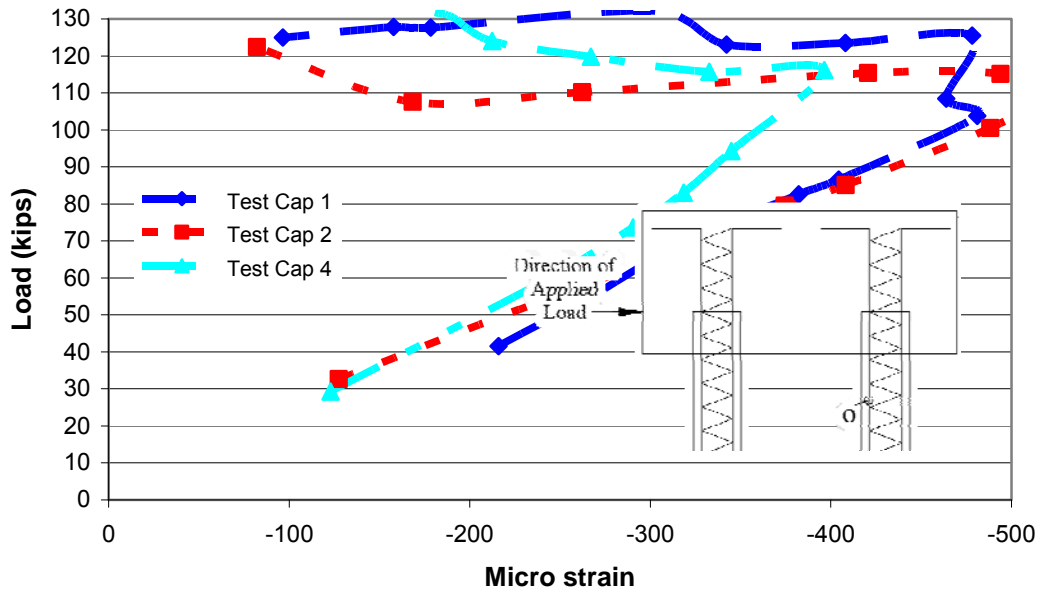


Figure 5-26 Strain gauge readings at location o.

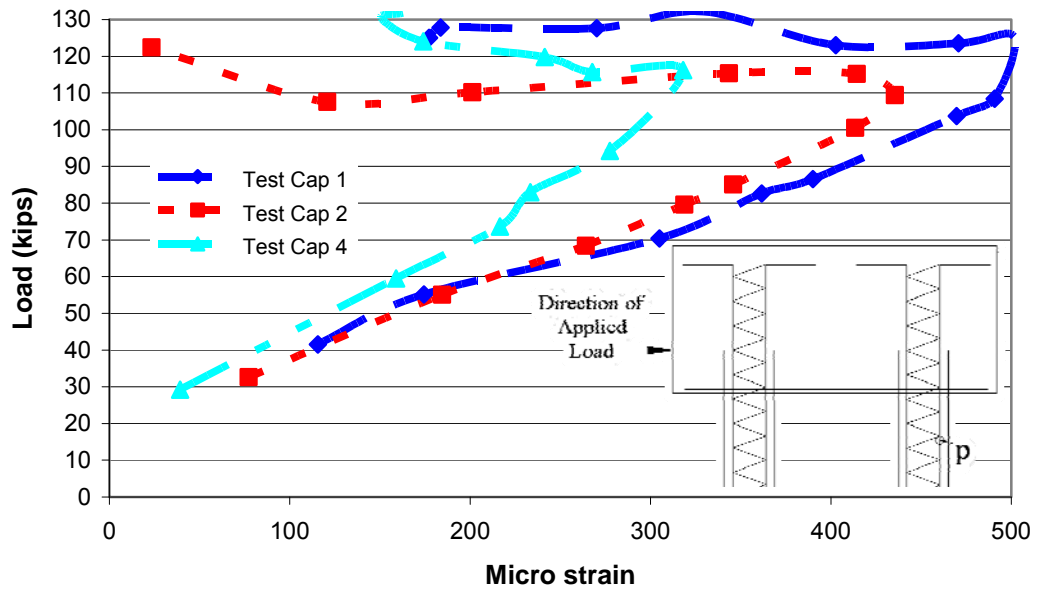


Figure 5-27 Strain gauge readings at location p.

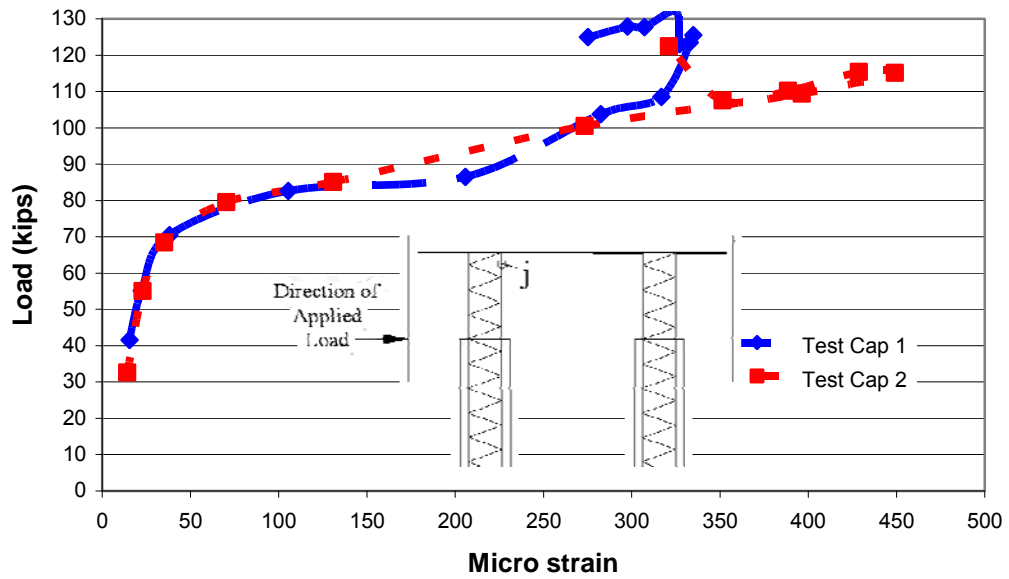


Figure 5-28 Strain gauge readings at location j.

The strain gauges located along the bottom reinforced grid at locations a, b, c, and d yielded quite variable yet relatively small strains from one another. While it was not possible to develop any consistent patterns from the measurements, it does appear that the tensile force in the bottom reinforcing grid was relatively small.

## 5.5 Comparison of Observed Moments

The observed moments developed within the pile were calculated using the equation

$$M = \frac{EI(\varepsilon_c - \varepsilon_t)}{h} \quad (5-2)$$

The composite EI before cracking was determined to be 12,195,440 kip-in<sup>2</sup> and the ultimate moment capacity for the section was determined to be 3500 in-kips. GROUP produced moment vs. depth curves presented in Figure 5-29 for loads of 80 to 120 kips. This plot indicates that the maximum negative moment occurs at the interface between the pile cap and the ground. The measured moment charts in Figures 5-30 and 5-31 confirm this behavior. The largest observed negative moments occur at location s-t which is at grade on the front pile. The observed moment is about 60% of the computed moment capacity of the pile assuming non-linear behavior. The maximum measured negative moment on the rear piles only reached about 40% of the moment capacity of the pile.

Below the pile cap-ground interface, the computed moments in Figure 5-29 decrease very quickly and reach zero at about 3.5 to 4.5 feet below the ground. The

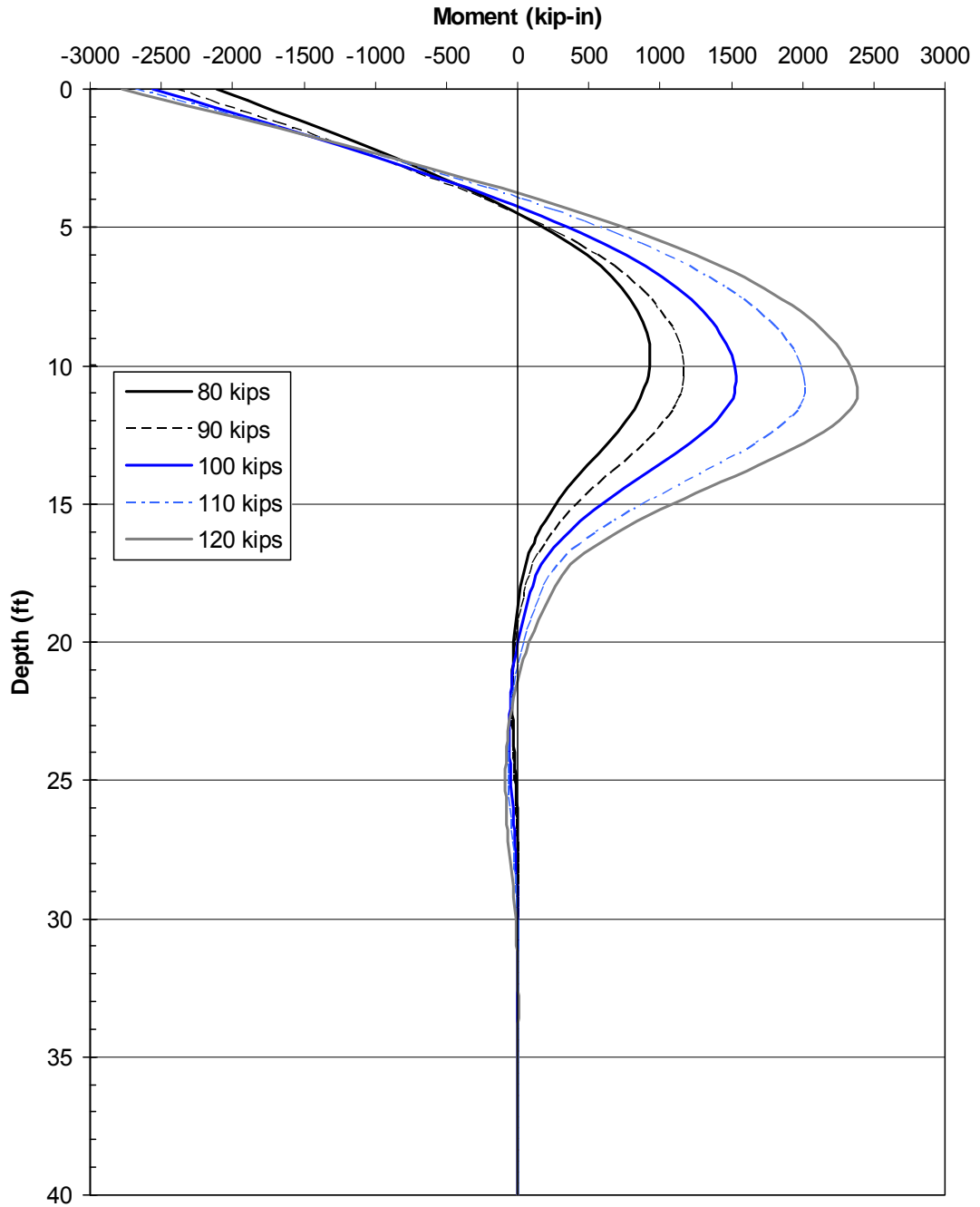


Figure 5-29 Moment vs. depth chart computed with GROUP.

strain gauges that were located 4 feet below the ground and attached to the vertical reinforcing bars generally confirm this pattern as the measured moments were much smaller. Below a depth of 4 feet, the computed moment increases to its largest positive value which occurs at a depth near 10 feet below cannot be confirmed by the strain data because the reinforcing cage did not extend to this depth.

The measured moments in figures below show a general increase with load until a maximum moment is reached at a load level of about 100 to 110 kips. This load level generally corresponds to the load level at which the back pile pulls out and the pile cap begins to rotate. Figure 5-31 shows the moments at a depth of 14 inches below grade at locations o-p and g-h. These gauges, as indicated in section 3, are at the same location but on opposite piles. The curves show that larger moments were observed on the front piles as predicted by GROUP.

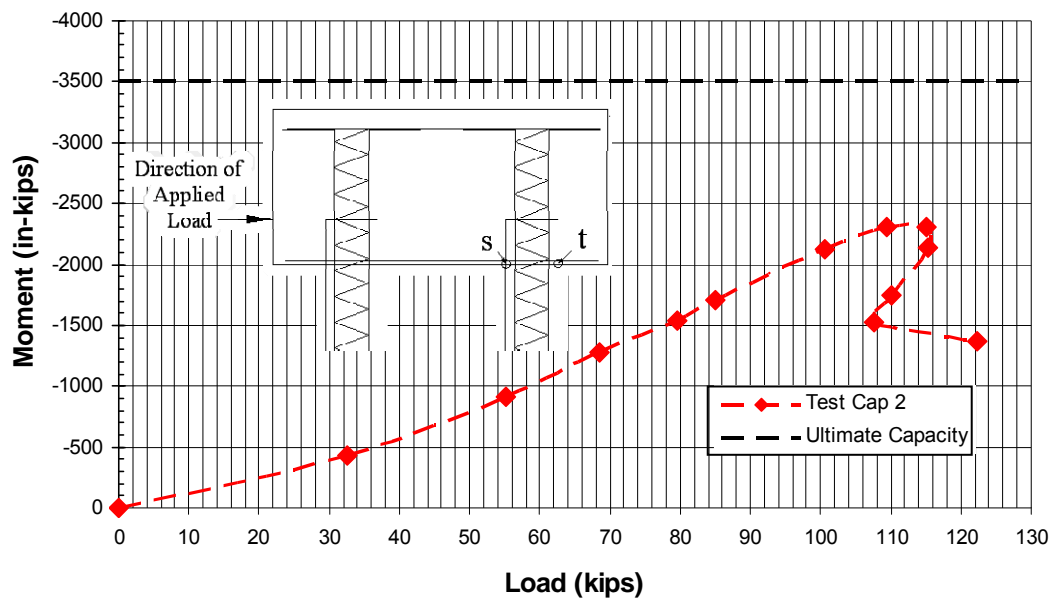


Figure 5-30 Observed moments at location s-t.

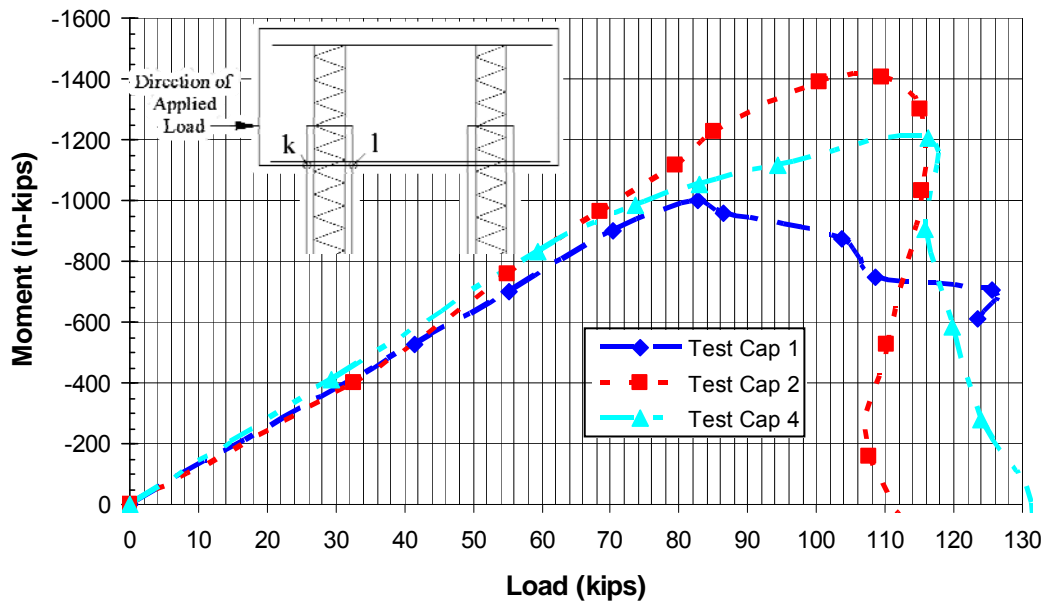


Figure 5-29 Observed moments at location k-l.

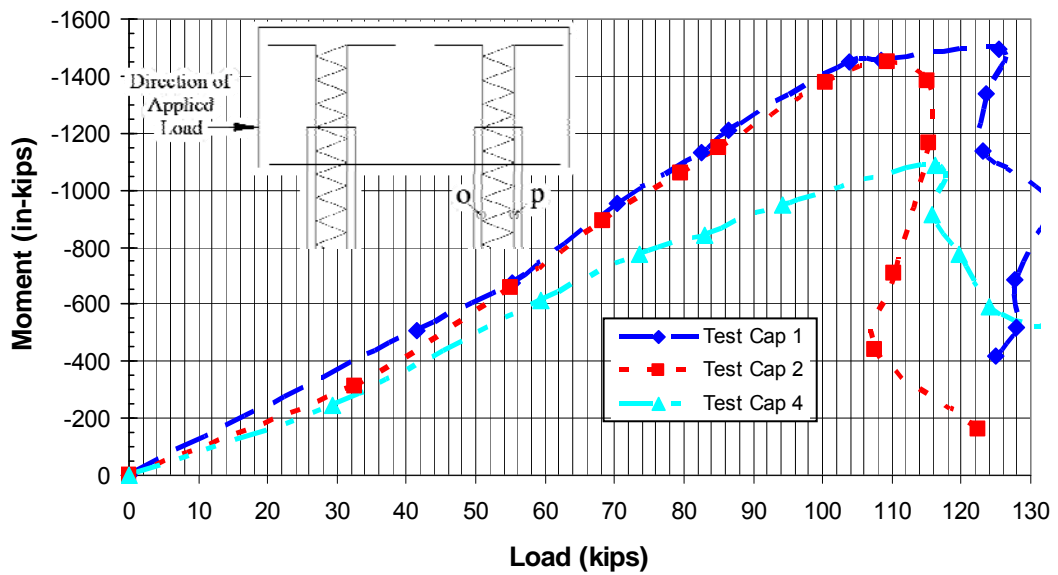


Figure 5-30 Observed moments at location o-p.

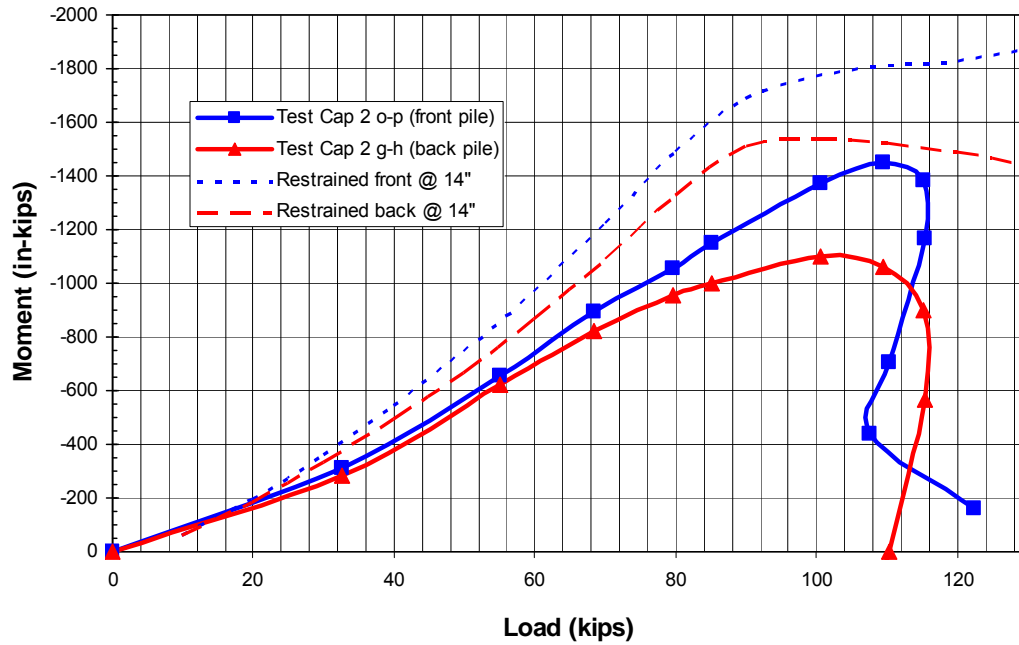


Figure 5-31 Observed and predicted moment vs. load at 14" below grade.

## 5.6 Comparison of Test Results

Each of the four tests were designed such that a proper comparison would be beneficial for future design. In current design with steel pipe piles it is typical to both embed the piles a sufficient depth into the pile cap as well as to provide a reinforcing cage extending from the top of the pile cap and into the piles. Figure 5-32 and Figure 5-33 plot load-deflection and load-rotation curves, respectively for all four lateral pile cap load tests to facilitate comparisons.

Comparing the performance of Pile Cap 1 with Pile Cap 2 shows that the additional pile embedment length may not be necessary for applied lateral loads. The reinforcement did an adequate job in connecting the piles to the cap even when the

embedment was only 6 inches. However, the moment only reached about 60% of the ultimate capacity of the pile.

Comparing the connection designs of Pile Cap 2 with Pile Cap 3 also proved to be valuable. Although the piles for both test caps were embedded one foot into the caps, the connection of Pile Cap 2 performed very well while that for Pile Cap 3 failed in the connection region. The connection for Pile Cap 2 included a reinforcing cage extending from the pile through the pile cap while Pile Cap 3 did not include any connection other than the pile embedment itself. This shows the importance of providing an adequate connection. As presented in section 4.3; Pile Cap 3 was designed to be able to resist the tensile and shear forces, yet the cap still failed. Based on Eq 2-1, the moment capacity of the pile to pile cap connection would have been exceeded for at a moment between 1700 and 2000 inch-kips. According to calculations with GROUP (See Figure 5-21) and measurements on other pile caps (see Figure 5-31), this moment developed at load levels between 80 and 90 kips. This load level corresponds to the load when the shear crack initiated at the level of the front pile and likely corresponds to a block failure against the front face of the pile.

Perhaps the most important comparison is the performance of Pile Cap 4 with the other three test caps. Pile Cap 4 performed very well, yielding lower deflections and rotations for a given load than any of the other three caps as shown in Figure 5-32 and Figure 5-33. The observed rotation from the front face string pots is shown in Figure 5-33 and the top face string pot data which was only gathered from Pile Cap 2 and 4 is shown in Figure 5-34. The largest variance between observed rotations occurs with the front face string pots of Pile Cap 2 which at low loads yield very small

rotations; this could be misleading data since it varies significantly from the other tests rotations from both the front and top string pots.

The observed data leads to the conclusion that this simple 2 foot embedment connection, which was 2/3 the cap height and about 2 times the piles diameter, is an adequate design and possibly the most favorable connection presented. However, this somewhat better performance might be a result of slightly different soil parameters or variances in construction.

The load-deflection and load-rotation curves computed by GROUP assuming elastically restrained conditions were in reasonable agreement with all the all of the test results. The computed stiffness for the two pile group was about 80 kips/inch and this value was essentially the same as the measured stiffness for all four test caps.

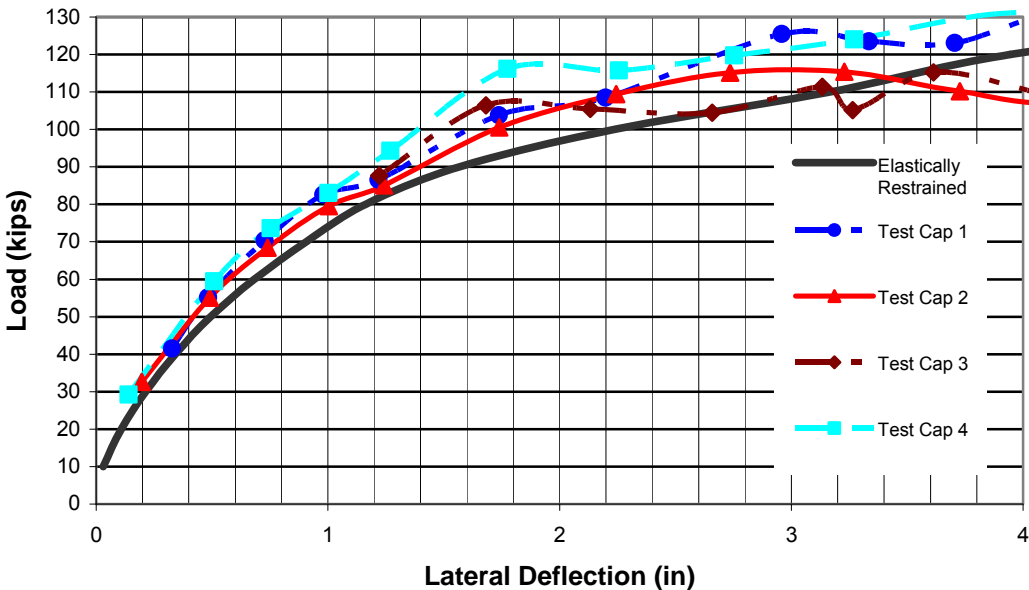


Figure 5-32 Deflection comparisons of all tests.

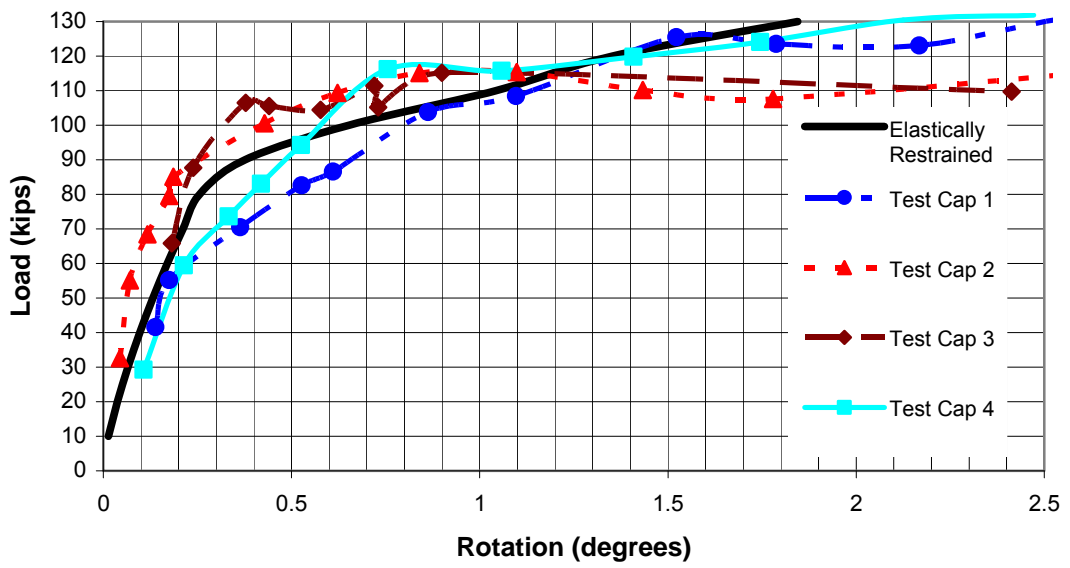


Figure 5-33 Rotation comparisons of all tests (front face).

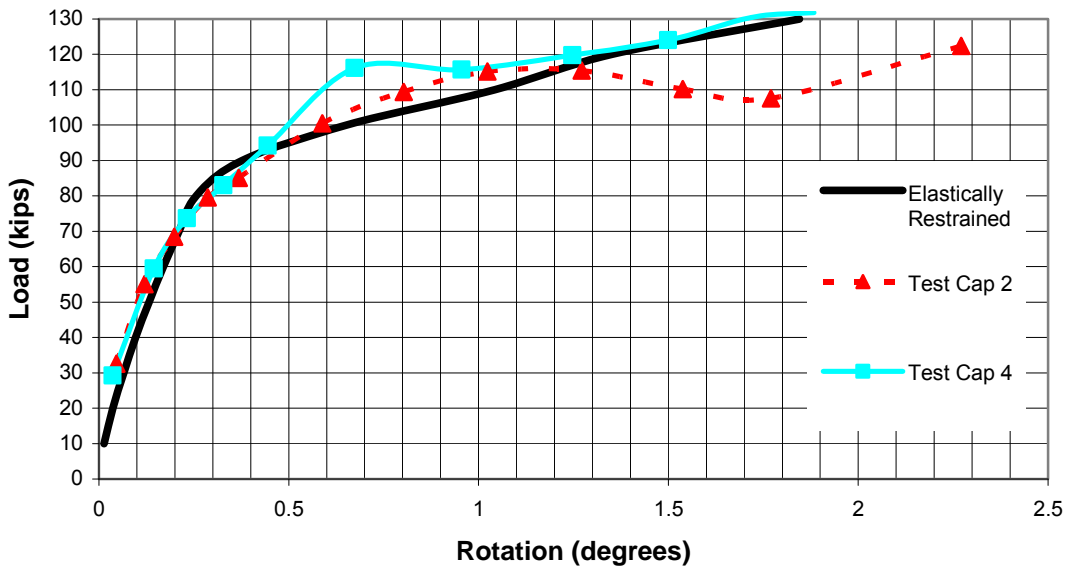


Figure 5-34 Rotation comparisons of all tests (top face).

## 6 CONCLUSIONS

### 6.1 Summary

To better understand the connection details involved with full-scale piles and pile caps, four pile cap configurations were built, analyzed and then tested. All of the tests consisted of the same cap details and the only variations were that of the connection detail. Each cap was 6 ½ feet long, 3 feet wide, and 3 feet tall, with two circular steel piles driven to a depth of 40 feet and spaced at 3½ feet on centers. Reinforcing grids with #7 bars spaced at 6 inches were placed in the longitudinal and transverse directions both top and bottom. There are two variations with the connection presented in this paper; the length of the pile extending into the cap (embedment length), and the amount of rebar extending down into the pile and into the cap.

Pile Cap 1 included a 6 inch pile embedment length and (4) 7 foot #6 bars extending to the top of the cap and 4 feet below grade. Pile Cap 2 included a 12 inch pile embedment length and the same rebar detail as Pile Cap 1. Pile Cap 3 included only a 12 inch pile embedment length with no reinforcement and a steel plate at the top of the pile. Finally, Pile Cap 4 included only a 24 inch pile embedment length with no reinforcing cage. All piles were filled with concrete with the exception of Pile Cap 3 which remained hollow in accordance with Oregon DOT practice.

String potentiometers, strain gauges and a load cell were attached to each pile cap during testing to measure deflection, rotation, strain, and applied force. This data has been collected and, when relevant, presented as graphs in this report. The pile caps were analyzed by hand calculations and two computer modeling programs; GROUP and LPILE. The results from these programs are presented and compared with measured response. In general, GROUP yielded estimations very similar to the observed data and therefore most of the data presented in this paper has been compared to those estimations.

Testing produced some surprising results. Although design equations based on embedment length predicted connection failure for Pile Caps 1, 2, and 3, only Pile Cap 3 experienced failure at the connection. Because Pile Caps 1 and 2 also contained a reinforcing cage, attention has focused on the additional moment capacity provided by this connection detail. Although the applied lateral force was sufficient to load the connections for Pile Caps 1 and 2 beyond the anticipated failure moment, pile pullout prevented a determination of the ultimate moment capacity of the connection. Failure of the connection for Pile Cap 3 led to the development of a crack which eventually propagated across the entire length of the pile cap. Pile Cap 4, with a 24 inch embedment, did not experience connection failure and provided a load-deflection curve that was slightly better than the other pile caps which were tested.

## **6.2 Conclusions**

Based on the results of the testing and analysis conducted during this investigation, the following conclusions can be drawn:

1. A pile embedded a sufficient depth into the cap can produce a connection with an equivalent capacity to those with a reinforced detail. Pile Cap 4 which relied solely upon its embedment length of 24 inches provided an adequate connection and performed as well or better than comparable caps which relied on a reinforced connection. This is consistent with predictions based on Eq. 2-1 which predicts that the moment capacity of this connection would exceed that of the pile.
2. Piles with inadequate embedment and no reinforcing dowels can result in an early seismic failure at the connection. Pile Cap 3 lacked both an adequate embedment length and reinforcement resulting in early failure due to large shear and tensile cracks as predicted by Eq. 2-1.
3. Despite shallow embedment, a connection detail which includes a steel reinforcing cage (typical of the UDOT standard design) can still develop moments equal to 40 to 60% of the moment capacity of the pile. This finding is consistent with test results on prestressed piles and H piles reported by Xiao (2003) and Xiao (2006). Pile Caps 1 and 2 both included a reinforced connection detail and performed successfully despite the fact that Pile Cap 1 had only six inches of embedment and Pile Cap 2 had only a twelve inch embedment.
4. Equations which only account for embedment effects in assessing the shear and moment capacity of a pile to pile cap connection (e.g. Eq. 2-1 or PCI Handbook method), can significantly underestimate the capacity of the

connection. According to these equations (Eqs 2-1, 2-2, and 4-8), both Pile Caps 1 and 2 should have experienced connection failures but did not.

5. Programs such as GROUP and LPILE are quite accurate when predicting deflections and rotations of pile caps. As shown in the graphs presented in this report the observed behavior was nearly identical to that predicted by GROUP although accuracy decreased at higher deflection levels.

### **6.3 Recommendation for Future Research**

Based on the experience from conducting these tests and a thorough literature review, we recommend that additional pile to pile cap testing be carried out in a laboratory setting. These tests should be aimed at evaluating the moment capacity of pipe piles with variable depths of embedment and with connections involving reinforcing cages as well as for piles without reinforcing cages. These tests in combination with previous test results should make it possible to develop equations to account for moment capacity provided by both embedment and flexure mechanisms. While the field testing provided improved understanding of the role of soil-pile interaction on the equations used to predict connection capacity, laboratory testing would make it possible to better see the structural failure mechanisms and potential spalling of the concrete cover.

### **6.4 Implementation of Results**

Based on the available test results, we recommend that connection details for 12 inch diameter steel pipe piles involve a minimum of either (a) 2 ft of embedment without additional steel dowels at the connection, or (b) at least 1 ft of embedment

with at least 4 #6 bars extending at least one development length into the concrete filled pile and into the pile cap. For other pile diameters, conservative estimates of the moment capacity of the connection can be obtained using the Marcakis and Mitchell (1980) which has been adopted in the current PCI Handbook.

## 7 REFERENCES

- Army Corps of Engineers (1984), Castilla, F, Martin, P. and Link, J. “Fixity of Members Embedded in Concrete.” Technical Report M-339, February 1984.
- Beatty, C.I. (1970). “Lateral test on pile groups.” *Foundation Facts*, VI(1), 18-21.
- Bruneau, M. and Marson, J. (2004). “Seismic Design of Concrete-Filled Circular Steel Bridge Piers.” *Journal of Bridge Engineering*, Vol. 9, No. 1, January 1, 2004.
- Group (1996). “A program for the analysis of a group of piles subjected to axial and lateral loading.” Version 4.0, by Lymon Reese, Shin Tower Wang, Jose A. Arrellaga, and Joe Hendrix. ENSOFT, Inc., Austin, Texas.
- Harris, K.A. Ph.D., and Petrou, M. F. Ph.D. (2001). “Behavior of Precast, Prestressed Concrete Pile to Cast-in-Place Pile Cap Connections.” *PCI JOURNAL*, V. 46, No. 4, July-August 2001, pp.82-92.
- Joen, P.H. and Park, R. (1990). “Simulated seismic load tests on prestressed concrete piles and pile-pile cap connections.” *PCI Journal*, Vol. 35 No. 6, p. 892-900.
- Kim, J.B., and Singh, L.P. (1974). “Effect of pile cap – soil interaction on lateral capacity of pile groups,” Master of Science, Bucknell University, Lewisburg, PA.
- LPILE (1997). “A program for the analysis of piles and drilled shafts under lateral loads.” By Lymon Reese, Shin Tower Wang, JoseA. Arrellaga, and Joe Hendrix, ENSOFT, Inc., Houston, Texas.
- MacGregor, J. G., Wight, J. K., (2005). *Reinforced Concrete Mechanics and Design*. Fourth Edition, Pearson Education Inc., Upper Saddle River, New Jersey.
- Marcakis, K., and Mitchell, D. (1980). “Precast Concrete Connections with Embedded Steel Members,” *PCI JORNAL*, V.25, No. 4, July-August 1980, pp.88-116.

- Mattock, A. H., and Gaafar, G. H., (1982). "Strength of Embedded Steel Sections as Brackets," *ACI Journal*, V. 79, No. 2, March-April 1982, pp 83-93
- Mokwa, R. L., (1999). "Investigation of the Resistance of Pile Caps to Lateral Loading." Dissertation etd-093099-180817, Department of Civil Engineering Virginia Tech.
- Mokwa, R. L., and Duncan, J.M. (2003). "Rotational Restraint of Pile Caps during Lateral Loading." *Journal of Geotechnical and Geoenvironmental Engineering*, Vol. 129, No.9, September 1, 2003.
- Ooi, P. S.K., Chang, B. K.F., and Wang, S. A. (2004). "Simplified Lateral Load Analyses of Fixed Head Piles and Pile Groups." *Journal of Geotechnical and Geoenvironmental Engineering*, Vol. 130, No. 11, November 1, 2004.
- Rollins, M., K, Weaver, T.J., and Peterson, K.T. (1997). "Statnamic lateral load testing of a full-scale fixed-head pile group." Report, UDOT, FHWA.
- Shama, A.A. and Mander, J.B. (2004) "Behavior of Timber Pile-to-Cap Connections under Cyclic Lateral Loading." *J. of Strutural Engienering, ASCE*, Vol. 130, No. 8, p. 1252-1262.
- Shama, A.A., Mander, J.B. and Blabac, B.A. (2002a). "Seismic Investigation of Steel Pile Bents: I. Evaluation of Performance." *Earthquake Spectra, EERI*, Vol. 18, No. 1, p. 121-142
- Shama, A.A., Mander, J.B. and Chen, S.S. (2002b). "Seismic Investigation of Steel Pile Bents: II. Retrofit and Vulnerabilty Analysis." *Earthquake Spectra, EERI*, Vol. 18, No. 1, p. 143-160.
- Stephens, J. and McKittrick, L. (2005) "Performance of Steel Pipe Pile-to-Concrete Bent Cap Connections Subject to Seismic or High Transverse Loading: Phase II." Report No. FHWA/MT-05-001/8144.

Shama, A., A, and Mander, J.B. (2001). "Seismic Performance and Retrofit of Steel Pile to Concrete Cap Connections." *ACI Structural Journal*, V.99, No.1, 2001, pp 185-192.

Silva, P. F., and Seible, F. (2001). "Seismic Performance Evaluation of Cast-in-Steel-Shell (CISS) Piles." *ACI Structural Journal*, V.98, No.1, 2001, pp 36-49.

Xiao, Y. (2003). "Experimental Studies on Precast Prestressed Concrete Pile to CIP Concrete Pile-Cap Connections." *PCI Journal*, PCI, Vol. 48, Issue 6, p. 82-91.

Xiao, Y., Wu, H., Yaprak, T.T., Martin, G.R., Mander, J.B. (2006). "Experimental Studies on Seismic Behavior of Steel Pile-to-Pile-Cap Connections." *J. of Bridge Engineering*, ASCE, Vol. 11, No. 2, p. 151-159.

Zafir, Z., and Vanderpool, W.E. (1998). "Lateral response of large diameter drilled shafts: I-15/US 95 load test program." *Proceedings of the 33<sup>rd</sup> Engineering Geology and Geotechnical Symposium*, University of Nevada, Reno, 161-176.

## Appendix A. Complete Test Results

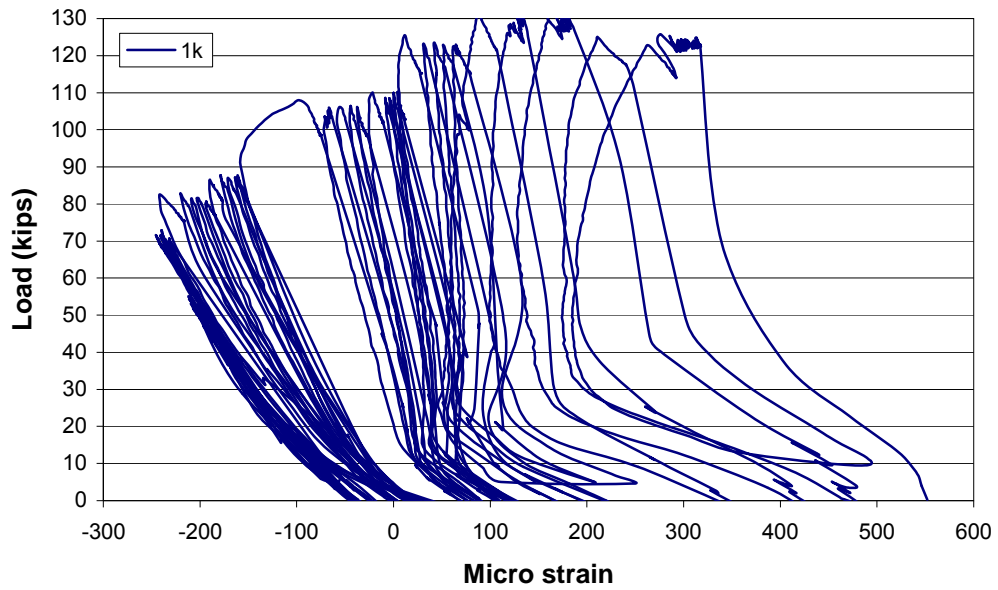


Figure A-0-1 Observed strain Pile Cap 1 location k.

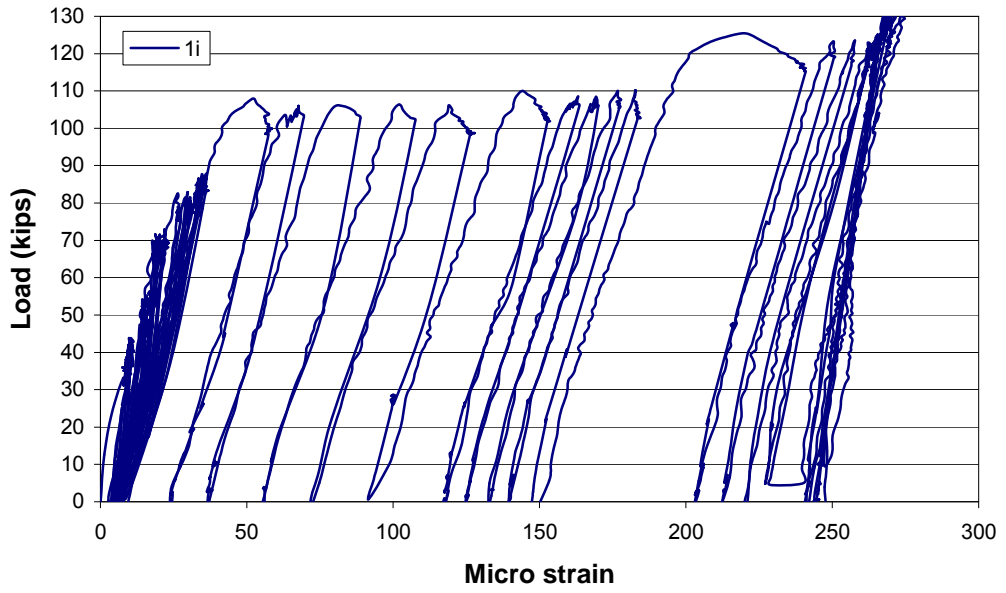


Figure A-0-2 Observed strain Pile Cap 1 location i.

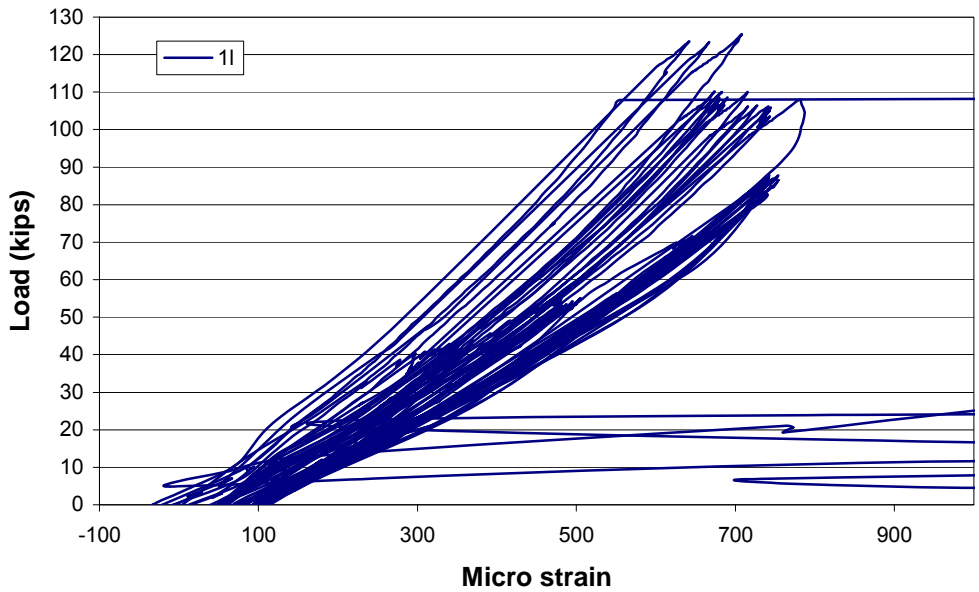
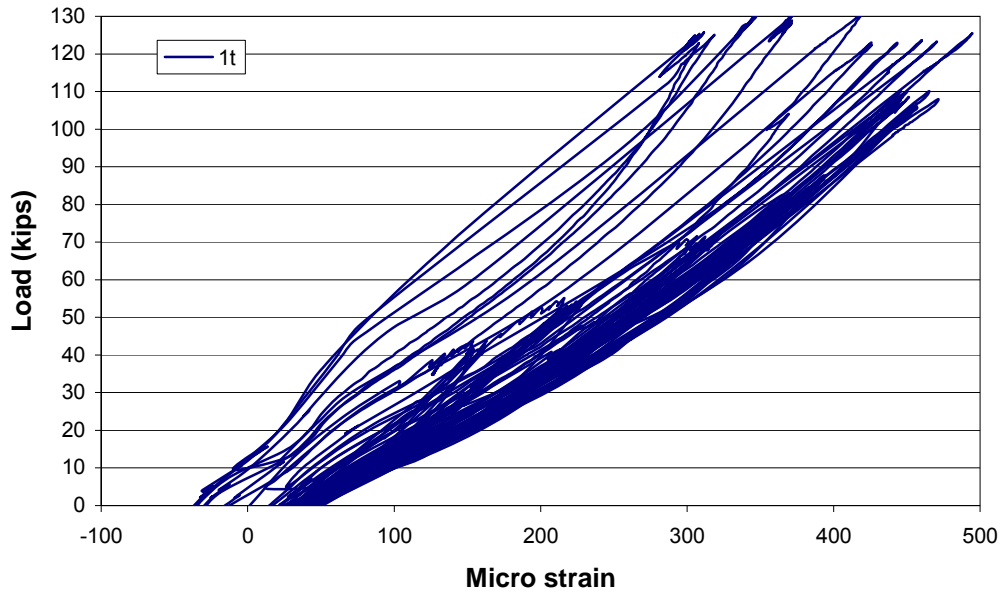
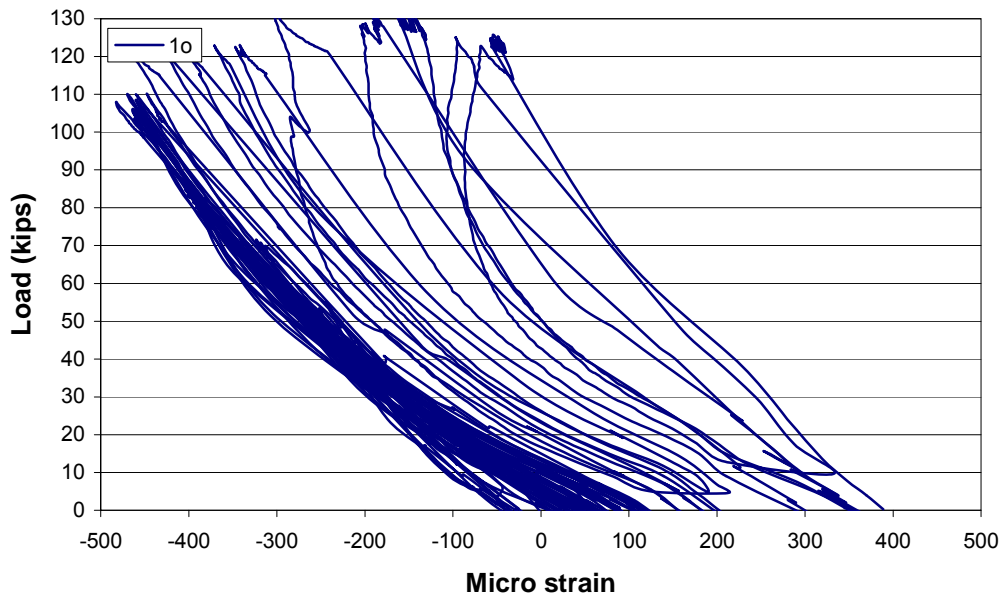


Figure A-0-3 Observed strain Pile Cap 1 location l.



**Figure A-0-4 Observed strain Pile Cap 1 location t.**



**Figure A-0-5 Observed strain Pile Cap 1 location o.**

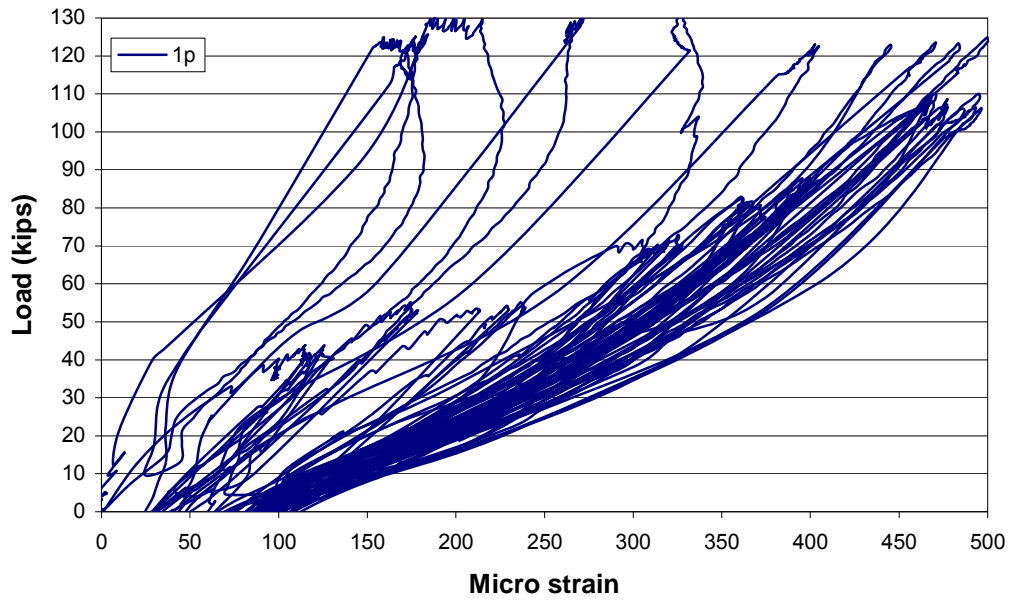


Figure A-0-6 Observed strain Pile Cap 1 location p.

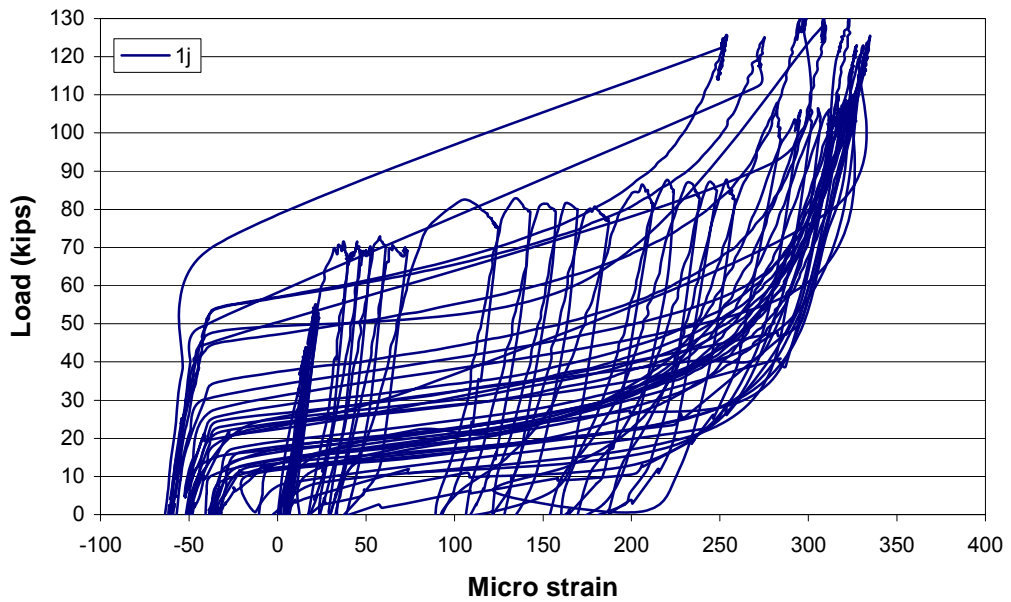


Figure A-0-7 Observed strain Pile Cap 1 location j.

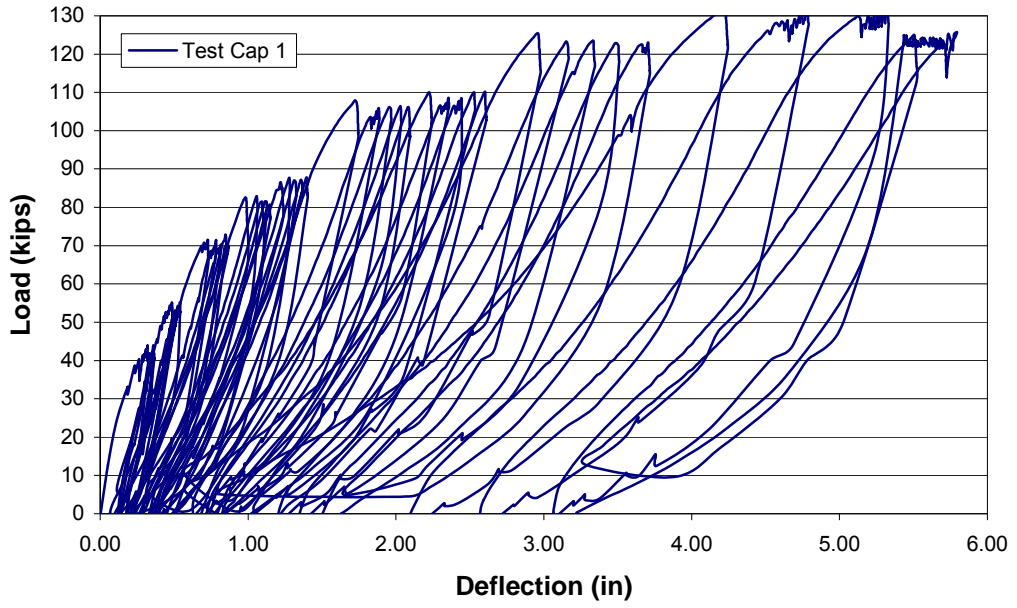


Figure A-0-8 Observed deflection Pile Cap 1.

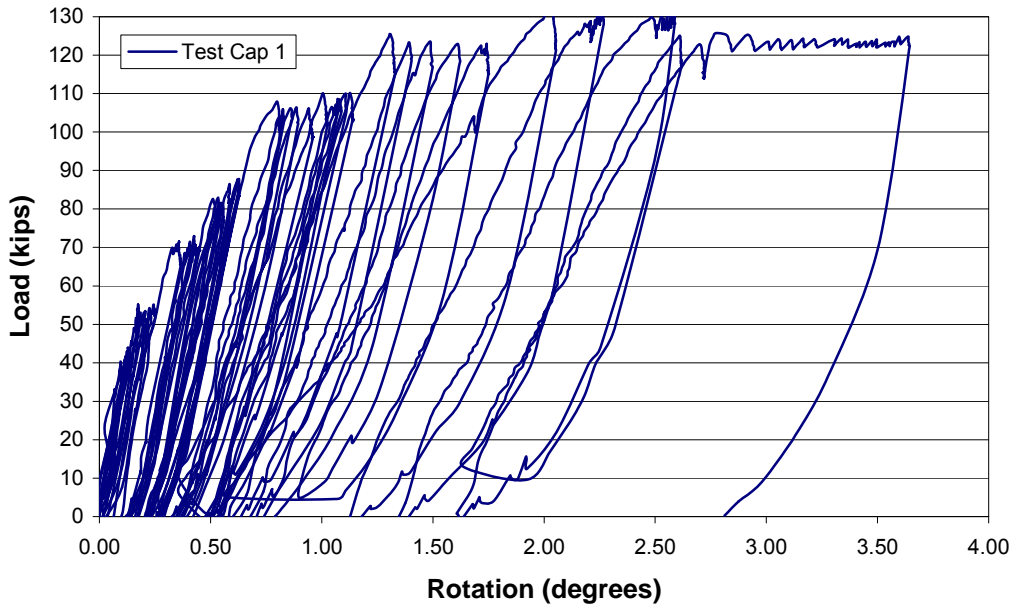
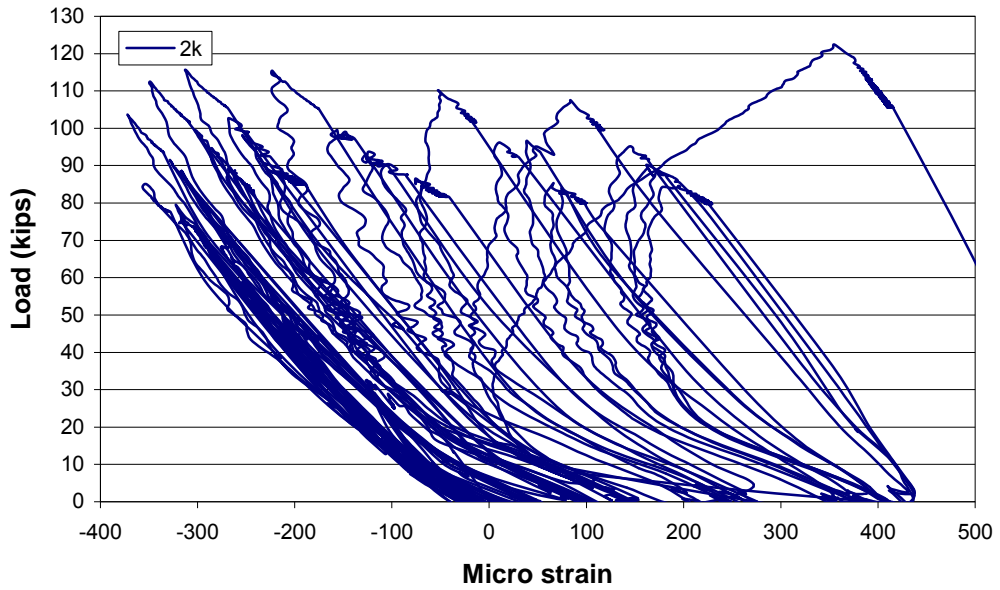
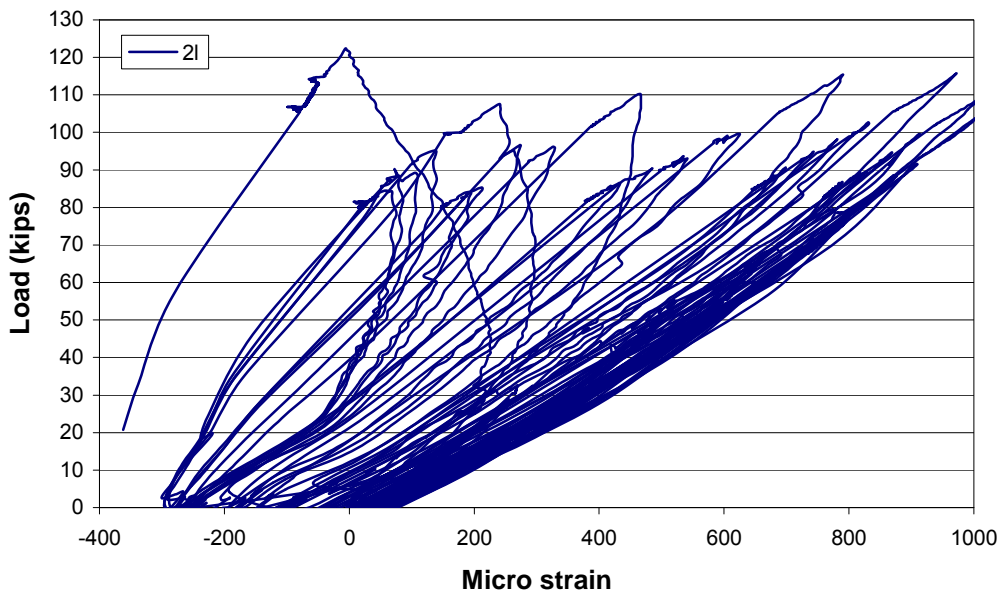


Figure A-0-9 Observed rotation Pile Cap 1.



**Figure A-0-10 Observed strain Pile Cap 2 location k.**



**Figure A-0-11 Observed strain Pile Cap 2 location l.**

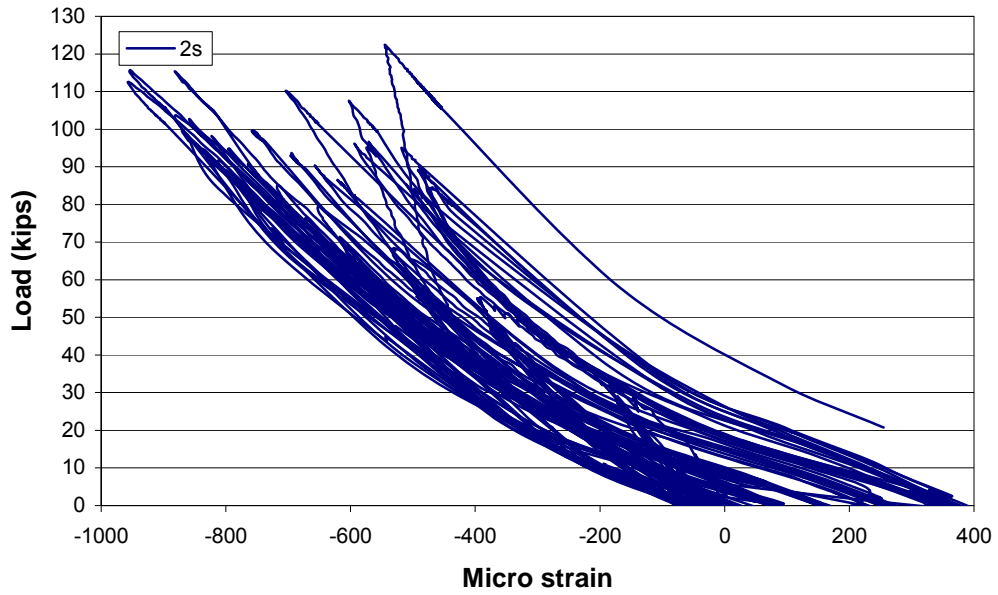


**Figure A-0-12 Observed strain Pile Cap 2 location s.**

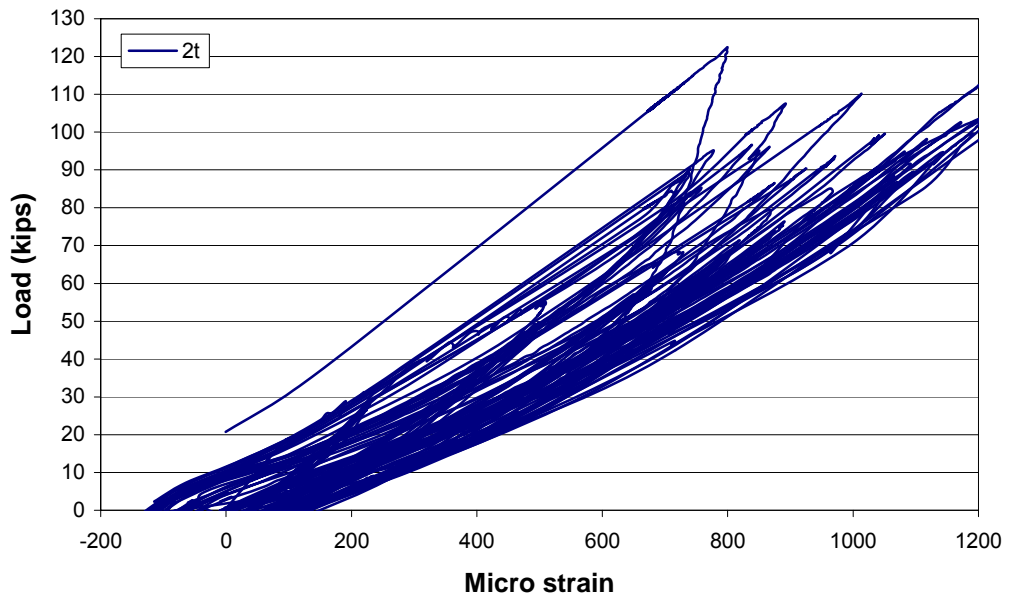


**Figure A-0-13 Observed strain Pile Cap 2 location t.**

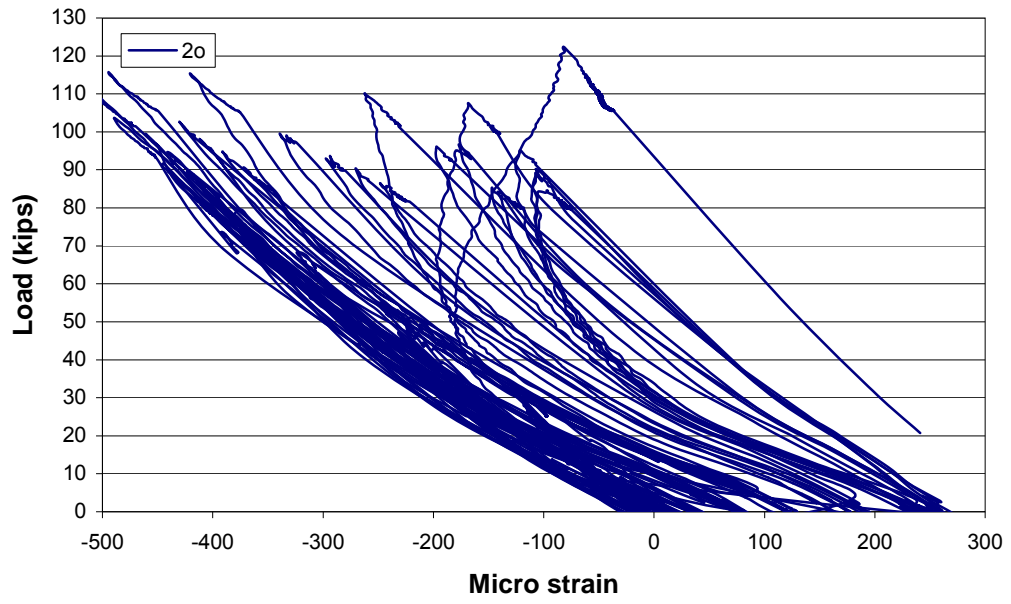


Figure A-0-14 Observed strain Pile Cap 2 location o.

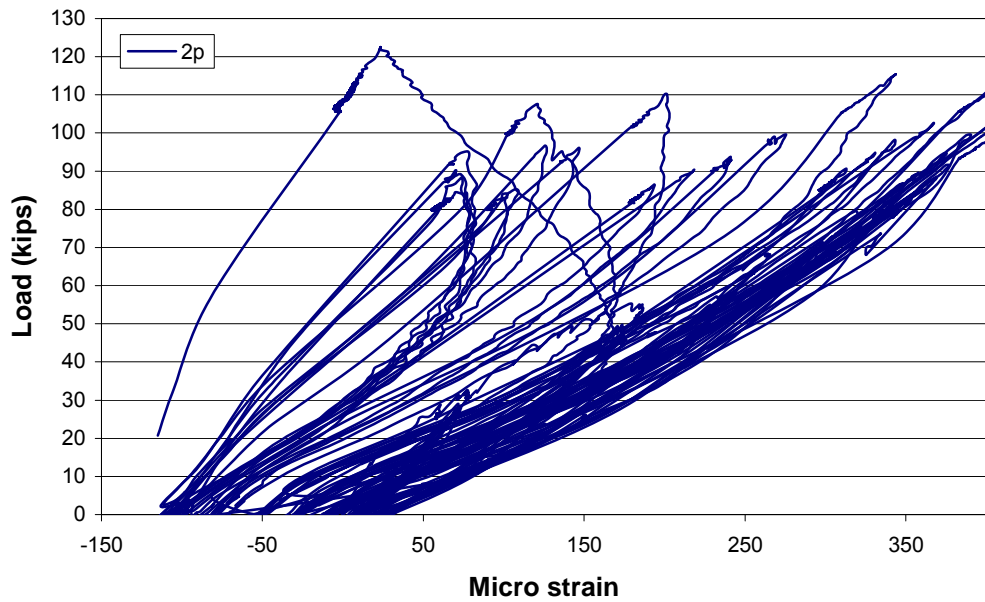


Figure A-0-15 Observed strain Pile Cap 2 location p.

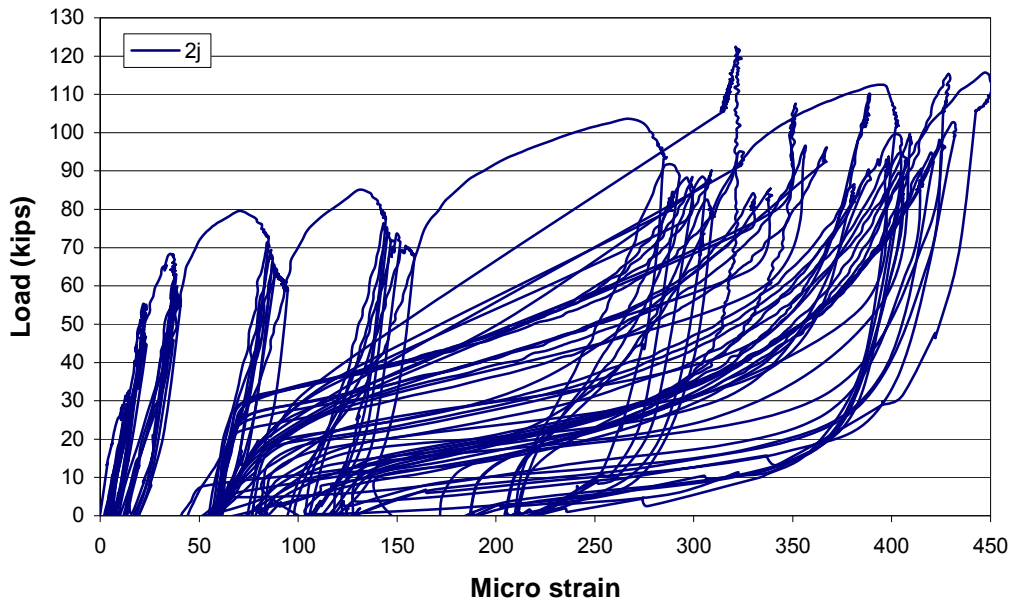


Figure A-0-16 Observed strain Pile Cap 2 location j.

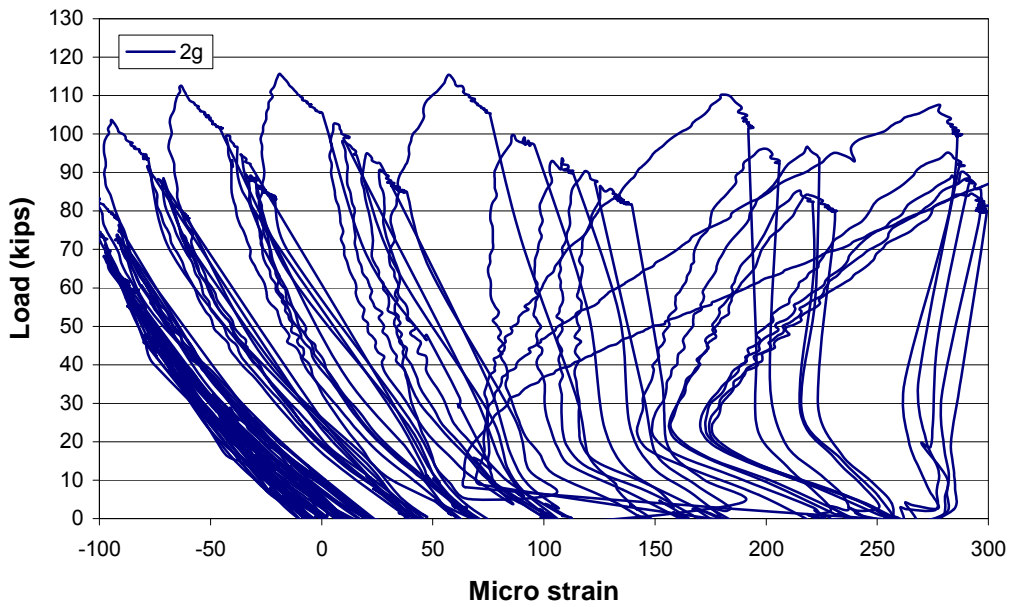
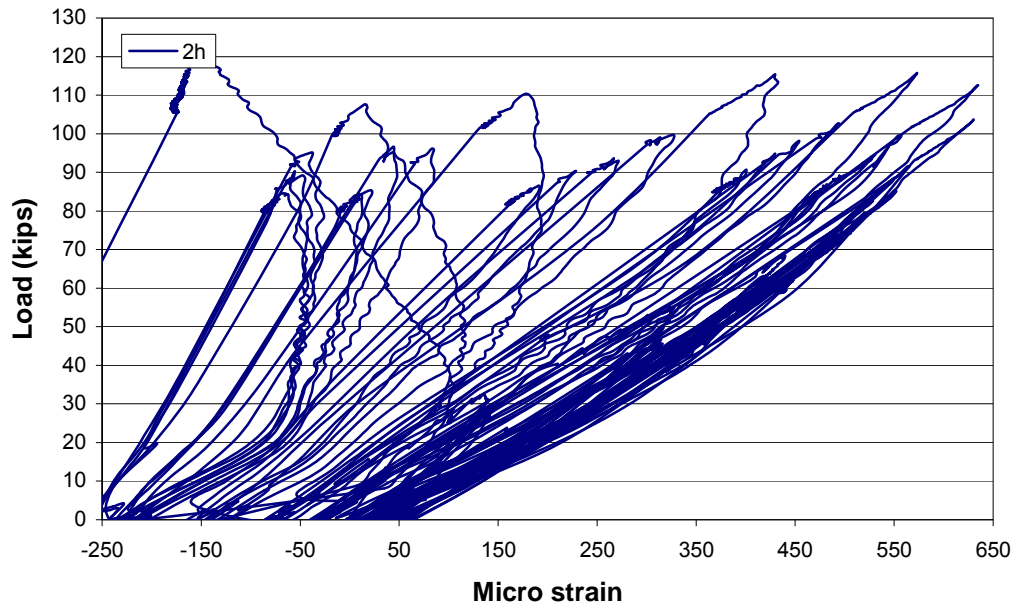
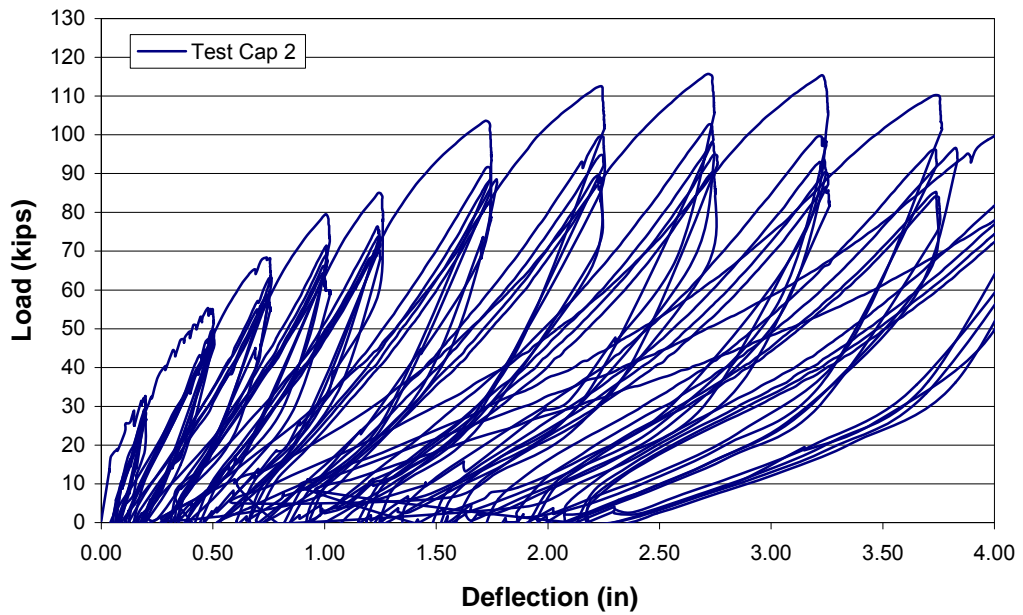


Figure A-0-17 Observed strain Pile Cap 2 location g.



**Figure A-0-18 Observed strain Pile Cap 2 location h.**



**Figure A-0-19 Observed deflection Pile Cap 2.**

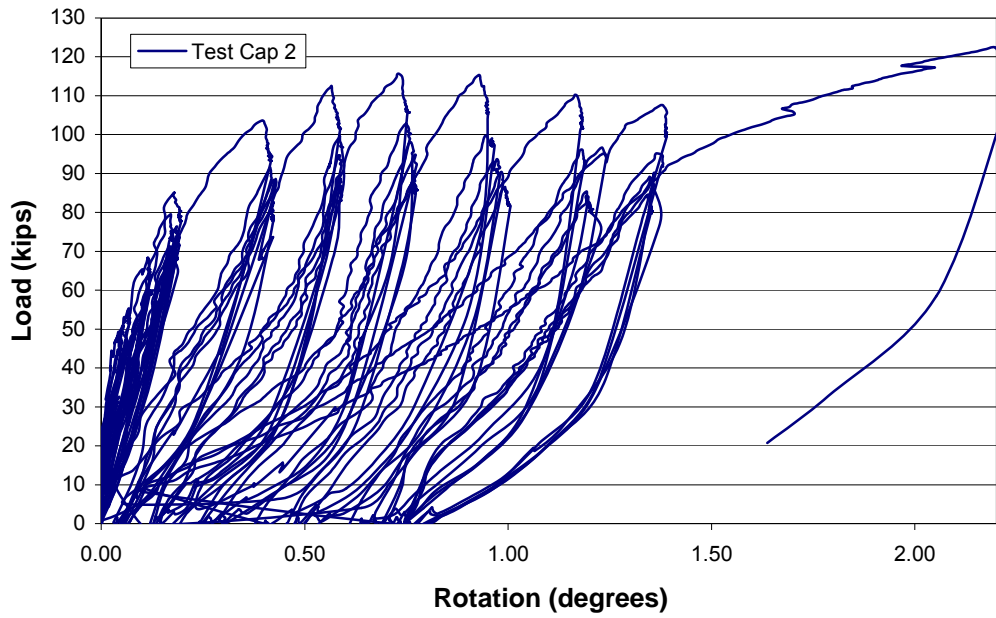


Figure A-0-20 Observed rotation Pile Cap 2.

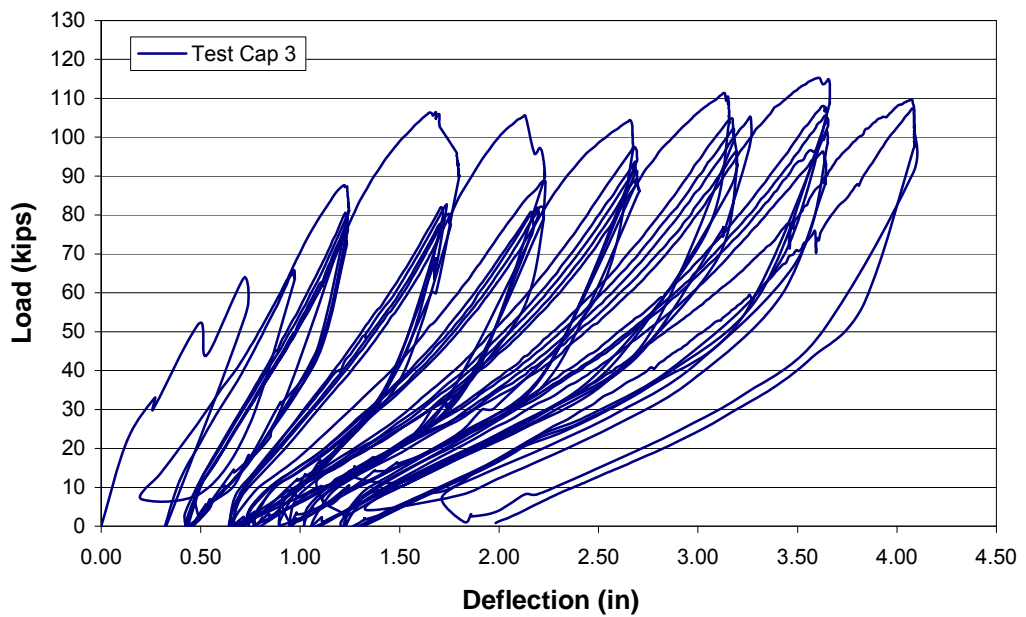


Figure A-0-21 Observed deflection Pile Cap 3.

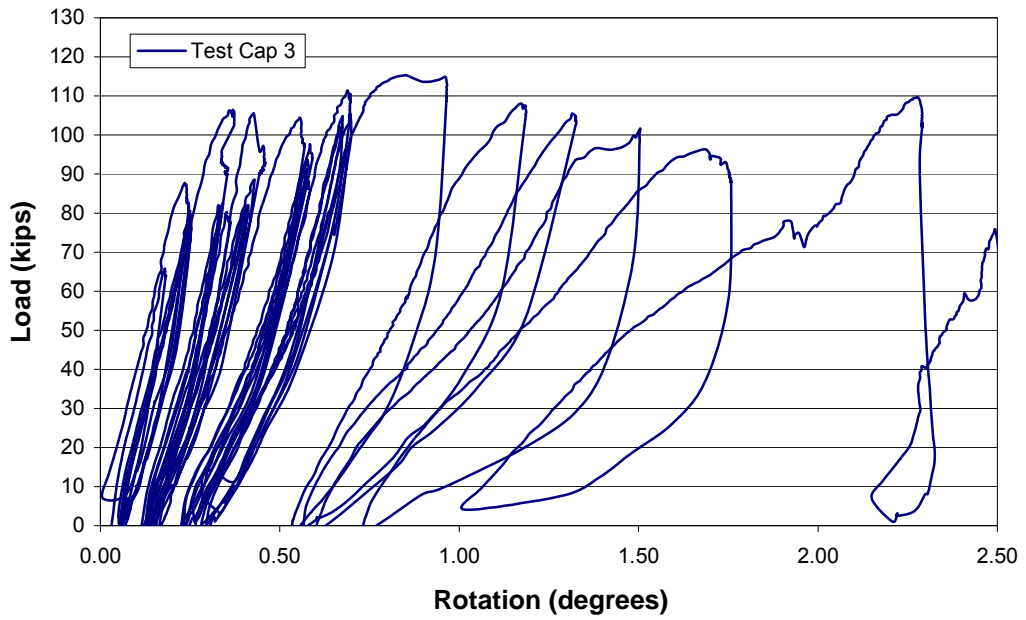


Figure A-0-22 Observed rotation Pile Cap 3.

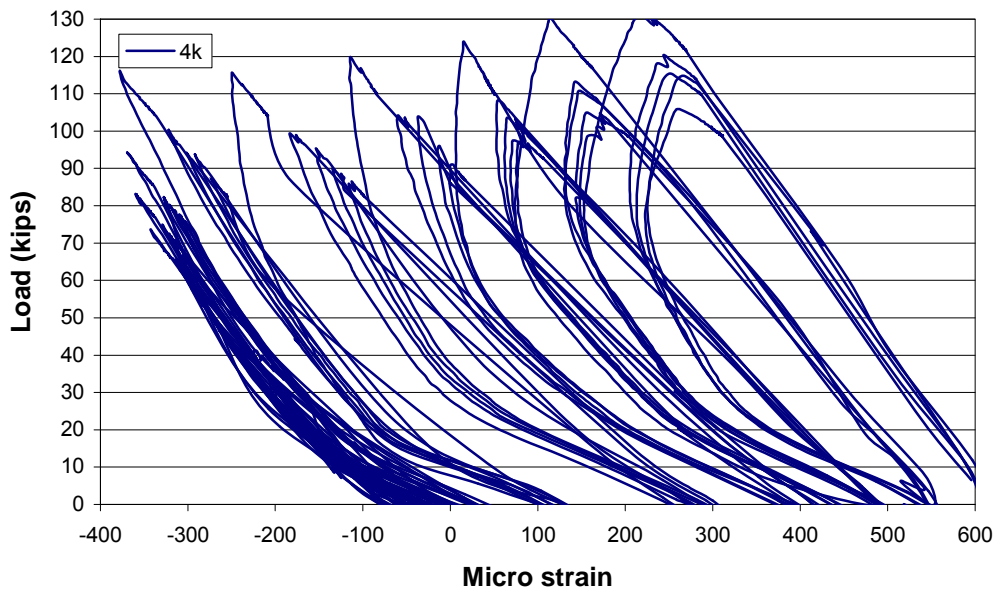
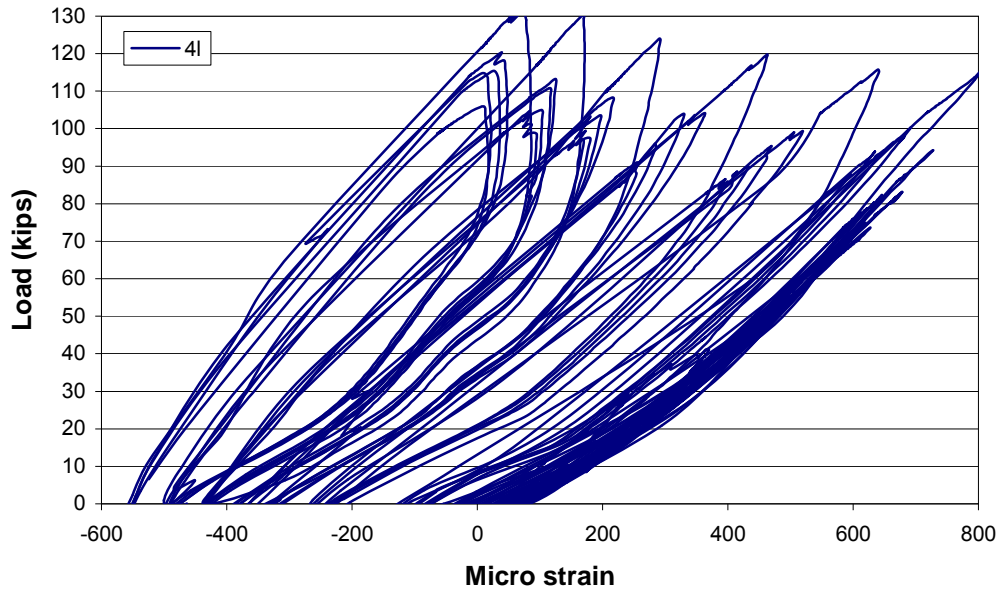
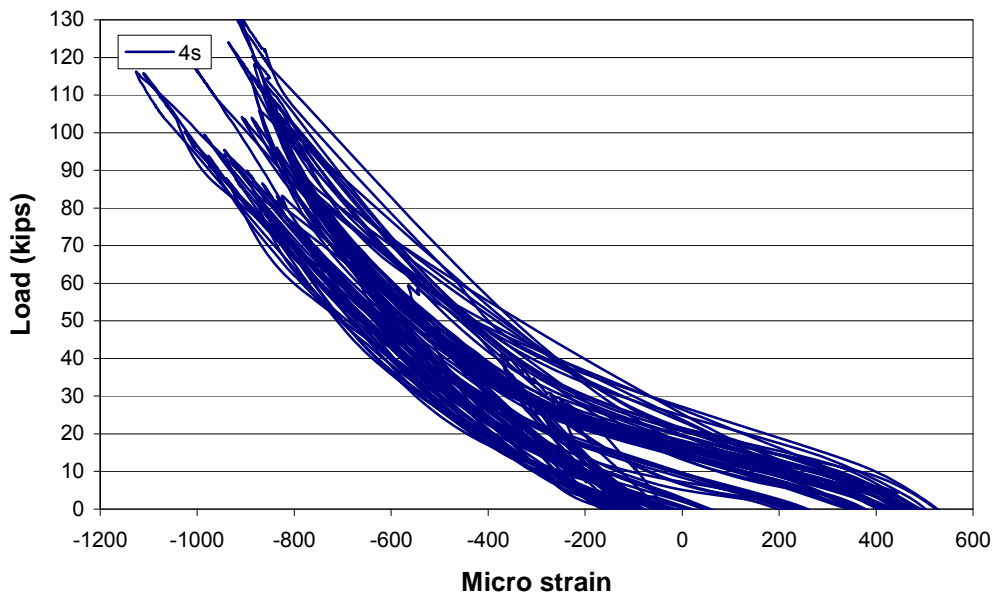


Figure A-0-23 Observed strain Pile Cap 4 location k.



**Figure A-0-24 Observed strain Pile Cap 4 location l.**



**Figure A-0-25 Observed strain Pile Cap 4 location s.**

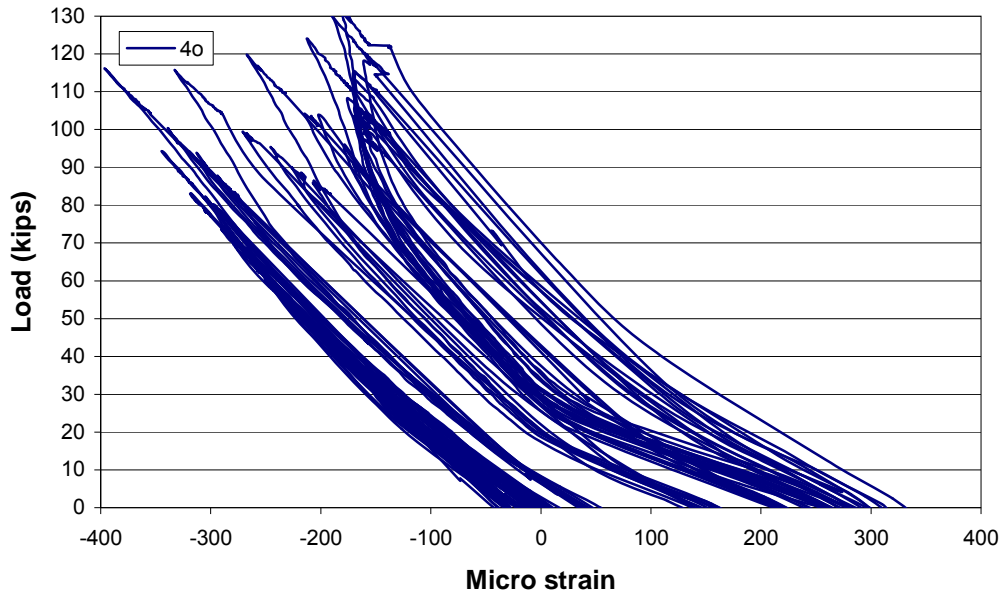


**Figure A-0-26 Observed strain Pile Cap 4 location o.**

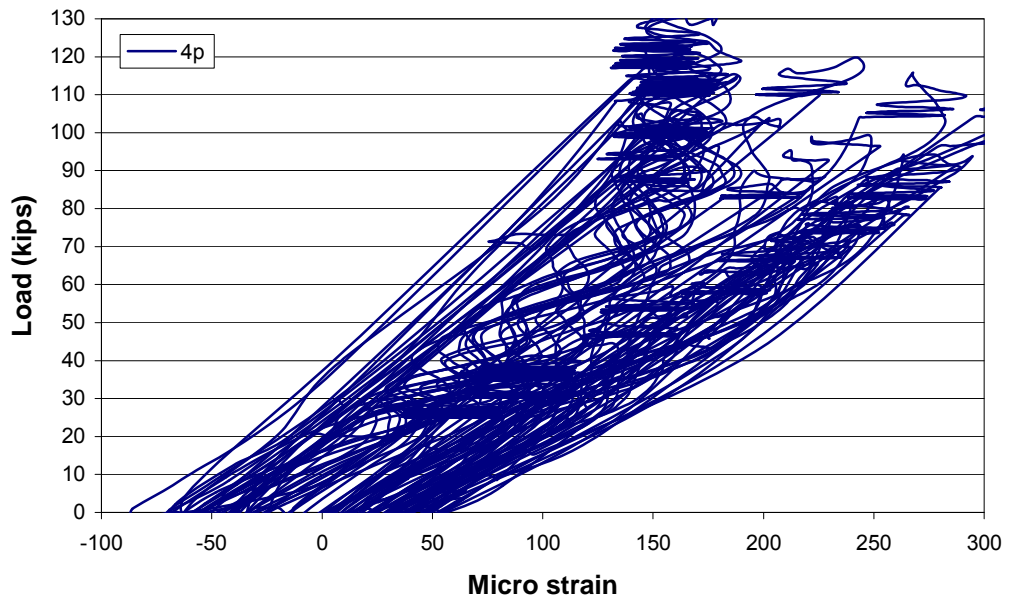


**Figure A-0-27 Observed strain Pile Cap 4 location p.**

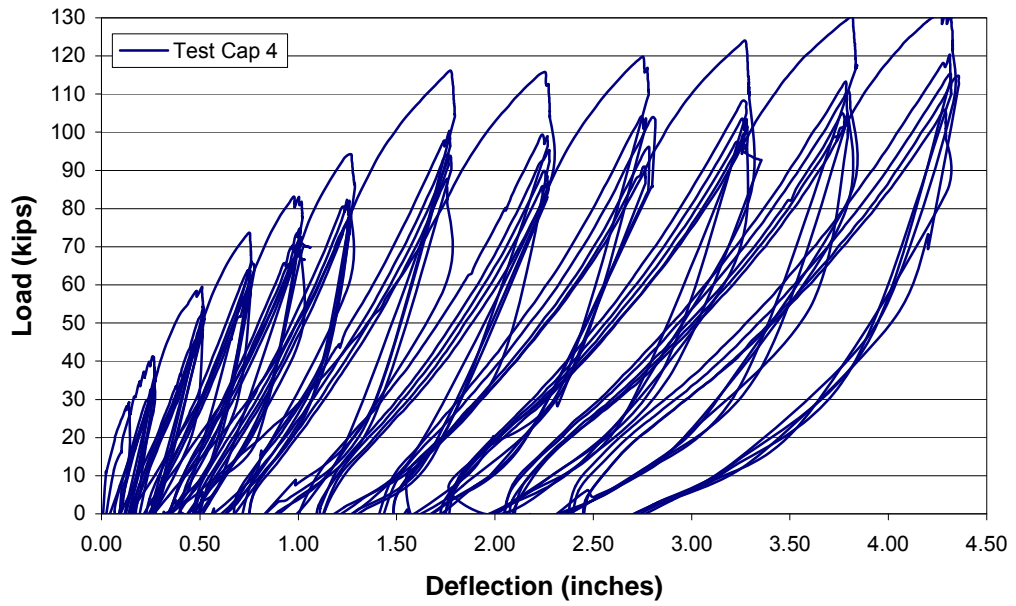


**Figure A-0-28 Observed deflection Pile Cap 4.**

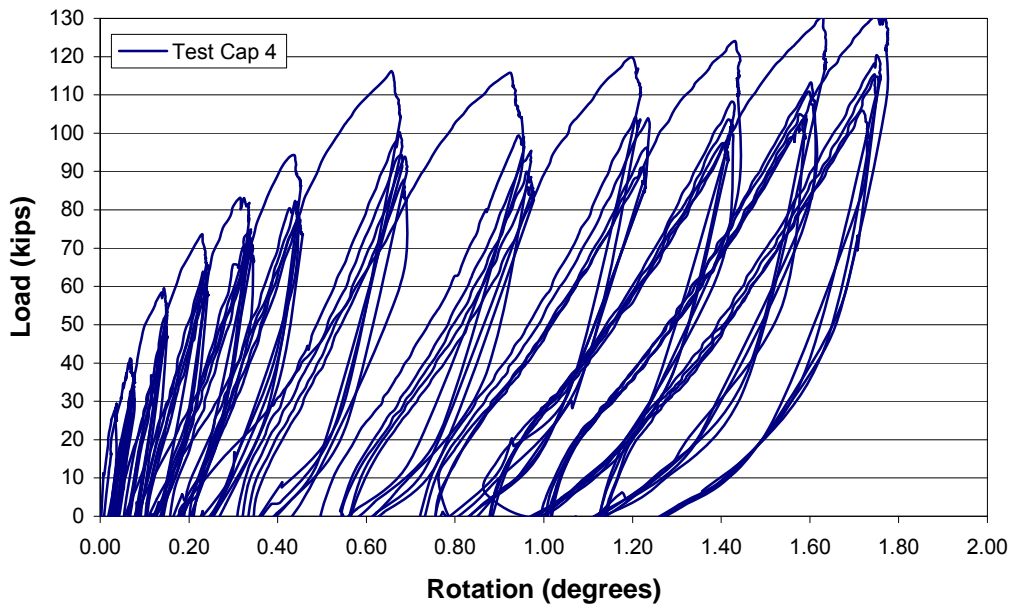


**Figure A-0-29 Observed rotation Pile Cap 4.**